NASA Contractor Report 187456
ICASE Report No. 90–72

ICASE

VORTEX INSTABILITIES IN 3D BOUNDARY LAYERS: THE RELATIONSHIP BETWEEN GÖRTLER AND CROSSFLOW VORTICES

Andrew P. Bassom
Philip Hall

Contract No. NAS1–18605
October 1990

Institute for Computer Applications in Science and Engineering
NASA Langley Research Center
Hampton, Virginia 23665–5225

Operated by the Universities Space Research Association

National Aeronautics and Space Administration
Langley Research Center
Hampton, Virginia 23665-5225

VORTEX INSTABILITIES IN 3D BOUNDARY LAYERS : THE RELATIONSHIP BETWEEN GÖRTLER AND CROSSFLOW VORTICES

Andrew P. Bassom and Philip Hall*
Department of Mathematics
North Park Road
University of Exeter
Exeter, Devon EX4 4QE
U.K.

ABSTRACT

The inviscid and viscous stability problems are addressed for a boundary layer which can support both Görtler and Crossflow vortices. The change in structure of Görtler vortices is found when the parameter representing the degree of three-dimensionality of the basic boundary layer flow under consideration is increased. It is shown that Crossflow vortices emerge naturally as this parameter is increased and ultimately become the only possible vortex instability of the flow. It is shown conclusively that at sufficiently large values of the crossflow there are no unstable Görtler vortices present in a boundary layer which, in the zero crossflow case, is centrifugally unstable. The results suggest that in many practical applications Görtler vortices cannot be a cause of transition because they are destroyed by the 3-D nature of the basic state. In swept wing flows the Görtler mechanism is probably not present for typical angles of sweep of about 20 degrees. Some discussion of the receptivity problem for vortex instabilities in weakly 3-D boundary layers is given; it is shown that inviscid modes have a coupling coefficient marginally smaller than those of the fastest growing viscous modes discussed recently by Denier, Hall and Seddougui (1990). However the fact that the growth rates of the inviscid modes are the largest in most situations means that they are probably the most likely source of transition.

*Research was supported by the National Aeronautics and Space Administration under NASA Contract No. NAS1-18605 while the author was in residence at the Institute for Computer Applications in Science and Engineering (ICASE), NASA Langley Research Center, Hampton, VA 23665.

§1. Introduction.

Recently there has been interest in the effect of boundary layer growth on instability mechanisms to which the boundary layers are susceptible. Here, we shall concentrate on the Görtler vortex mechanism which has been shown to occur in both two- and three-dimensional boundary layer flows over concave walls. Much of the early theoretical work concerned with Görtler vortices addressed the problem of the linear stability of external two-dimensional flows over such concave walls. Early contributions were made by, among others, Görtler (1940), Smith (1955) and Hämmerlin (1956). Later Hall (1982a, b) argued that much of this early work was fundamentally flawed for all the analyses invoked the parallel flow approximation (which essentially assumes that the basic flow in which the vortices lie is independent of the streamwise co-ordinate and so neglects the effect of boundary layer growth). This approximation enables the linear stability equations to be expressed as ordinary differential equations but Hall illustrated that this assumption is unjustifiable except in the limit of small vortex wavelength, and indeed this is the explanation for the considerable inconsistencies in the results of the previous studies. Additionally, in the case of small vortex wavelength the Görtler instability may be described by an asymptotic structure which takes account of boundary layer growth in a rational manner and thence the parallel flow assumption is rendered superfluous in the only situation in which it has any relevance whatsoever.

Hall (1982a) examined boundary layer flow over the cylinder $y = 0$, $-\infty < z < \infty$ where the z-axis is a generator of the cylinder and y measures the distance normal to the surface. The x- co-ordinate measures distance along the curved surface, which is taken to have variable curvature $(1/b)\,\kappa\left(\frac{x}{l}\right)$ where b and l are lengthscales. The Reynolds number Re, the curvature parameter δ and the Görtler number G are defined by

$$Re = \frac{U_0 l}{\nu}, \qquad \delta = \frac{l}{b}, \qquad G = 2Re^{\frac{1}{2}}\delta, \tag{1.1}$$

where U_0 is a typical flow velocity in the x direction and ν the kinematic viscosity of the fluid. Hall (1982a) investigated the flow characteristics when Re is large and δ is small such that in the limit $\delta \longrightarrow 0$ G is held fixed at an O(1) value. By scaling the spanwise co-ordinate z on the boundary layer thickness, it was demonstrated that for a non-dimensional vortex wavenumber $\epsilon^{-1} \gg 1$ linearised vortex modes within a two-dimensional basic flow are neutrally stable at a Görtler number $G = g_0\epsilon^{-4} + \ldots$, where g_0 is a known O(1) constant whose precise value is dependent upon the properties of the basic

flow under consideration. For larger wavelengths the problem is fully nonparallel and the linear stability equations, which now take the form of a set of partial differential equations, have to be solved numerically, see Hall (1983). This paper showed two significant features of this nonparallel flow problem, namely that the ideas of a unique stability curve and of unique growth rates at a specified downstream location are inapplicable to the Görtler problem because the location where a vortex commences to grow is dependent upon the position and the shape of the the imposed disturbance.

Questions concerning the development of nonlinear nonparallel vortices within growing boundary layers were addressed by Hall (1988). This numerical investigation showed that as the nonlinear disturbance evolves the perturbation energy becomes concentrated in the fundamental and mean flow correction; a conclusion consistent with the weakly nonlinear theory of Hall (1982*b*) valid for small wavelength vortices. It is well known that Görtler vortices set up in an experiment conserve their wavelength as they move downstream. Since the boundary layer itself thickens it follows that the local nondimensional vortex wavenumber becomes large as the vortex develops. Thus the small wavelength limit in the external Görtler problem is appropriate to the ultimate development of any fixed wavelength vortex and hence sufficiently far downstream in many flows the asymptotic work of Hall (1982*a*, *b*) becomes applicable.

As with all weakly nonlinear investigations, the results of Hall (1982*b*) are valid only within a neighbourhood of the point where the imposed perturbation is neutrally stable. For vortices of wavenumber $\epsilon^{-1} \gg 1$, their development downstream of the point of neutral stability is governed by the solution of a pair of coupled nonlinear partial differential equations which adopt a simple asymptotic structure at large values of X, where ϵX ($X = O(1)$) denotes the distance of the vortex downstream of the neutral point. Formally, for large X, Hall & Lakin (1988) showed that this asymptotic structure could be used to deduce the flow configuration for fully nonlinear Görtler vortices, at which point the mean flow correction generated by the presence of the vortices is as large of the basic (undisturbed) flow itself. The vortex structure derived by Hall & Lakin (1988) essentially consists of a core region in which the vortex is concentrated and which is bounded by two thin layers in which the vortex activity is reduced to zero exponentially. Further work by Hall & Seddougui (1989) has shown that these thin layers are susceptible to secondary instabilities which take the form of travelling waves confined within these layers. This theoretical

investigation, together with the weakly nonlinear account of this form of secondary instability described by Seddougui & Bassom (1990), provides good qualitive agreement with several experimental observations, notably those of Peerhossaini & Wesfreid (1988a, b).

All the work described above has addressed problems which arise when Görtler vortices occur in two–dimensional boundary layers but in many practical situations in which Görtler vortices are known to arise the basic boundary layer is three–dimensional. For example, in the case of a boundary layer flow over a three–dimensional obstacle or the flow over a turbine blade the three–dimensionality of the basic flow is potentially crucial and should not be neglected. Most significantly, the development of laminar flow airfoils has given rise to designs which have two areas of concave curvature on the lower side of the airfoil and when the wing is swept the boundary layer flow is fully three–dimensional and the previously mentioned analyses are largely inapplicable.

The first attempt to describe this three–dimensionality effect was given by Hall (1985) who examined the Görtler mechanism in flow over an infinitely long swept cylinder. The results obtained were quite general and did not require a precise description of the particular boundary layer under investigation. Hall (1985) showed that it is the relative size of the crossflow and chordwise flow over the cylinder which is critical in determining the vortex structure. He demonstrated that as this ratio, say λ, was increased from zero the first significant change in the vortex structure from that in the two–dimensional case occurs when $\lambda \sim Re^{-\frac{1}{2}}$, where Re is the (large) Reynolds number defined in (1.1). Then the vortices become time dependent and unlike the two–dimensional case, the high wavenumber modes no longer have vortex boundaries aligned with the flow direction. Indeed, as the crossflow increases further, the neutral vortices have axes perpendicular to the vortex lines of the basic flow. The neutral Görtler number for the vortices was predicted by a large wavenumber asymptotic analysis, the results of which suggested that for O(1) values of the ratio of the crossflow and chordwise velocity fields the Görtler mechanism is probably unimportant compared with Tollmien–Schlichting and crossflow type instabilities.

An investigation into the effect of crossflow on weakly nonlinear Görtler vortices was made by Bassom (1989). Rather than concentrate on vortices within a growing boundary layer with the inherent difficulties of providing an adequate description of boundary layer growth, that work considered vortices within a curved channel. This has the advantage that the problem can be described by solution of ordinary differential equations as opposed to partial differential equations. Bassom (1989) showed that for this problem

equilibrium, streamwise independent weakly nonlinear vortices could only persist below a certain threshold value of the crossflow.

One aim in the present paper is to extend some recent work by Denier, Hall & Seddougui (1990) (hereafter referred to as DHS) into a three–dimensional setting. The principal aim of DHS was to investigate the problem of providing a rational theory for the receptivity of Görtler vortices and specifically how the vortices may be triggered by wall roughness elements. In the course of this work, DHS reconsidered the stability of a vortex in a high Görtler number flow by implementing a linear, spatial stability analysis. In particular, for $G \gg 1$, they considered the structure of vortices in two different wavenumber regimes: they reworked the analysis of Hall (1982*a*) for high $O\left(G^{\frac{1}{4}}\right)$ wavenumbers and also examined O(1) wavenumber vortices. This latter disturbance mode is governed by inviscid equations. By considering the region between these two wavenumber regimes, DHS identified a new structure which is relevant for vortices of wavenumber $O\left(G^{\frac{1}{6}}\right)$ and which has the property that the vortices are trapped in a thin layer of thickness $O\left(G^{-\frac{1}{6}}\right)$ at the wall. This is in contrast to the structure identified previously by Hall (1982*a*) who demonstrated that vortices of wavenumber $O\left(G^{\frac{1}{4}}\right)$ are confined to a thin layer embedded within the boundary layer at *some well–defined* position.

Of paramount importance, DHS showed that within the $O\left(G^{\frac{1}{6}}\right)$ wavenumber regime there exists a unique most unstable Görtler vortex according to linear stability theory. Hence the most dangerous mode within a two–dimensional boundary layer has been found and our objective now is to extend the work of DHS to consider the effect of introducing crossflow into the boundary layer flow.

As previously mentioned, DHS conducted a purely spatial analysis of the instability modes. Here, we firstly add a crossflow into the situation considered by DHS and assess its effect; we continue to use the spatial approach. For the O(1) wavenumber modes at $G \gg 1$ we show that crossflow first has a significant effect on the two–dimensional results once this parameter becomes $O(Re^{-\frac{1}{2}}G^{\frac{1}{2}})$. By examining the properties of the vortices when subject to this size of crossflow we can identify several limits of note. We show that as the crossflow increases the vortex structure takes on an identity which is essentially that of a crossflow instability, a mechanism first investigated by Gregory, Stuart & Walker (1955). Additionally, if both the crossflow and the wavenumber of this inviscid vortex increase appropriately we can obtain a mode whose structure is dominated by viscous effects. It is found that when this occurs the ratio of crossflow to chordwise flow becomes $O(Re^{-\frac{1}{2}}G^{\frac{3}{6}})$

and the (large) wavenumber of the vortices is that considered by DHS and which pertains to the most unstable Görtler vortex in a two-dimensional flow. Consequently, we have the basis for explaining how the stability characteristics of the modes found by DHS are changed by the presence of crossflow. We demonstrate that the introduction of crossflow into the problem can have a stabilising effect, at least according to our linear theory. In particular, whereas in DHS it was shown that stationary vortices are necessarily unstable at $O\left(G^{\frac{1}{6}}\right)$ wavenumbers, this is no longer true once crossflow terms are introduced. In addition, for certain crossflow values there exist neutrally stable vortex modes whilst at large enough values of the crossflow no vortex instabilities induced by centrifugal effects persist.

We then develop our description of the disturbance motion by allowing the vortices to be time dependent. Unfortunately, as in DHS, for all the problems treated here the equations which determine the vortices form a pair of coupled ordinary differential equations with associated boundary conditions and this system is only amenable to a numerical solution for O(1) parameter values. We study this numerical problem for a number of particular parameter choices and also investigate the asymptotic description of the vortex structure in both the limits of large and of small vortex wavelengths.

The procedure for the remainder of the paper is as follows. In the coming section we formulate the problem at hand and obtain the differential equations which determine the (essentially inviscid) structure for vortices of O(1) wavenumber. After considering the solutions to this problem, we move on in section 3 to examine the viscous structure which describes the large wavenumber $O(G^{\frac{1}{6}})$ vortices in the presence of crossflow. At this stage we include both the crossflow and temporal terms described in the preceding paragraphs and then subsequently we study particular cases. In section 4 we briefly consider the zero frequency crossflow problem and in the ensuing section examine the effect of allowing the disturbance to have periodic temporal dependence. We then proceed to investigate various asymptotic limits which describe the behaviour of the vortex modes in both low and high wavenumber cases and conclude with some discussion.

§2. Formulation.

Our aim here is to obtain the equations which determine the structure of high wavenumber vortices in a slightly three-dimensional boundary layer. As in Hall (1985), we consider

a boundary layer flowing over the cylinder $y = 0$, $-\infty < z < \infty$ so that the z-axis is a generator of the cylinder and y measures the distance normal to the surface. The x co-ordinate measures distance along the curved surface, which is supposed to have variable curvature $(1/b)\chi\left(\frac{x}{l}\right)$ where b and l are length scales. We define the Reynolds number Re, the Görtler number G and the curvature parameter δ as in (1.1) where U_0 is a typical flow velocity in the streamwise direction. The Reynolds number is assumed to be large, whilst δ is sufficiently small so that as $\delta \longrightarrow 0$ the parameter G is fixed and is order one. Again following Hall (1985), the basic three-dimensional boundary layer is taken to be of the form

$$\mathbf{u} = U_0\left[\bar{u}(X,Y), Re^{-\frac{1}{2}}\bar{v}(X,Y), Re^{-\frac{1}{2}}\lambda^*\bar{w}(X,Y)\right]\left(1 + O\left(Re^{-\frac{1}{2}}\right)\right), \tag{2.1a}$$

where

$$X = \frac{x}{l}, \qquad Y = \left(\frac{y}{l}\right)Re^{-\frac{1}{2}}, \tag{2.1b}$$

and λ^* is supposed to be O(1). To compute this boundary layer profile in practice, $\bar{u}$ and $\bar{v}$ are determined by numerically integrating the two-dimensional boundary layer equations and the crossflow $\bar{w}$ is then found from the spanwise momentum equation.

We now define the variable $Z = Re^{\frac{1}{2}}z/l$ and perturb the basic flow. If t is a time variable scaled on l/U_0 and if $E \equiv \exp(iaZ)$ then we disturb (2.1a) by writing

$$\begin{aligned}\mathbf{u} = U_0\big[&\bar{u} + \delta U(t,X,Y)E, \bar{v}Re^{-\frac{1}{2}} + \delta Re^{-\frac{1}{2}}V(t,X,Y)E,\\ &\lambda^*Re^{-\frac{1}{2}}\bar{w} + \delta Re^{-\frac{1}{2}}W(t,X,Y)E\big]\left(1 + O\left(Re^{-\frac{1}{2}}\right)\right),\end{aligned} \tag{2.2a}$$

where $\delta \ll 1$. Similarly, we perturb the basic pressure $\bar{p}$ by writing

$$p = \bar{p} + Re^{-1}P(t,X,Y)E. \tag{2.2b}$$

Substituting the expressions (2.2) into the governing continuity and Navier–Stokes equations and linearising yields the perturbation equations

$$U_X + V_Y + iaW = 0, \tag{2.3a}$$

$$U_t + \bar{u}U_X + U\bar{u}_X + \bar{v}U_Y + V\bar{u}_Y + \lambda^*\bar{w}iaU = U_{YY} - a^2U, \tag{2.3b}$$

$$V_t + \bar{u}V_X + U\bar{v}_X + \bar{v}V_Y + V\bar{v}_Y + \lambda^*\bar{w}iaV + G\chi(X)\bar{u}U = -P_Y + V_{YY} - a^2V, \tag{2.3c}$$

$$W_t + \bar{u}W_X + \lambda^*U\bar{w}_X + \bar{v}W_Y + \lambda^*V\bar{w}_Y + \lambda^*\bar{w}iaW = -iaP + W_{YY} - a^2W. \tag{2.3d}$$

The scalings (2.2) are those appropriate to Görtler vortices (see Hall (1982a) for futher discussion). We note the key features that the streamwise velocity disturbance is asymptotically larger than the other components and that with these scalings the pressure term drops out of the streamwise momentum equation (2.3b). Further, viscous effects are brought into the perturbation equations (2.3) by the choice of spanwise and normal scalings.

At this stage we consider the spatial inviscid Görtler modes of O(1) wavenumber; in the context of the viscous equations (2.3) this corresponds to taking the limit $G \gg 1$. DHS showed that for $\lambda^* = 0$, $a = O(1)$ the vortex structure is found by considering expansions of the forms

$$U = \left\{ u_0(x,Y) + G^{-\frac{1}{2}} u_1(x,Y) + \ldots \right\} \exp\left(G^{\frac{1}{2}} \int \beta dx \right), \tag{2.4}$$

together with similar expansions for $G^{-\frac{1}{2}}V$, $G^{-\frac{1}{2}}W$ and $G^{-1}P$. Substitution of (2.4) in (2.3) yields the problem for the amplification rate β

$$-\beta^2 \bar{u} \left[\left(\frac{\partial^2}{\partial Y^2} - a^2 \right) v_0 - \frac{\bar{u}_{YY}}{\bar{u}} v_0 \right] = a^2 \chi \bar{u}_Y v_0, \tag{2.5a}$$

with associated boundary conditions

$$v_0 = 0 \qquad \text{at} \quad Y = 0, \qquad v_0 \longrightarrow 0 \qquad \text{as} \quad Y \longrightarrow \infty. \tag{2.5b}$$

DHS observed that the most unstable spatial mode which is a solution of (2.5) may be written in the form

$$v_0 = \bar{u} \exp(-aY), \qquad \beta^2 = \frac{a\chi}{2}, \tag{2.5c}$$

which is valid for all a. Thus we have the somewhat remarkable result that, so long as $\bar{u}$ vanishes at the wall, the fastest growing inviscid mode has growth rate independent of the basic state.

We are concerned with inclusion of sufficient crossflow in the problem so that the governing equations (2.5) are altered by this effect. We find that this occurs when $\lambda^* = O(G^{\frac{1}{2}})$ and then we write

$$(U,V,W,P) = \left\{ U_0(Y) + \ldots, G^{\frac{1}{2}} V_0(Y) + \ldots, G^{\frac{1}{2}} W_0(Y) + \ldots, \; G P_0(Y) + \ldots \right\} \times \exp\left(G^{\frac{1}{2}} \int \beta dx \right), \tag{2.6a}$$

$$\lambda^* = \bar{\bar{\lambda}} G^{\frac{1}{2}}. \tag{2.6b}$$

At this stage we concentrate on a purely spatial approach so that on substituting (2.6) into (2.3) we obtain, in turn,

$$(\beta U_0 + iaW_0) + \frac{dV_0}{dY} = 0, \tag{2.7a}$$

$$\left(\beta\bar{u} + i\bar{\bar{\lambda}}a\bar{w}\right) U_0 + \bar{u}_Y V_0 = 0, \tag{2.7b}$$

$$\left(\beta\bar{u} + i\bar{\bar{\lambda}}a\bar{w}\right) V_0 + \chi\bar{u}U_0 = -\frac{dP_0}{dY}, \tag{2.7c}$$

$$\left(\beta\bar{u} + i\bar{\bar{\lambda}}a\bar{w}\right) W_0 + \bar{\bar{\lambda}}\bar{w}_Y V_0 = -iaP_0. \tag{2.7d}$$

¿From (2.7) we can easily show that

$$\left(-i\beta\bar{u} + \bar{\bar{\lambda}}a\bar{w}\right)^2 \left(\frac{d^2V_0}{dY^2} - a^2V_0\right) - \left(-i\beta\bar{u} + \bar{\bar{\lambda}}a\bar{w}\right)\left(-i\beta\bar{u}_{YY} + \bar{\bar{\lambda}}a\bar{w}_{YY}\right) V_0 = a^2\chi\bar{u}\bar{u}_Y V_0. \tag{2.8a}$$

The above equation then controls the inviscid growth of vortices in a weakly three-dimensional boundary layer; it is of course the appropriate generalisation due to wall curvature of the well-known Rayleigh equation for unidirectional flows.

Equation (2.8a) needs to be solved subject to suitable boundary conditions. Firstly, we demand the typical inviscid condition at the surface of the cylinder $y = 0$ so that

$$V_0 = 0 \qquad \text{at} \quad Y = 0. \tag{2.8b}$$

In addition, to ensure that the disturbance is confined within the boundary layer,

$$V_0 \longrightarrow 0 \qquad \text{as} \quad Y \longrightarrow \infty. \tag{2.8c}$$

These boundary conditions, when added to (2.8a), constitute an eigenproblem for the spatial growth rate β in terms of the scaled wavenumber a and the scaled crossflow $\bar{\bar{\lambda}}$. We notice that since this problem is a localised one about some point $x = x_*$ we may scale the curvature parameter χ out of the problem by appropriately redefining β and $\bar{\bar{\lambda}}$. Consequently, for the remainder of the work described here we shall take $\chi \equiv 1$.

To fix our ideas upon some definite boundary layer flow we chose to consider (2.8) when $\bar{u}$ is given by the Falkner–Skan profile

$$\bar{u} = f'(Y): \qquad f''' + ff'' + \frac{1}{2}\left(1 - \left(f'\right)^2\right) = 0, \quad f(0) = f'(0) = 0, \quad f'(\infty) = 1. \tag{2.9a}$$

This flow is closely related to the steady flow in the boundary layer along a surface of revolution near a forward stagnation point, see Jones & Watson (1963). Cooke (1950) showed that for a flow over an infinite yawed wedge at zero angle of attack then if the streamwise basic flow is given by (2.9a) then the spanwise component $\bar{w}$ satisfies

$$\bar{w} = g: \qquad g'' + fg' = 0, \qquad g(0) = 0, \quad g(\infty) = 1. \tag{2.9b}$$

The dependences of $\bar{u}$ and $\bar{w}$ on Y are depicted in Figure (2.1). We observe that the Blasius profile would not be a suitable choice for $\bar{u}$ and $\bar{w}$ for then we retrieve the scenario described in Hall (1985). Hall showed that in flows with zero pressure gradient and with $\bar{u}$ and $\bar{w}$ therefore linearly related the whole problem of Görtler vortices in three-dimensional boundary layers becomes degenerate and can be reduced to a two-dimensional case. Consequently, we needed to focus our attention on other physically realistic three-dimensional flows and the choice (2.9) was motivated by these requirements.

Given this basic flow we then solved (2.8) for a variety of parameter regimes. We firstly considered the effect of increasing the crossflow $\bar{\bar{\lambda}}$ on the vortex growth rate β_r (β_r denotes the real part of the complex number β). The results are illustrated in Figure (2.2) for a selection of $\bar{\bar{\lambda}}$ values and we can make some immediate deductions. When $\bar{\bar{\lambda}} = 0$ we of course return to the case of DHS and β is given by (2.5c). However, as $\bar{\bar{\lambda}}$ is increased then for most prescribed wavenumbers a the corresponding growth rate decreases so that the effect of increasing the crossflow is to stabilise the vortex flow.

For small crossflows $\bar{\bar{\lambda}}$ (less than some critical value, say $\bar{\bar{\lambda}}_c \approx 4.7$) we observe that although the vortex is more stable than in the two-dimensional base flow case, we still have $\beta_r > 0$ so that the vortex remains unstable for all a. Once $\bar{\bar{\lambda}}$ reaches the value $\bar{\bar{\lambda}}_c$ however, Figure (2.2) indicates that there exists a region of wavenumber space in which vortices can no longer persist; indeed, for $\bar{\bar{\lambda}} > \bar{\bar{\lambda}}_c$ there exist cut-off values $a_1(\bar{\bar{\lambda}})$ and $a_2(\bar{\bar{\lambda}})$ such that the vortices only exist for $a < a_1$ or $a > a_2$. As $\bar{\bar{\lambda}}$ increases yet further, we see that a_1 decreases and a_2 increases and in addition the growth rates β_r in the lower wavenumber regime grow. In Figure (2.3) we have illustrated the dependence of β_r upon $\bar{\bar{\lambda}}$ for those values of a less than $a_1(\bar{\bar{\lambda}})$. We can infer from this figure that as $\bar{\bar{\lambda}} \longrightarrow \infty$ the value $a_1(\bar{\bar{\lambda}})$ converges to some non-zero value, say $a_{1\infty}$, and this behaviour is explained in the asymptotic work elucidated shortly.

Figure (2.4) shows the behaviour of the imaginary part of β, β_i, as the wavenumber a and the crossflow $\bar{\bar{\lambda}}$ vary. We immediately deduce from Figure (2.4a) that, for $0 < \bar{\bar{\lambda}} < \bar{\bar{\lambda}}_c$,

β_i is negative for all a and becomes increasingly more negative as $a \longrightarrow \infty$. In addition, we know from the solution (2.5c) of DHS that $\beta_i = 0$ for all a when we consider a purely two-dimensional flow ($\bar{\bar{\lambda}} = 0$). For values of $\bar{\bar{\lambda}} > \bar{\bar{\lambda}}_c$, see Figure (2.4b), we find, as previously mentioned, that the unstable vortex cannot persist in some wavenumber range which increases in extent as $\bar{\bar{\lambda}}$ grows. In Figure (2.4b) this feature is indicated by the gap in the possible values of β_i for $\bar{\bar{\lambda}} > \bar{\bar{\lambda}}_c$. As $\bar{\bar{\lambda}}$ is increased yet further, see Figure (2.4c), β_i becomes progressively more negative for any prescribed wavenumber a and here we have plotted the dependence $\beta_i(a)$ for $a < a_1(\bar{\bar{\lambda}})$.

We turn now to consider various asymptotic solutions of (2.8). Firstly, we study the case $\bar{\bar{\lambda}} \gg 1$, $a < a_1$; i.e. the left-hand solution branches in Figures (2.2b), (2.4b) and those branches sketched in Figures (2.3), (2.4c). If we write

$$\beta = \hat{\beta}\bar{\bar{\lambda}} + o(\bar{\bar{\lambda}}), \tag{2.10a}$$

and substitute this expansion into (2.8a) we obtain at leading order

$$\left(-i\hat{\beta}\bar{u} + a\bar{w}\right)\left(\frac{d^2V_0}{dY^2} - a^2V_0\right) - \left(-i\hat{\beta}\bar{u}'' + a\bar{w}''\right)V_0 = 0. \tag{2.10b}$$

Since curvature efects are now negligible at zeroth order this is a standard Rayleigh equation and we now have a connection between our three-dimensional vortex flow and the work of Gregory, Stuart & Walker (1955) (hereafter referred to as GSW) who were concerned with a description of stationary crossflow vortices formed in the boundary layer above a rotating disc. This instability is due to the inflectional character of the basic velocity profile and GSW showed with china-clay techniques that the crossflow instability took the form of a regularly spaced pattern of spiral vortices which was stationary relative to the disc. Stuart (in GSW), using inviscid theory, suggested that the instability could be associated with a particular inflectional profile in which the inflection point coincided with a point of zero velocity somewhere in the flow. His calculation gave the predicted number of vortices to be approximately four times the observed value of about 30, but the angle of 13° between the axes of the vortices and the radius vector was in excellent agreement with their experiments.

We can appeal to Stuart's inviscid analysis and note that there is a solution of (2.10b) with boundary conditions (2.8b, c) for which a is real and β purely imaginary if there exists a point $\bar{Y} \neq 0$ at which

$$\left(-i\hat{\beta}\bar{u}(\bar{Y}) + a\bar{w}(\bar{Y})\right) = \left(-i\hat{\beta}\bar{u}''(\bar{Y}) + a\bar{w}''(\bar{Y})\right) = 0. \tag{2.11}$$

Some numerical work shows that for the basic profiles (2.9) a suitable solution of (2.11) may be found and then $\hat{\beta}_i/a \approx -0.85$. Consequently, we have, recalling (2.10), neutrally stable crossflow vortex type solutions of (2.8) if $\bar{\bar{\lambda}} \gg 1$, $a = O(1)$ and

$$\frac{\beta_i}{a\bar{\bar{\lambda}}} \approx -0.85. \tag{2.12}$$

On figure (2.4*c*) we indicate, for each crossflow parameter considered, those points for which (2.12) is satisfied. We can conclude that the asymptotic result (2.12) is very accurate for surprisingly modest values of $\bar{\bar{\lambda}}$. Once conditions (2.11) & (2.12) are satisified, the Rayleigh equation (2.10*b*) has regular singular points at $Y = 0$ and $Y = \bar{Y}$ and the solution of this equation with boundary conditions (2.8*b*) forms an eigenvalue problem for the GSW wavenumber $\hat{a}$. We recall that earlier we observed that for $\bar{\bar{\lambda}} > \bar{\bar{\lambda}}_c$ the vortex mode can only persist for wavenumbers a less than $a_1(\bar{\bar{\lambda}})$ and greater than $a_2(\bar{\bar{\lambda}})$ and that as $\bar{\bar{\lambda}} \longrightarrow \infty$, a_1 tends to a non-zero constant $a_{1\infty}$. It is now easy to see that $a_{1\infty}$ is the GSW wavenumber $\hat{a}$. We have chosen not to compute the precise value of $\hat{a}$ here for its value is dependent on the choice of the basic boundary layer flow and our present purpose is to concentrate on the underlying description of vortices in three-dimensional flows as opposed to concentrating on profiles (2.9) in particular. However, from Figure (2.3), we can deduce that for the basic flow (2.9), $\hat{a} \approx 1.3$.

Thus within the context of inviscid stability theory we now see the relationship between Görtler and crossflow vortices. For a two-dimensional boundary layer which is centrifugally unstable the growth rate of the most dangerous mode is given by (2.5c), the exact solution found by DHS. When the crossflow is increased from zero a maximum value of the growth rate develops at some wavenumber and the growth rate curve to the right of this point eventually crosses the zero growth rate axis. Thus at a finite value of the crossflow a finite band of unstable wavenumbers persists to the right of $a = 0$. At this stage we can identify this unstable band of modes as crossflow vortices since at even larger crossflows they reduce to the modes of GSW. At larger values of the wavenumber an unstable band of modes persists up to $a = \infty$ for all values of the crossflow; it is perhaps appropriate to think of these modes as the remnants of the Görtler mechanism. However we shall see below that at high wavenumbers viscous effects become important and that when these effects are allowed for these remnants vanish completely at large enough crossflows.

Having examined the asymptotic description of modes for which $\bar{\bar{\lambda}} > 1$, $a = O(1)$ we next consider vortex states at high wavenumbers a. In Figure (2.5) we show the dependence

of the eigenvalue β of (2.8a) for a range of crossflows in the cases $a = 5$ and $a = 10$. We observe, as already commented upon, that increasing $\bar{\bar{\lambda}}$ tends to decrease the growth rate β_r and we expect that for each fixed $a \gg 1$ there exists a corresponding crossflow value at which the vortex is completely stabilised by the crossflow. This deduction is consistent with the results previously illustrated in Figure (2.2) where as the crossflow increases the wavenumber range over which vortices are unable to persist steadily widens. We can also conclude from earlier results that for $a \gg 1$ and $\bar{\bar{\lambda}}$ not large the vortex flow will remain unstable for as $a \longrightarrow \infty$, $\beta_r \sim a^{\frac{1}{2}}$ when $\bar{\bar{\lambda}} = 0$ and it is not expected that an O(1) increase in the scaled crossflow $\bar{\bar{\lambda}}$ could result in a reduction in the growth rate by this dramatic amount. Consequently, we anticipate that near neutral vortices will be described for $a \gg 1$, $\bar{\bar{\lambda}} \gg 1$.

When $a \gg 1$, following DHS it is deduced from (2.8) that the vortices will be confined to a thin region of thickness $O(a^{-1})$ adjacent to the cylinder wall $y = 0$. We therefore find it convenient to write

$$\xi = aY, \tag{2.13a}$$

and suppose that around $y = 0$ the basic flow velocities have regular Taylor expansions of the forms

$$\bar{u} = \mu_{11}a^{-1}\xi + \frac{1}{2}\mu_{12}a^{-2}\xi^2 + \ldots, \qquad \bar{w} = \mu_{21}a^{-1}\xi + \frac{1}{2}\mu_{22}a^{-2}\xi^2 + \ldots. \tag{2.13b}$$

When $\bar{\bar{\lambda}}$ is gradually increased we find that the stability characteristics of the vortices are first altered significantly once $\bar{\bar{\lambda}} \sim O(a^{\frac{1}{2}})$. If we write $\bar{\bar{\lambda}} = a^{\frac{1}{2}}\hat{\lambda}$, $\hat{\lambda} = O(1)$ we are led to the expansion

$$\beta = i\left(a^{\frac{3}{2}}\beta_0 + a^{\frac{1}{2}}\beta_1 + \ldots\right), \tag{2.13c}$$

with β_0 and β_1 real. If in turn we expand $V_0 = V_{00} + a^{-1}V_{01} + \ldots$ and substitute into (2.8a) we obtain at the leading two orders the relationships

$$\beta_0\mu_{11} + \hat{\lambda}\mu_{21} = 0, \tag{2.14a}$$

and

$$\begin{aligned}\left[\beta_1\mu_{11}\xi + \frac{1}{2}\left(\beta_0\mu_{12} + \hat{\lambda}\mu_{22}\right)\xi^2\right]^2\left(\frac{d^2V_{00}}{d\xi^2} - V_{00}\right) - \\ \left[\beta_1\mu_{11}\xi + \frac{1}{2}\left(\beta_0\mu_{12} + \hat{\lambda}\mu_{22}\right)\xi^2\right]\left[\beta_0\mu_{12} + \hat{\lambda}\mu_{22}\right]V_{00} = (\mu_{11})^2\,\xi V_{00},\end{aligned} \tag{2.14b}$$

which needs to be solved subject to $V_{00} = 0$ at $\xi = 0$ and as $\xi \longrightarrow \infty$ (recall that we scaled $\chi \equiv 1$). This problem needs a fully numerical solution but here we merely remark that this equation has a critical layer structure at the position

$$\xi = -\frac{2\beta_1\mu_{11}}{\left(\beta_1\mu_{12} + \hat{\lambda}\mu_{22}\right)}, \tag{2.14c}$$

and that this structure has to be fully analysed in order that the numerical scheme be effected. We are presently considering this problem in further work and hope to be able to report on this in the near future. However the structure outlined above is certainly consistent with our numerical calculations which suggest the emergence of a critical layer structure when a approaches the cut-off wavenumber a_1.

For the present purposes, we can infer that Görtler vortex states require, at wavenumbers $a \gg 1$, a crossflow of size $O(a^{\frac{1}{2}})$ in order to have a significant effect on their stability. Further, in this case the whole vortex structure is compressed into a thin $O(a^{-1})$ region close to the cylinder surface. Of course, in the development of the inviscid equations (2.7) which describe the vortex we found that for O(1) wavenumber vortices in a crossflow of size $O(G^{\frac{1}{2}})$ (see (2.6*b*)) the viscous terms are negligible. However, as $a \longrightarrow \infty$ the extent of the structure reduces so that at some stage we expect that the viscous terms become significant and no longer negligible. Guided by the asymptotic results (2.13) & (2.14), study of the fundamental equations (2.3) suggest that viscous terms are crucial and so a new regime is acheived when

$$a = O(G^{\frac{1}{6}}), \tag{2.15a}$$

and then

$$\bar{\bar{\lambda}} = O\left(G^{\frac{1}{10}}\right) \qquad \text{and} \qquad \beta = O\left(G^{\frac{3}{10}}\right). \tag{2.15b,c}$$

Recalling the original scalings (2.4), (2.6) we then have a viscous structure in operation for $O(G^{\frac{1}{6}})$ wavenumber vortices in crossflows of size $O(G^{\frac{3}{6}})$ and then the vortices develop on a streamwise lengthscale of $O(G^{-\frac{4}{6}})$. Interestingly, DHS identified the unique most unstable vortex within a two-dimensional base flow as occuring within this wavenumber band and developing on this lengthscale.

In this section we have restricted ourselves to calculations pertinent to stationary vortices. Much of the above analysis can be modified in a straightforward manner to account for time-dependence of the vortices. However, our objective has been to concentrate on understanding the fundamental connections between the inviscid vortex modes and the

GSW crossflow instability and viscous, high–wavenumber vortex structures. There are natural non–stationary counterparts of the GSW stationary instability (see Bassom & Gajjar (1988) for an example) and these will match with time–dependent inviscid vortices in a manner virtually identical to that described here. Further remarks relating our inviscid modes to the crossflow instability mechanism will be made in the conclusions. However, we now move on to examine the salient properties of the high wavenumber viscous structures suggested by scalings (2.15).

§3. The viscous modes.

Following the discussion of the solution properties of the principally inviscid modes considered in the previous section we now examine the effect of crossflow on the stability of the viscous modes whose scalings are suggested by the asymptotic results (2.15). The wavenumber of these vortices is predicted to be $O\left(G^{\frac{1}{6}}\right)$, i.e. is that found by DHS for the most unstable vortex in two-dimensional flow. For no crossflow, DHS showed that the vortex is then confined to an $O(G^{-\frac{1}{6}})$ thick region which lies immediately adjacent to the cylinder $y = 0$ and that the spatial growth rate of the instability is $O(G^{\frac{4}{6}})$ in the streamwise direction. We have, from (2.15b), that when the scaled crossflow $\lambda^* = O\left(G^{\frac{3}{6}}\right)$ (where λ^* is defined in (2.2a)) it is to be expected that a significant deviation in the stability characteristics of the flow from those which occur in the zero crossflow case. Then, following DHS, we write

$$a = k_0 G^{\frac{1}{6}}, \tag{3.1a}$$

where k_0 is $O(1)$ and seek disturbances confined to the layer in which $\psi = O(1)$ where

$$\psi = k_0 G^{\frac{1}{6}} Y. \tag{3.1b}$$

Then we consider modes for which the perturbation velocities (U, V, W) and pressure P take the forms

$$\begin{aligned}(U, V, W, P) = \\ \left(U_0 + G^{-\frac{1}{6}} U_1 + \ldots, G^{\frac{2}{6}} V_0 + G^{\frac{1}{6}} V_1 + \ldots, G^{\frac{3}{6}} W_0 + G^{\frac{2}{6}} W_1 + \ldots, G^{\frac{3}{6}} P_0 + G^{\frac{2}{6}} P_1 + \ldots\right) \\ \times \exp\left[G^{\frac{4}{6}} \int^X \left(\beta_0(X) + G^{-\frac{1}{6}} \beta_1(X) + \ldots\right) dX - iG^{\frac{2}{6}} \int^t \left(\Omega_0(t) + G^{-\frac{1}{6}} \Omega_1(t) + \ldots\right) dt\right]\end{aligned} \tag{3.2a}$$

and we fix the crossflow parameter at $O(G^{\frac{3}{6}})$ so that

$$\lambda^* = \hat{\lambda} G^{\frac{3}{6}}. \tag{3.2b}$$

Here the unknowns $U_0, U_1, V_0, \ldots, P_0, P_1, \ldots$ are functions of ψ alone.

We substitute (3.1) and (3.2) into (2.3) and compare like powers of the large parameter G. In this process, we need to expand the basic flow about $Y = 0$ and so, as in (2.13), we assume that

$$\bar{u} = \mu_{11}(X) Y + \frac{1}{2}\mu_{12}(X) Y^2 + \frac{1}{6}\mu_{13}(X) Y^3 + \ldots, \tag{3.3a}$$

$$\bar{w} = \mu_{21}(X)Y + \frac{1}{2}\mu_{22}(X)Y^2 + \frac{1}{6}\mu_{23}(X)Y^3 + \ldots, \tag{3.3b}$$

$$\bar{v} = O(Y^2), \quad \text{for} \quad Y \ll 1. \tag{3.3c}$$

¿From leading orders in (2.3a) we have

$$\beta_0 U_0 + ik_0 W_0 = 0, \tag{3.4a}$$

$$\beta_1 U_0 + \beta_1 U_0 + k_0 \frac{dV_0}{d\psi} + ik_0 W_1 = 0, \tag{3.4b}$$

and similar manipulation for (2.3b) yields

$$\frac{\beta_0 \mu_{11}}{k_0} + i\hat{\lambda}\mu_{21} = 0, \tag{3.5a}$$

$$\left[\frac{d^2}{d\psi^2} - 1 + \frac{i\Omega_0}{k_0^2} - \frac{\beta_1\mu_{11}\psi}{k_0^3} - \frac{i\hat{\lambda}}{2k_0^3\mu_{11}}\left(\mu_{11}\mu_{22} - \mu_{21}\mu_{12}\right)\psi^2\right] U_0 = \frac{\mu_{11}}{k_0^2} V_0, \tag{3.5b}$$

and

$$\begin{aligned}&\left[\frac{d^2}{d\psi^2} - 1 + \frac{i\Omega_0}{k_0^2} - \frac{\beta_1\mu_{11}\psi}{k_0^3} - \frac{i\hat{\lambda}}{2k_0^3\mu_{11}}\left(\mu_{11}\mu_{22} - \mu_{21}\mu_{12}\right)\psi^2\right] U_1 - \frac{\mu_{11}}{k_0^2} V_1 \\ &= \left[\frac{i\hat{\lambda}}{6\mu_{11}k_0^4}\left(\mu_{11}\mu_{23} - \mu_{21}\mu_{13}\right)\psi^3 + \frac{\beta_1\mu_{12}\psi^2}{2k_0^4} + \frac{\beta_2\mu_{11}\psi}{k_0^3} - \frac{i\Omega_1}{k_0^2}\right] U_0 + \frac{\mu_{12}\psi}{k_0^3} V_0.\end{aligned} \tag{3.5c}$$

On considering the spanwise momentum equation (2.3d), at leading orders we just retrieve a trivial combination of (3.4a), (3.5a) and (3.5b). The third order terms imply that

$$\begin{aligned}&\left[\frac{d^2}{d\psi^2} - 1 + \frac{i\Omega_0}{k_0^2} - \frac{\beta_1\mu_{11}\psi}{k_0^3} - \frac{i\hat{\lambda}}{2k_0^3\mu_{11}}\left(\mu_{11}\mu_{22} - \mu_{21}\mu_{12}\right)\psi^2\right] W_1 - \frac{\hat{\lambda}\mu_{21}}{k_0^2} V_1 \\ &= \left[\frac{i\hat{\lambda}}{6\mu_{11}k_0^4}\left(\mu_{11}\mu_{23} - \mu_{21}\mu_{13}\right)\psi^3 + \frac{\beta_1\mu_{12}\psi^2}{2k_0^4} + \frac{\beta_2\mu_{11}\psi}{k_0^3} - \frac{i\Omega_1}{k_0^2}\right] W_0 + \frac{\hat{\lambda}\mu_{22}\psi}{k_0^3} V_0 + \frac{iP_0}{k_0}.\end{aligned} \tag{3.6}$$

Eliminating U_1 and W_1 between (3.4b), (3.5c) and (3.6) yields an equation for the leading pressure term P_0 of the form

$$\begin{aligned}P_0 = k_0\frac{d^3V_0}{d\psi^3} - k_0\frac{dV_0}{d\psi} + \left(\frac{i\hat{\lambda}\psi}{k_0^2\mu_{11}}\left(\mu_{11}\mu_{22} - \mu_{21}\mu_{12}\right) + \frac{\beta_1\mu_{11}}{k_0^2}\right) V_0 \\ + \frac{i\Omega_0}{k_0}\frac{dV_0}{d\psi} - \frac{\beta_1\mu_{11}\psi}{k_0^2}\frac{dV_0}{d\psi} - \frac{i\hat{\lambda}}{k_0^2\mu_{11}}\left(\mu_{11}\mu_{22} - \mu_{21}\mu_{12}\right)\psi^2\frac{dV_0}{d\psi}.\end{aligned} \tag{3.7a}$$

Finally, leading order terms in the remaining momentum equation (2.3c) give that

$$\frac{dP_0}{d\psi} = k_0\left[\frac{d^2}{d\psi^2} - 1 + \frac{i\Omega_0}{k_0^2} - \frac{\beta_1\mu_{11}\psi}{k_0^3} - \frac{i\hat{\lambda}}{2k_0^3\mu_{11}}\left(\mu_{11}\mu_{22} - \mu_{21}\mu_{12}\right)\psi^2\right]V_0 - \frac{\chi\mu_{11}\psi}{k_0^2}U_0, \tag{3.7b}$$

so that on eliminating P_0 between $(3.7a, b)$ and simplifying we obtain

$$\begin{aligned}\left[\frac{d^2}{d\psi^2} - 1 + \frac{i\Omega_0}{k_0^2} - \frac{\beta_1\mu_{11}\psi}{k_0^3} - \frac{i\hat{\lambda}}{2k_0^3\mu_{11}}\left(\mu_{11}\mu_{22} - \mu_{21}\mu_{12}\right)\psi^2\right]\left(\frac{d^2}{d\psi^2} - 1\right)V_0 \\ + \frac{i\hat{\lambda}}{k_0^3\mu_{11}}\left(\mu_{11}\mu_{22} - \mu_{21}\mu_{12}\right)V_0 = -\frac{\chi\mu_{11}\psi}{k_0^3}U_0.\end{aligned} \tag{3.8}$$

It is of interest here to note that if we had chosen the crossflow to have been of the more obviously significant size $O(G^{\frac{2}{6}})$ then the quadratic terms in ψ in the above equations would be replaced by linear ones. Then β_1 can be redefined to remove these terms so that such a weak crossflow does not have a significant efect on the viscous modes. To summarise thus far, the leading order vortex quantities U_0, V_0 satisfy the sixth order system $(3.5b)$, (3.8). To simplify this pair we introduce the parameters $\bar{k}$, $\bar{\beta}$, $\bar{U}$ and $\bar{V}$ defined by

$$k_0 = \left(\chi\mu_{11}^2\right)^{\frac{1}{6}}\bar{k}, \quad \beta_1 = \chi^{\frac{3}{6}}\mu_{11}^{\frac{1}{6}}\bar{\beta}, \quad U_0 = \mu_{11}\bar{U} \quad \text{and} \quad V_0 = \chi^{\frac{2}{6}}\mu_{11}^{\frac{4}{6}}\bar{V}. \tag{3.9a-d}$$

Further, if we write

$$\Omega_0 = \chi^{\frac{2}{6}}\mu_{11}^{\frac{4}{6}}\bar{\Omega} \qquad \text{and} \qquad \bar{\lambda} = \frac{\hat{\lambda}\left(\mu_{11}\mu_{22} - \mu_{12}\mu_{21}\right)}{2\mu_{11}^{\frac{11}{6}}\chi^{\frac{3}{6}}}, \tag{3.9e, f}$$

and substitute (3.9) in $(3.5b)$ and (3.8), we obtain our final equations to determine $\bar{U}$ and $\bar{V}$, i.e.

$$\left(\frac{d^2}{d\psi^2} - 1 + \frac{i\bar{\Omega}}{\bar{k}^2} - \frac{\bar{\beta}\psi}{\bar{k}^3} - \frac{i\bar{\lambda}\psi^2}{\bar{k}^3}\right)\left(\frac{d^2}{d\psi^2} - 1\right)\bar{V} + \frac{2i\bar{\lambda}}{\bar{k}^3}\bar{V} = -\frac{\psi\bar{U}}{\bar{k}^3}, \tag{3.10a}$$

$$\left(\frac{d^2}{d\psi^2} - 1 + \frac{i\bar{\Omega}}{\bar{k}^2} - \frac{\bar{\beta}\psi}{\bar{k}^3} - \frac{i\bar{\lambda}\psi^2}{\bar{k}^3}\right)\bar{U} = \frac{\bar{V}}{\bar{k}^2}. \tag{3.10b}$$

We need to impose suitable boundary conditions on the solutions of (3.10). First, in order to ensure that the disturbance is confined to the thin $O(G^{-\frac{1}{6}})$ zone close to the wall we demand that the perturbation quantities decay exponentially as $\psi \longrightarrow \infty$. Additionally, to satisfy the requirement of zero disturbance velocities on the wall $\psi = 0$, $\bar{U} = \bar{V} = 0$

on $\psi = 0$ and the continuity equation (3.4b) further implies that $d\bar{V}/d\psi = 0$ on $\psi = 0$. Hence, in all, our six boundary conditions are

$$\bar{U} = \bar{V} = \frac{d\bar{V}}{d\psi} = 0, \qquad \text{at} \quad \psi = 0, \tag{3.11a}$$

$$\bar{U} = \bar{V} = \frac{d\bar{V}}{d\psi} \longrightarrow 0 \qquad \text{as} \quad \psi \longrightarrow \infty. \tag{3.11b}$$

Now (3.10) and (3.11) constitute an eigenproblem to be solved for the scaled vortex frequency $\bar{\Omega}$, scaled spatial growth rate $\bar{\beta}$ and scaled crossflow $\bar{\lambda}$. We note that once the eigenfunctions $\bar{U}$, $\bar{V}$ are determined we can retrieve the spanwise velocity component of the vortex by applying (3.4a) and (3.9).

The equations solved by DHS are precisely (3.10) with $\bar{\Omega} = \bar{\lambda} = 0$. They demonstrated that for all $\bar{k}$ we then have $\bar{\beta} > 0$ so that the corresponding vortex flow is unstable. Further, as $\bar{k} \longrightarrow 0$, $\bar{\beta} \sim \bar{k}^{\frac{1}{2}}$ and as $\bar{k} \longrightarrow \infty$, $\bar{\beta} \sim \bar{k}^{-2}$. The behaviour as $\bar{k} \longrightarrow 0$ matches with (2.5c) which determines the growth rate of O(1) wavenumber vortices in two-dimensional flow. Since $\bar{\beta} \longrightarrow 0$ as both $\bar{k} \longrightarrow 0$ and as $\bar{k} \longrightarrow \infty$ there is a most unstable vortex at some intermediate value of $\bar{k}$ which DHS calculated to be $\bar{k} = 0.476$ with corresponding $\bar{\beta} = 0.312$. The dependence of $\bar{\beta}$ upon $\bar{k}$ as found by DHS is illustrated in Figure (3.1). Our interest is with non-zero $\bar{\Omega}$ and $\bar{\lambda}$, but before we consider any specific calculations we make one observation concerning (3.10). We see that if $(\bar{\Omega}, \bar{\beta}, \bar{\lambda})$ is an eigenvalue set of (3.10) & (3.11) then so is $(-\bar{\Omega}^*, \bar{\beta}^*, -\bar{\lambda})$ for real crossflows $\bar{\lambda}$ and where an asterisk denotes complex conjugate. Evidently we can therefore restrict our attention to postive crossflow parameters and do so for the remainder of the paper. As a first detailed examination of (3.10), (3.11) we will study the effect of introducing the crossflow $\bar{\lambda}$ whilst maintaining a zero frequency $\bar{\Omega}$— this case is treated in the forthcoming section.

§4. Solution of (3.10) for the zero frequency case.

We first consider the solution of governing equations (3.10) with associated boundary conditions (3.11) for the steady vortex problem ($\bar{\Omega} = 0$). Naturally, this problem had to be tackled numerically and the solution technique used in practice was based on a method

suggested by Malik, Chuang & Hussaini (1982). In the zero frequency work described in this section we solved

$$\left(\frac{d^2}{d\psi^2} - 1 - \frac{\bar{\beta}\psi}{\bar{k}^3} - \frac{i\bar{\lambda}\psi^2}{\bar{k}^3}\right)\left(\frac{d^2}{d\psi^2} - 1\right)\bar{V} + \frac{2i\bar{\lambda}}{\bar{k}^3}\bar{V} = -\frac{\psi\bar{U}}{\bar{k}^3}, \tag{4.1a}$$

$$\left(\frac{d^2}{d\psi^2} - 1 - \frac{\bar{\beta}\psi}{\bar{k}^3} - \frac{i\bar{\lambda}\psi^2}{\bar{k}^3}\right)\bar{U} = \frac{\bar{V}}{\bar{k}^2}, \tag{4.1b}$$

by prescribing values for the real scaled wavenumber $\bar{k}$ and the crossflow $\bar{\lambda}$. Then (4.1) with its associated boundary conditions (3.11) were solved for the complex-valued spatial growth rate $\bar{\beta}$. Recalling the definitions (3.2a), (3.9b) we can see that when $Re(\bar{\beta}) > 0$ the vortex is unstable and, conversely, for $Re(\bar{\beta}) < 0$ the disturbance is stable. As remarked already we can, without loss of generality, restrict ourselves to considering $\bar{\lambda} > 0$.

Malik *et. al.* (1982) described a boundary value method for solving eigenvalue problems. In these methods the differential equations to be solved are reduced to a set of linear algebraic equations using either a finite difference discretisation or a spectral representation and the eigenvalues are found by solving the characteristic determinant of a generalised eigenvalue problem. The particular method devised by Malik *et. al.* uses a fourth order accurate (Euler–Maclaurin) finite difference scheme with nodal points distributed so as to resolve any singular layers. These authors used their scheme to examine the temporal and spatial stability of a three-dimensional compressible boundary layer flow over a swept wing. For further detials of this numerical method the reader is referred to Malik *et. al.* (1982).

To implement the solution procedure for (4.1) we decided to perform a sequence of runs with a gradually increasing crossflow $\bar{\lambda}$ and a fixed wavenumber $\bar{k} = \frac{1}{2}$. This choice of $\bar{k}$ is not significant, and we duly performed further tests at other values of $\bar{k}$ in order to ensure that the results were qualitively similar to those we describe here. For zero crossflow we were, of course, just repeating the calculation of DHS presented in Figure (3.1) for which $\bar{\beta}$ is real and the vortex is unstable for all $\bar{k} > 0$. For non-zero crossflows the spatial dependence parameter $\bar{\beta}$ becomes truly complex and some solutions of (4.1) are shown in Figure (4.1). Here we have fixed $\bar{k} = \frac{1}{2}$ and we observe that as $\bar{\lambda}$ increases $Re(\bar{\beta})$ decreases so that the vortex becomes progressively stabilised. When $\bar{\lambda} = 0$, $\bar{\beta} = 0.313$ (from DHS) and $Re(\bar{\beta})$ vanishes when $\bar{\lambda} \approx 0.406$, at which point $Im(\bar{\beta}) \approx -0.91$ (see Figure (4.1b)). As the crossflow increases yet further $Re(\bar{\beta})$ becomes negative and hence we have the situation of a stable vortex flow. The form of behaviour of $\bar{\beta}$ when $\bar{k} = \frac{1}{2}$ is

typical of that for other wavenumbers and so we may conclude, at least for these stationary vortices, that the effect of increasing the crossflow is to stabilise the flow.

We then extended our computations by fixing the crossflow parameter $\bar{\lambda}$ and solving (4.1) for a selection of wavenumbers $\bar{k}$. The results obtained are illustrated in representative Figures (4.2a,b). Here we plot the dependence of $Re(\bar{\beta})$ upon $\bar{k}$. In Figure (4.2a) we have fixed $\bar{\lambda} = 0.414$, i.e. a little larger than the value at which the vortex of wavenumber $\bar{k} = 0.5$ becomes neutrally stable. It is clearly seen that although $Re(\bar{\beta}) < 0$ for $\bar{k} = 0.5$, there is a range of wavenumbers, approximately $0.37 < \bar{k} < 0.44$, over which $Re(\bar{\beta})$ is still positive. Consequently, at this crossflow value there remains an interval of wavelengths for which the stationary vortex is unstable. However, from Figure (4.2b) it is plain that when $\bar{\lambda}$ is increased further (here $\bar{\lambda} = 0.434$) we have $Re(\bar{\beta}) < 0$ for all wavenumbers and hence when the crossflow becomes this large the flow is completely stabilised. More detailed calculations showed that this occurs whenever the crossflow is greater than approximately 0.416.

There are two natural asymptotic regimes to investigate within the context of the present problem. The first deals with the large wavenumber limit $\bar{k} \longrightarrow \infty$. We do not address this limit here because it also arises when making large wavenumber studies of the temporal problem dealt with in section 5. Consequently, we shall focus our attention on $\bar{k} \longrightarrow \infty$ there. Second is the case of small scaled wavenumber $\bar{k} \longrightarrow 0$. We can develop a formal asymptotic solution of (4.1), (3.11) in this limit but rather than concentrate on small wavenumbers for stationary vortices alone we shall consider a slightly wider class of flows and shall investigate small wavelength vortices with small frequencies. Of course we can recover the asymptotic solution for stationary vortices without formal difficulty but also, much more importantly, considering small wavenumber vortices of the type just described will allow us to tie this analysis in with results for the temporal case in section 5.

§4.1 *Solutions of (3.10) for* $\bar{k} \ll 1$.

Guided by the eigensolutions of the problem (4.1) for small $\bar{k}$ it is found that for $\bar{k} \ll 1$, $\bar{\Omega} = O(\bar{k}^{\frac{4}{7}})$ the solution vortex of (3.10) is neutrally stable for a scaled crossflow of size $O(\bar{k}^{\frac{1}{7}})$. To demonstrate this we suppose that

$$\bar{\Omega} = \hat{\Omega}\bar{k}^{\frac{4}{7}} + \ldots, \qquad \bar{\lambda} = C\bar{k}^{\frac{1}{7}} + \ldots, \qquad \bar{\beta} = iD\bar{k}^{\frac{6}{7}} + \ldots. \tag{4.2}$$

Here we have assumed that $\bar{\beta}$ is purely imaginary so that D is real and with the scalings as in (4.2) the solution structure divides into a number of distinct regions. For the moment we take $\hat{\Omega} > 0$ as we will subsequently find that a modified asymptotic structure is required for the case $\hat{\Omega} \leq 0$.

Close to $\psi = 0$ we write

$$\psi = \bar{k}^{\frac{5}{7}}\theta, \qquad \bar{V} = V_0 + \ldots, \qquad \bar{U} = \bar{k}^{-\frac{4}{7}}U_0 + \ldots. \tag{4.3}$$

Substitution of (4.2) & (4.3) into governing equations (3.10) shows that

$$\left(\frac{d^2}{d\theta^2} - i\hat{\Omega} - iD\theta - iC\theta^2\right)\frac{d^2V_0}{d\theta^2} + 2iCV_0 = -\theta U_0, \tag{4.4a}$$

$$\left(\frac{d^2}{d\theta^2} - i\hat{\Omega} - iD\theta - iC\theta^2\right)U_0 = V_0. \tag{4.4b}$$

We expect the disturbance to be largely confined within this $O(\bar{k}^{\frac{5}{7}})$ layer and so we demand that as $\theta \longrightarrow \infty$ the solution decays. Inspection of (4.4) then imposes the conditions

$$V_0 \propto \frac{1}{\theta} + \ldots, \qquad U_0 \propto \frac{1}{\theta^3} + \ldots \qquad \text{as} \quad \theta \longrightarrow \infty. \tag{4.5a}$$

Additionally, boundary conditions (3.11a) demand that

$$U_0 = V_0 = \frac{dV_0}{d\theta} = 0 \qquad \text{at} \quad \theta = 0. \tag{4.5b}$$

Now (4.4), (4.5) together form an eigenvalue problem for the O(1) real constants C and D. Before considering this further, we need to check that the disturbance decays correctly so as to ensure that the boundary conditions (3.11b) applicable as $\psi \longrightarrow \infty$ are indeed met.

Inspection of (3.10) subject to the scalings (4.2) suggests that when $\psi = O(1)$ the velocity components of the vortex behave according to

$$\bar{U} = \bar{k}^{\frac{11}{7}}\hat{U} + \ldots, \qquad \bar{V} = \bar{k}^{\frac{8}{7}}\hat{V} + \ldots, \tag{4.6}$$

using (4.3) and (4.5a). Substitution of (4.6) into (3.10a) yields the equations

$$-\psi^2\left(\frac{d^2}{d\psi^2} - 1\right)\hat{V} + 2\hat{V} = 0, \tag{4.7a}$$

and

$$-iC\psi^2\hat{U} = \hat{V}. \tag{4.7b}$$

To match with (4.5a) requires $\hat{V} \propto \frac{1}{\psi}$ as $\psi \longrightarrow 0$ and the solution of (4.7a) with this property is

$$\hat{V} = \bar{E}\psi^{\frac{1}{2}} K_{\frac{3}{2}}(\psi), \tag{4.8}$$

where $\bar{E}$ is some constant and $K_\nu(\psi)$ is the modified Bessel function of order ν. Solution (4.8) has the required exponential decay as $\psi \longrightarrow \infty$ and so, therefore, $\hat{U}$ also decays exponentially (see (4.7b)). Hence we have obtained the complete asymptotic description of the solutions of (3.10) & (3.11) for neutral modes when $\bar{k} \ll 1$, $\bar{\Omega} = O(\bar{k}^{\frac{4}{7}})$, $\bar{\Omega} > 0$.

Technically, to complete our description of this limit the solution of (4.4), (4.5) is desired for various values of $\hat{\Omega}$. We have not done this here for this aspect is not within our principal objectives. The asymptotic work above demonstrates that for $\bar{k} \ll 1$ only a small scaled crossflow, $O(\bar{k}^{\frac{1}{7}})$ is required to completely stabilise a vortex of positive frequency $O(\bar{k}^{\frac{4}{7}})$. This is an exceptionally tiny frequency and so in practice the scaled frequency parameter $\hat{\Omega}$ defined in (4.2) is likely to be large. It can be shown (and details are available from the authors) that for $\hat{\Omega} \gg 1$ we have $C = O(\hat{\Omega}^{\frac{1}{6}})$ and $D = O(\hat{\Omega}^{\frac{5}{6}})$ and this information matches with further asymptotic limits to be discussed in the following section.

The above describes the asymptotic solution of *(3.10) & (3.11) for $\bar{k} \ll 1$ and $\bar{\Omega}$ small* but positive. We can show however that for $\bar{\Omega}$ negative a completely different structure must come into play, and in order to illustrate this revised case we will work with stationary vortices ($\bar{\Omega}$=0) although our analysis may be easily modified to account for $|\bar{\Omega}| \ll 1$, $\bar{\Omega} < 0$. In the stationary case we need to solve (4.1) for $\bar{k} \ll 1$. We write

$$\begin{aligned} \bar{\beta} &= i\bar{k}^{\frac{1}{2}}\hat{\beta} + \ldots, & \bar{\lambda} &= \bar{k}^{\frac{1}{2}}\hat{\lambda} + \ldots, \\ \bar{V} &= \bar{V}_0 + \ldots, & \bar{U} &= \bar{k}^{\frac{1}{2}}\bar{U}_0 + \ldots, \end{aligned} \tag{4.9}$$

in the region where $\psi = O(1)$. Substituting these expansions in (4.1) yields

$$-i\left(\hat{\beta}\psi + \hat{\lambda}\psi^2\right)\left(\frac{d^2}{d\psi^2} - 1\right)\bar{V}_0 + 2i\hat{\lambda}\bar{V}_0 = -\psi\bar{U}_0, \tag{4.10a}$$

$$-i\left(\hat{\beta}\psi + \hat{\lambda}\psi^2\right)\bar{U}_0 = \bar{V}_0, \tag{4.10b}$$

so that

$$\left(\hat{\beta}\psi + \hat{\lambda}\psi^2\right)^2\left(\frac{d^2\bar{V}_0}{d\psi^2} - \bar{V}_0\right) - 2\hat{\lambda}\left(\hat{\beta}\psi + \hat{\lambda}\psi^2\right)\bar{V}_0 = \psi\bar{V}_0, \tag{4.10c}$$

which is an eigenproblem for the quantities $\hat{\beta}$ and $\hat{\lambda}$ when we impose the inviscid condition $\bar{V}_0 \longrightarrow 0$ as $\psi \longrightarrow 0$ and demand that $\bar{V}_0 \longrightarrow 0$ as $\psi \longrightarrow \infty$. For neutral modes we need $\hat{\beta}$ real and from the numerical work illustrated in Figures (4.1) & (4.2) we saw that for positive crossflows $\bar{\lambda}$ in (4.1) the neutrally stable vortices satisfying (4.1) typically had $Im(\hat{\beta}) < 0$. Consequently, in terms of (4.9) we anticipate that the eigenvalues $\hat{\beta}$, $\hat{\lambda}$ of (4.10c) are such that $\hat{\beta} < 0$, $\hat{\lambda} > 0$ and so (4.10c) has a critical layer structure surrounding $\psi = -\hat{\beta}/\hat{\lambda}$. Of course, the critical layer problem (4.10c) is closely related to (2.14b) (in fact it is just a scaled version of (2.14b)) which governs the large wavenumber inviscid modes studied in section 2. As discussed there, in order that a numerical solution on (4.10c) be possible a detailed analysis of the critical layer structure is required and which we will consider in a future article. However, the pertinent result from this critical layer problem is that it represents the description of how the neutrally stable vortex modes are affected as we pass from the parameter regime of section 2 to those considered in this section.

Although the above description is specific to stationary vortices it is easily generalised to account for disturbances of frequencies $\bar{\Omega} = O(\bar{k}^{\frac{1}{2}})$ and negative. The effect of the non-zero frequency is to introduce two extra constants into the critical layer equation (4.10c) but the overall properties of the problem are virtually unaffected. Again inclusion of these non-zero frequencies provides scope for further discussion of the critical layer problem.

To summarise thus far, we have shown that for small frequencies the effect of increasing crossflow in the fundamental equations (3.10) with boundary conditions (3.11) is to tend to stabilise the vortex flow. Interestingly, we have also demonstrated that for small non-dimensional wavenumbers the structure of the neutrally stable modes is dependent largely on the sign of the frequency of the modes. For frequencies $\bar{\Omega} > 0$ the vortex structure is dictated by the solution of eigenproblem (4.4) whereas for $\bar{\Omega} \leq 0$ we obtain a critical layer structure which matches with the large wavenumber inviscid modes described by (2.14). Having studied the low frequency problem we now move on to consider larger frequencies, indeed we examine the case for which the scaled frequency $\bar{\Omega} = O(1)$.

§5. The vortex problem (3.10) for O(1) frequencies.

Here we examine the properties of Görtler vortices of wavenumber $O(G^{\frac{1}{6}})$ and frequency $O(G^{\frac{2}{6}})$ in the presence of crossflow of size $O(G^{\frac{3}{6}})$. In this case, of course, the scaled parameters $\bar{\Omega}$, $\bar{\beta}$ and $\bar{\lambda}$ in (3.10) are all order one quantities. For the purpose of this section we will concentrate almost exclusively on neutrally stable states for the results of the previous sections have suggested how the stability of the flow will be altered by changing particular parameter values which give rise to neutral modes. To solve for neutral modes we again used the method described in section 4 subject to a few slight changes. We then specified the O(1) frequency $\bar{\Omega}$ and the wavenumber $\bar{k}$ in (3.10) and treated these coupled ordinary differential equations as an eigenproblem for the crossflow parameter $\bar{\lambda}$ and the spatial development quantity $\bar{\beta}$ which was supposed to be purely imaginary. In this way we ensured that the resulting eigenvalues corresponded to neutrally stable modes.

Some sample results are illustrated in Figures (5.1) – (5.3) where we show the dependence of the crossflow $\bar{\lambda}$ and the parameter $\bar{\beta}$ on the scaled wavenumber $\bar{k}$ for the three frequencies $\bar{\Omega} = 1, 0$ and -1. Briefly, we can see that neutral modes appear to be possible over the complete range of wavenumbers $\bar{k}$ and that for large $\bar{k}$ the crossflow needed to produce neutrally stable modes is quite small. However, a striking difference between the neutral modes is observed depending on whether $\bar{\Omega} > 0$ or $\bar{\Omega} \leq 0$. In the former case (see Figure (5.1a)), as $\bar{k} \longrightarrow 0$ $\bar{\lambda}$ tend to an O(1) value whereas in the latter case $\bar{\lambda} \longrightarrow 0$ as $\bar{k} \longrightarrow 0$ (Figures (5.2a, 5.3a)). A discussion of the asymptotic properties of these two cases is given later. We note here that on recalling the results of section 4 together with the zero crossflow calculation of DHS we can infer that for crossflows greater than the neutral mode values on Figures (5.1a – 5.3a) the corresponding vortex motions are stable whilst the opposite is true for lesser crossflows.

We can be confident that the results shown in Figures (5.1–5.3) are sufficient to demonstrate that increasing crossflow again stabilises these non-stationary vortex modes in a similar way as was described for the stationary case in section 4. As before, there exist several regimes in which asymptotic description of (3.10) & (3.11) is possible. We first concentrate on properties of this eigenproblem in the high wavenumber limit, $\bar{k} \gg 1$.

§5.1 *The high-wavenumber* ($\bar{k} \gg 1$) *limit*

In this limit we are concerned with obtaining an asymptotic solution of the system (3.10), (3.11) for $\bar{k} \gg 1$, $\bar{\Omega} = O(1)$. We can initially consider the problem in the context of neutrally stable modes in the spirit of the calculations just described. It has been seen that for low wavenumber modes the vortex structure appears to be critically dependent on the sign of the frequency $\bar{\Omega}$ but inspection of Figures (5.1–5.3) suggest that this is unlikely to be the case for high wavenumber modes and consequently there is no need to specify $\bar{\Omega}$ further than taking it to be of order unity. An idea of the expected structure can be gleaned by studying Figure (5.4). Here we present the eigenfunctions of (3.10) & (3.11) when this pair of equations is solved for neutral modes with $\bar{\Omega} = 0$ and $\bar{k} \approx 1.35$. Unfortunately, for values of $\bar{k}$ much larger than this value we found that it was difficult to obtain satisfactory numerical convergence but the evidence of Figure (5.4) and close inspection of the governing equations are sufficient in order to strongly suggest that the disturbance is confined to an O(1) thick region which moves away from $\psi = 0$ as $\bar{k} \longrightarrow \infty$. If we write

$$\psi = c\bar{k}^5 + \tilde{\psi}, \tag{5.1a}$$

$$\bar{\beta} = i\left(\beta_0 \bar{k}^3 + \beta_1 \bar{k}^{-2} + \ldots\right), \tag{5.1b}$$

and

$$\bar{\lambda} = \lambda_0 \bar{k}^{-2} + \lambda_1 \bar{k}^{-7} + \ldots, \tag{5.1c}$$

together with the eigenfunction expansions

$$\bar{U} = U_0 + \bar{k}^{-5} U_1 + \ldots, \qquad \bar{V} = \bar{k}^2 V_0 + \bar{k}^{-3} V_1 + \ldots, \tag{5.1d}$$

and substitute (5.1) into (3.10) we find the following. At leading orders we obtain

$$\beta_0 = -\lambda_0 c, \tag{5.2}$$

and, at next order,

$$\begin{aligned} \left[\frac{d^2}{d\tilde{\psi}^2} - 1 + i\beta_0\tilde{\psi} - i\left(\beta_1 c + \lambda_1 c^2\right)\right]\left[\frac{d^2}{d\tilde{\psi}^2} - 1\right] V_0 &= -cU_0, \\ \left[\frac{d^2}{d\tilde{\psi}^2} - 1 + i\beta_0\tilde{\psi} - i\left(\beta_1 c + \lambda_1 c^2\right)\right] U_0 &= V_0. \end{aligned} \tag{5.3}$$

By redefining $\hat{\psi} = \tilde{\psi} - ((\beta_1 c + \lambda_1 c^2)/\beta_0)$ we simplify these equations to

$$\left[\frac{d^2}{d\hat{\psi}^2} - 1 + i\beta_0\hat{\psi}\right]\left[\frac{d^2}{d\hat{\psi}^2} - 1\right] V_0 = -cU_0, \tag{5.4a}$$

$$\left[\frac{d^2}{d\hat{\psi}^2} - 1 + i\beta_0\hat{\psi}\right] U_0 = V_0, \tag{5.4b}$$

which need to be solved for real β_0 and c subject to the boundary conditions

$$U_0, \quad V_0, \quad \frac{dV_0}{d\hat{\psi}} \longrightarrow 0, \qquad \text{as} \quad \hat{\psi} \longrightarrow \pm\infty. \tag{5.5}$$

The precise solutions of (5.4) & (5.5) are relatively unimportant– the crucial conclusion we can draw from this asymptotic work is that for an O(1) frequency we only need a very small $O(\bar{k}^{-2})$ crossflow to stabilise modes with wavenumber $\bar{k} \gg 1$. In passing, we notice that the eigenproblem (5.4) may be used to deduce other results. In particular, we have the result that the description of the asymptotic problem $\bar{k} \longrightarrow \infty$ is independent of the order one value of $\bar{\Omega}$:– a result which is in keeping with the numerical evidence presented earlier. Indeed, the above is valid for all frequencies $\bar{\Omega} = o(\bar{k}^2)$ so that in particular it is valid for the high wavenumber limit of the zero frequency work examined in section 4.

We now make some comments about the low wavenumber limit, $\bar{k} \longrightarrow 0$.

§5.2 *The low wavenumber ($\bar{k} \ll 1$) limit for $\bar{\Omega} > 0$*

We have already observed that different eigenproperties of (3.10), (3.11) are expected for $\bar{k} \ll 1$ and that the sign of $\bar{\Omega}$ is crucial in determining these properties. Consequently, here we take $\bar{\Omega} > 0$ and examine the case $\bar{\Omega} < 0$ later (the zero frequency case has already been dealt with). When $\bar{\Omega} > 0$, $\bar{k} \ll 1$ the eigenfunctions of (3.10) are concentrated in a thin region near $\psi = 0$, see Figure (5.5). In this figure we illustrate the eigenfunctions $\bar{U}$, $\bar{V}$ for the case $\bar{\Omega} = 1$, $\bar{k} = 1.3 \times 10^{-2}$. This suggests seeking a multi-zoned asymptotic solution structure of (3.10) for $\bar{k} \ll 1$, $\bar{\Omega} = O(1)$, and we now show how this may be achieved. Initially, we suppose that the crossflow $\bar{\lambda}$ and spatial dependence $\bar{\beta}$ assume the forms

$$\bar{\lambda} = \lambda_0 + \lambda_1 \bar{k}^{\frac{1}{4}} + \lambda_2 \bar{k}^{\frac{1}{2}} + \ldots, \tag{5.6a}$$

$$\bar{\beta} = i\left[\beta_0 \bar{k}^{\frac{1}{2}} + \beta_1 \bar{k}^{\frac{3}{4}} + \beta_2 \bar{k} + \ldots\right], \tag{5.6b}$$

and we recall that we are seeking neutral disturbances so that the O(1) constants $\lambda_0, \lambda_1, \ldots$, $\beta_0, \beta_1, \ldots$ are real. After experimentation, we can infer that the disturbance is largely trapped in an $O(\bar{k}^{\frac{3}{4}})$ thick region which is located at a distance $O(\bar{k}^{\frac{1}{2}})$ from $\psi = 0$. Guided by this, when

$$\psi = \bar{k}^{\frac{1}{2}}\psi_0 + \bar{k}^{\frac{3}{4}}\tilde{\psi}, \tag{5.7a}$$

say, with $\psi_0 = O(1)$, we need to expand

$$\bar{U} = U_0\bar{k}^{-\frac{1}{2}} + U_1\bar{k}^{-\frac{1}{4}} + U_2 + \ldots, \qquad \bar{V} = V_0 + V_1\bar{k}^{\frac{1}{4}} + V_2\bar{k}^{\frac{1}{2}} + \ldots. \tag{5.7b}$$

Substituting (5.6), (5.7) in (3.10) yields that in this region (refer to it as zone I),

$$\bar{\Omega} + \beta_0\psi_0 + \lambda_0\psi_0^2 = 0, \tag{5.8a}$$

$$\beta_0 + 2\psi_0\lambda_0 = \beta_1\psi_0 + \lambda_1\psi_0^2 = 0. \tag{5.8b,c}$$

If we define $\hat{\bar{\Omega}} = \beta_2\psi_0 + \lambda_2\psi_0^2 - (\beta_1^2/4\lambda_0)$ and write

$$\tilde{\psi} = \frac{\beta_1}{2\lambda_0} + \hat{\tilde{\psi}},$$

we deduce that within zone I the leading order disturbance quantities U_0, V_0 satisfy

$$\left[\frac{d^2}{d\hat{\tilde{\psi}}^2} - i\hat{\bar{\Omega}} - i\lambda_0\hat{\tilde{\psi}}^2\right]\frac{d^2V_0}{d\hat{\tilde{\psi}}^2} + 2i\lambda_0V_0 = -\psi_0U_0, \tag{5.9a}$$

$$\left[\frac{d^2}{d\hat{\tilde{\psi}}^2} - i\hat{\bar{\Omega}} - i\lambda_0\hat{\tilde{\psi}}^2\right]U_0 = V_0. \tag{5.9b}$$

For the disturbance to be effectively confined to zone I we require the solutions to decay as $\hat{\tilde{\psi}} \longrightarrow \pm\infty$. We can show that the potentially most dangerous mode is even in $\hat{\tilde{\psi}}$, and in addition it is easy to prove that

$$V_0 \propto \frac{1}{\hat{\tilde{\psi}}}, \qquad U_0 \propto \frac{i}{\lambda_0\hat{\tilde{\psi}}^3}, \qquad \text{as} \quad |\hat{\tilde{\psi}}| \longrightarrow \infty. \tag{5.10}$$

In the course of his investigation into Görtler vortices at $O(G^{\frac{1}{4}})$ wavenumbers in three-dimensional boundary layers, Hall (1985) considered the eigenproblem (5.9), (5.10). He found that the relevant eigenvalues are

$$\frac{\psi_0}{\lambda_0^{\frac{1}{2}}} = 4.71 \qquad \text{and} \qquad \frac{\hat{\bar{\Omega}}}{\lambda_0^{\frac{1}{2}}} = -3.59. \tag{5.11a,b}$$

Even though we now have enough information to determine λ_0 and β_0 via (5.8a,b) and (5.11a), we must check that this zone I solution obtained above can be satisfactorily matched to the requisite boundary conditions (3.11). Since zone I is fixed at a distance $O(\bar{k}^{\frac{1}{2}})$ from the wall $\psi = 0$ it is natural to define a second region, zone II, by

$$\psi = \bar{k}^{\frac{1}{2}}\theta. \tag{5.12}$$

By (5.7b) and (5.10), within II the eigenfunctions must expand according to

$$\bar{V} = v_0\bar{k}^{\frac{1}{4}} + \ldots, \qquad \bar{U} = u_0\bar{k}^{\frac{1}{4}} + \ldots. \tag{5.13}$$

Substitution of (5.6), (5.12) & (5.13) into the governing equations (3.10) yields, on application of the results (5.8), that

$$(\theta - \psi_0)^2 \frac{d^2v_0}{d\theta^2} - 2v_0 = 0, \tag{5.14a}$$

and

$$i\lambda_0(\theta - \psi_0)^2 u_0 = -v_0. \tag{5.14b}$$

Strictly, of course, we need to consider the regions $\theta < \psi_0$ and $\theta > \psi_0$ separately, and we shall concentrate on the former first.

The region $\theta < \psi_0$

We first recall that the boundary conditions (3.11a) need to be satisfied at $\theta = 0$ and, guided by result (5.10), we solve (5.14a) subject to the conditions $v_0 \longrightarrow \frac{1}{\theta} + \ldots$ as $\theta \longrightarrow \psi_0$, $v_0 = 0$ at $\theta = 0$. This yields

$$v_0 = \frac{\psi_0^3 - (\psi_0 - \theta)^3}{\psi_0^3(\psi_0 - \theta)}, \tag{5.15a}$$

and, by (5.14b),

$$u_0 = \frac{i\left[\psi_0^3 - (\psi_0 - \theta)^3\right]}{\lambda_0\psi_0^3(\psi_0 - \theta)^3}. \tag{5.15b}$$

We see that (5.15) satisfies only two of $u_0 = v_0 = \frac{dv_0}{d\theta} = 0$ at $\theta = 0$ and to force the third condition to be met we now add a viscous layer, zone III, at $\theta = 0$. If in this layer we define the O(1) co-ordinate

$$\phi = \bar{k}\xi, \tag{5.16}$$

and the expansions

$$\bar{U} = \hat{u}_0 \bar{k}^{\frac{3}{4}} + \ldots, \qquad \bar{V} = \hat{v}_0 \bar{k}^{\frac{3}{4}} + \ldots, \tag{5.17}$$

then to satisfy (3.11a) and to match with (5.15) we require

$$\hat{u}_0 = \hat{v}_0 = \frac{d\hat{v}_0}{d\xi} = 0 \qquad \text{at} \quad \xi = 0 \tag{5.18a}$$

and

$$\hat{u}_0 \longrightarrow \frac{3i}{\bar{\Omega}\psi_0^2}\xi + \ldots, \qquad \hat{v}_0 \longrightarrow \frac{3\xi}{\psi_0^2} + \ldots, \qquad \text{as} \quad \xi \longrightarrow \infty. \tag{5.18b}$$

Substituting (5.16), (5.17) into (3.10) yields

$$\left(\frac{d^2}{d\xi^2} - i\bar{\Omega}\right)\frac{d^2\hat{v}_0}{d\xi^2} = 0, \qquad \left(\frac{d^2}{d\xi^2} - i\bar{\Omega}\right)\hat{u}_0 = \hat{v}_0. \tag{5.19}$$

The solutions of (5.19) satisfying (5.18) are

$$\hat{v}_0 = \frac{3(1-i)}{\psi_0^2\sqrt{2\bar{\Omega}}}\left[\exp\left(-(1+i)\xi\sqrt{\frac{\bar{\Omega}}{2}}\right) - 1\right] + \frac{3\xi}{\psi_0^2},$$

and

$$\hat{u}_0 = \left[\hat{H} - \frac{3(1-i)}{2m\psi_0^2\sqrt{2\bar{\Omega}}}\xi\right]\exp\left(-(1+i)\xi\sqrt{\frac{\bar{\Omega}}{2}}\right) + \frac{3i(1-i)}{\psi_0^2\bar{\Omega}\sqrt{2\bar{\Omega}}} + \frac{3i\xi}{\bar{\Omega}\psi_0^2},$$

where $m^2 = i\bar{\Omega}$ and $\hat{H}$ is chosen so that $\hat{u}_0(0) = 0$. In this way we have shown that the solution proposed so far satisfies the required conditions at $\psi = 0$. We now need to reconsider the $O(\bar{k}^{\frac{1}{2}})$ zone, zone II, where $\psi = \bar{k}^{\frac{1}{2}}\theta$ and $\theta > \psi_0$. Here expansions (5.13) and equations (5.14) again apply but this time we need to solve (5.14) so that $v_0 \longrightarrow \frac{1}{\theta} + \ldots$ as $\theta \longrightarrow \psi_0$ and $v_0 \longrightarrow 0$ as $\theta \longrightarrow \infty$. The required solution is simply

$$v_0 = \frac{1}{(\theta - \psi_0)}, \tag{5.20a}$$

and then

$$u_0 = \frac{i}{\lambda_0(\theta - \psi_0)^3}. \tag{5.20b}$$

To complete the structure we are led to consider a fourth zone, IV, where $v = O(1)$ and from (5.20) this means that the eigenfunctions have behaviours of the forms

$$\bar{V} = \hat{v}_0 \bar{k}^{\frac{3}{4}} + \ldots, \qquad \bar{U} = \hat{u}_0 \bar{k}^{\frac{7}{4}} + \ldots. \tag{5.21}$$

To match with (5.20) requires $\hat{v}_0 \longrightarrow \frac{1}{\psi} + \ldots$ and $\hat{u}_0 \longrightarrow \frac{i}{\lambda_0 \psi^3} + \ldots$ as $\psi \longrightarrow 0$. Substitution into (3.10) finally gives that

$$\psi^2 \frac{d^2 \hat{v}_0}{d\psi^2} - (2 + \psi^2)\hat{v}_0 = 0, \tag{5.22a}$$

$$\hat{u}_0 = \frac{i\hat{v}_0}{\lambda_0 \psi^2}. \tag{5.22b}$$

The solution of (5.22a) with the required algebraic growth as $\psi \longrightarrow 0$ together with exponential decay as $\psi \longrightarrow \infty$ is

$$\hat{v}_0 \propto \psi^{\frac{1}{2}} K_{\frac{3}{2}}(\psi), \tag{5.23}$$

where $K_\nu(\psi)$ is the modified Bessel function of order ν. Clearly, $\hat{u}_0$ also has exponential decay as $\psi \longrightarrow \infty$ and so we have a complete asymptotic solution of (3.10), (3.11) for $\bar{\Omega}$ =O(1), $\bar{k} \ll 1$ and $\bar{\beta}$ imaginary. The full four zoned structure of this solution is summarised in Figure (5.6). Returning to (5.8a,b) and (5.11) yields that

$$\lambda_0 \approx 0.46\bar{\Omega}^{\frac{1}{6}}, \qquad \psi_0 \approx 1.47\bar{\Omega}^{\frac{3}{6}} \qquad \text{and} \quad \beta_0 \approx -1.36\bar{\Omega}^{\frac{5}{6}}. \tag{5.24}$$

Hence we conclude that for small wavenumber vortices, a crossflow of approximately $0.46\bar{\Omega}^{\frac{1}{6}} + \ldots$ is required to stabilise the flow. We note also that as $\bar{\Omega} \longrightarrow 0$ in (5.24) our predictions match with the solution of the $\bar{k} \ll 1$, $\bar{\Omega} = O(\bar{k}^{\frac{4}{7}})$ problem described in section 4.1. Having now obtained the solution structure for $\bar{k} \ll 1$, $\bar{\Omega} > 0$ we turn now to consider the second case, $\bar{\Omega} < 0$.

§5.3 *The low wavenumber ($\bar{k} \ll 1$) limit for $\bar{\Omega} < 0$*

Having deduced the difference in behaviours of solution properties of (3.10), (3.11) when $\bar{k} \ll 1$ depending on the sign of $\bar{\Omega}$ we now study the case $\bar{\Omega} < 0$. From Figure (5.2) we conclude that the most fundamental difference between the two cases is that for $\bar{\Omega} < 0$ both $\bar{\beta}$ and $\bar{\lambda}$ tend to zero as $\bar{k} \longrightarrow 0$ in order that neutrally stable modes may be obtained. In order to study the structure here we show the eigenfunctions of the problem (3.10) when $\bar{\Omega} = -1$ and $\bar{k} = 8.7 \times 10^{-3}$, see Figure (5.7). Clearly the eigenfunctions are confined to a thin region centred away from the wall $\psi = 0$ and suggests that some critical layer type structure is operational. This is in agreement with the low frequency

work of the previous section where we proved that when $\bar{\Omega}$ is negative a similar critical layer approach is required, see equations (4.10).

To describe the detailed structure we suppose that across the majority of the flow, where $c = O(1)$, we write

$$V = V_0 + \ldots \qquad U = \bar{k}^{\frac{1}{3}} U_0 + \ldots \tag{5.25a}$$

and suppose that the streamwise dependence parameter $\bar{\beta}$ and scaled crossflow $\bar{\lambda}$ take the forms

$$\bar{\beta} = i\left(\beta_0 \bar{k}^{\frac{1}{3}} + \ldots\right) \qquad \text{and} \qquad \bar{\lambda} = \left(\lambda_0 \bar{k}^{\frac{1}{3}} + \ldots\right). \tag{5.25b}$$

Substitution in (3.10) yields that V_0 satisfies

$$\left(\beta_0 c - \lambda_0 c^2\right)^2 \left(\frac{d^2 V_0}{dc^2} - V_0\right) - 2\lambda_0 \left(\beta_0 c + \lambda_0 c^2\right) V_0 = c V_0. \tag{5.26}$$

This equation, which is identical to (4.10c), needs to be solved subject to $V_0 = 0$ at $c = 0$ and $V_0 \longrightarrow 0$ as $c \longrightarrow \infty$. As before, there is a critical layer structure at $c = -\beta_0/\lambda_0$ which needs further study before a full numerical solution of (5.26) can be effected. However, we can draw the general conclusion that for $\bar{\Omega} < 0$ the crossflow needed to maintain neutrally stable vortices vanishes as $\bar{k} \longrightarrow 0$.

In addition to the work on neutral modes described here we have performed a few calculations for non neutral modes. In Figure (5.8) we show the effect of crossflow on the stability of the vortices. We considered the two frequencies $\bar{\Omega} = -1.1$ and took the crossflow parameter $\lambda = .1, .2, .3, .4$ and, for various wavenumbers $\bar{k}$, solved (3.10), (3.11) for the complex valued $\bar{\beta}$. Figure (5.8) shows the growth rate curves for vortices with the above crossflow parameters . We can see (as has already been commented upon) that for a fixed wavelength vortex an increasing crossflow progressively stabilises the flow. Furthermore we see that instability occurs only for a finite range of values of the wavenumber; and we note that the width of this unstable band decreases as the crossflow increases. We also note that the flow is more unstable when the imposed frequency is positive. We now conclude with some further observations and some discussion.

§6. Conclusions.

In the previous sections we have described the process by which the Görtler vortex instability mechanism is destroyed by the introduction of a weak crossflow into a centrifugally unstable basic state. We choose to concentrate on the situation when the crossflow is of size $Re^{-\frac{1}{2}}$ because that is the crucial size at which the crossflow first has a significant effect on Görtler vortices. In addition we elect to concentrate on the large Görtler number limit because that limit describes inviscid Görtler vortices and nonparallel effects can be accounted for using asymptotic means. We found that at order one wavenumbers the introduction of a crossflow causes the growth rate–wavenumber curve of inviscid theory to split into two distinct parts. Thus above a critical size of the crossflow a finite band of unstable modes exists to the right of $a = 0$. This band of modes takes on the asymptotic structure of crossflow vortices when the crossflow is increased further. The growth rates of these modes increases monotonically with the crossflow parameter and will become formally of order $Re^{\frac{1}{2}}$ when the crossflow is comparable to the streamwise basic velocity field. The second branch of unstable modes occurs at progressively higher wavenumbers as the crossflow increases. The growth rates of these modes at any fixed value of the crossflow increases like $a^{\frac{1}{2}}$ for large a so it would appear at first sight that, at a fixed value of the crossflow, the viscous modes have the highest growth rates. However this is not the case since viscous effects, as in DHS, serve so as to stop this monotonic growth of β with a. In the absence of any crossflow the growth rate peaks at wavenumber of size $G^{\frac{1}{6}}$ and has a maximum of order $G^{\frac{3}{6}}$. At higher values of a the growth rate tends to zero and the right hand branch neutral structure of Hall (1982a) is retrieved. In the presence of a crossflow we showed that the second, semi-infinite band of unstable modes predicted on inviscid grounds becomes reduced to a finite band at high wavenumbers when the crossflow is formally of order $G^{\frac{3}{6}}$. At this stage the growth rates of the crossflow vortices associated with the modes to the right of $a = 0$ have growth rates of size $G^{\frac{3}{6}}$ comparable with those of the viscous modes. However as the crossflow is increased further the growth rates of the crossflow vortices increase whilst the viscous modes become stabilized. We further note that the unstable band of modes which emerge to the right of a_2 connect with the viscous modes in an inviscid manner; by this we simply mean that their structure is governed by a critical layer scenario near a_2.

In Figure (6.1) we have sketched the growth rate–wavenumber dependence determined above for the three situations: (a) $\lambda^* \sim G^{\frac{1}{2}}$, (b) $\lambda^* \sim G^{\frac{3}{6}}$, (c) $\lambda^* \gg G^{\frac{3}{6}}$. In (a) the crossflow

is strong enough only to alter the inviscid modes which have growth rate of size $G^{\frac{1}{2}}$; the viscous modes have growth rates of order $G^{\frac{3}{8}}$ and are not affected by the crossflow. In (b) both modes have growth rates of order $G^{\frac{3}{8}}$ but the inviscid modes are now independent of the wall curvature at zeroth order; thus the inviscid modes have deformed into crossflow vortices. The viscous modes at this stage depend on the crossflow and become completely stabilized at a finite value of $\lambda^*/G^{\frac{3}{8}}$. However before this occurs there are two points at which the growth rate has a local maximum. The relative importance of the maxima associated with the viscous and inviscid modes switches over as the crossflow increases. In (c) only the crossflow vortex mode remains and at zeroth order it is independent of the curvature of the wall.

The question of which of the possible modes discussed above is the most likely to be observed in an experiment can only be answered by a receptivity calculation of the type given by DHS for Görtler vortices in two-dimensional boundary layers. In fact the analysis given in Secion 6 of the latter paper is easily modified to discuss the receptivity problem for the viscous modes described by (3.10). Since this type of disturbance is concentrated near the wall then, following the analysis of DHS, it is a relatively simple matter to show that the 'coupling' coefficient associated with a roughness element at the wall is $O(1)$. By this we simply mean that the streamwise velocity component of a mode stimulated by an obstacle at the wall is comparable to the fluid velocity induced near the obstacle. However, as in DHS, the coupling coefficient depends on the vortex wavenumber and, if all modes are excited, sufficiently far downstream of the obstacle the fastest growing linear mode will dominate the flowfield. We shall concentrate on the case (b) above since by taking the appropriate limits in that situation (a) and (c) can be recovered.

We suppose then that the obstacle stimulates disturbances on a spanwise lengthscale comparable to the boundary layer lengthscale; this means that the inviscid modes satisfying (2.8a) will be stimulated. We shall now briefly describe how the coupling coefficient for this type of mode can be derived.

Suppose then that the roughness element defined by

$$Y = h(X, Z), \tag{6.1}$$

generates a disturbance field governed by (2.3). We assume that there are no oscillations in the free-stream so that the disturbed flow will be steady. Following DHS it is straightforward to show that the system (2.3) must now be solved subject to

$$U = -\bar{u}_Y h, \qquad V = 0, \qquad W = -\bar{w}_Y \bar{\lambda}^*, \qquad \text{at} \quad Y = 0 \tag{6.2}$$

instead of $U = V = W = 0$ at $Y = 0$. More precisely we note that we must replace ia by a partial Z derivative in (2.3) unless the X and Z dependences of h are separable. For simplicity we asume that this is the case so that without loss of generality we can take h to be function of X alone in the following discussion. However we note that, if we wish to generate the flowfields in a neighbourhood of the obstacle, the particular Z dependence of h must be accounted for when inverting the Fourier transform (in Z) of the disturbance. Here we are merely interested in finding the coupling coefficients associated with stationary vortices of wavelength comparable with boundary layer lengthscale so it is sufficient to take $h = h(X)$.

Since the forcing takes place at the wall we must in effect determine how an inviscid disturbance satisfying (2.8a) adjusts in a viscous wall layer so as to satisfy the correct boundary condition at the wall. It is easy to see that this layer must be of thickness $G^{-\frac{1}{6}}$ so that (6.2) suggests the following expansions for (U, V, W, P) in the wall layer where $Y = G^{\frac{1}{6}} q$,

$$(U, V, W, P) = (U^0 + \ldots, G^{\frac{1}{3}} V^0 + \ldots, G^{\frac{1}{2}} W^0 + \ldots, G^{\frac{5}{6}} P^0 + \ldots) \left(1 + O(G^{-\frac{1}{6}})\right), \quad (6.3)$$

The X dependence of the disturbance field is now taken care of using a Laplace transform. We suppose that h varies on a $G^{\frac{1}{2}}$ lengthscale in the X direction. Thus we write

$$h = \begin{cases} 0, & \text{if } X < X_0, \\ H(G^{\frac{1}{2}}[X - X_0]), & \text{if } X > X_0, \end{cases}$$

and determine the flow induced beyond $X = X_0$. Thus we now let β be the Laplace transform variable with respect to the variable $G^{\frac{1}{2}}[X - X_0]$. After a little work we can show that in the wall layer U^0 and W^0 are related by

$$\beta U^0 + iaW^0 = 3\bar{h} N^{\frac{4}{3}} \int_q^\infty Ai(N^{\frac{1}{3}} q) dq, \quad (6.4a)$$

where $\bar{h}$ is the transform of H and

$$N = \beta \mu_{11} + ia\mu_{21},$$

whilst Ai is the Airy function. The function V^0 is then given by

$$V^0 = -3\bar{h} N \int_0^q \left(\int_q^\infty Ai(N^{\frac{1}{3}} b) db \right) dq. \quad (6.4b)$$

We see that the above solution has V^0 tending to a constant V^0_∞ when $q \longrightarrow \infty$ so that in the main part of the boundary layer the appropriate expansions of U, V, W are

$$(U, V, W) = (G^{-\frac{1}{6}} U_0 + \ldots, G^{\frac{1}{3}} V_0 + \ldots, G^{\frac{1}{3}} W_0 + \ldots) \left(1 + O(G^{-\frac{1}{6}})\right) .$$

The function V_0 is then found to satisfy (2.8a): but the appropriate boundary conditions for this equation now become

$$V_0 = V^0_\infty, \qquad \text{at} \quad Y = 0, \qquad V_0 \longrightarrow 0 \qquad \text{as} \quad Y \longrightarrow \infty.$$

For given values of the transform variables β and a this inhomogeneous differential system for V_0 can be solved. However if $\beta = \bar{\beta}$ an eigenvalue of (2.8a, b, c) then the solution of the forced problem near $\bar{\beta}$ must be found by writing

$$V_0 = \frac{V_{00}}{(\beta - \bar{\beta})} + \cdots, \tag{6.5}$$

where $V_{00} = \Delta \bar{V}_0$. Here $\bar{V}_0$ is the eigensolution of (2.8a, b, c) with $\beta = \bar{\beta}$. The constant Δ may be written as

$$\Delta = \frac{V^0_\infty \bar{V}_0'(0)}{\int_0^\infty M(q) \bar{V}_0(q) dq}.$$

Here the function M is obtained by differentiating the left hand side of equation (2.8a) with respect to β and then setting $V_0 = \bar{V}_0$. Having determined V_0 we then see that in the main part of the boundary layer the disturbed downstream velocity component in β, a space near $\beta = \bar{\beta}$ is given by

$$U = \frac{-G^{-\frac{1}{6}} \Delta \bar{V}_0 \bar{u}_Y}{(\beta - \bar{\beta})(\beta \bar{u} + i \bar{\bar{\lambda}} a \bar{w})}, \tag{6.6}$$

It follows that when the Fourier-Laplace transform $U(\beta, a, Y)$ is inverted then the pole at $\bar{\beta}$ will lead to exponentially growing eigensoluti[illegible]roportional to $\Delta G^{-\frac{1}{6}} e^{\beta G^{\frac{1}{3}}(X - X_0)}$ Thus the coupling coefficient for inviscid vortex modes is of order $G^{-\frac{1}{6}}$ so that wall roughness is a more efficient stimulator of the viscous modes which, from DHS, have an $O(1)$ coefficient. However as the size of the crossflow is increased the growth rates of the inviscid modes increases to be larger than the viscous growth rates so this slight difference in size of the coupling coefficients will be irrelevant beyond a critical size for the crossflow and the observed instability will be a Rayleigh instability rather than a centrifugal one.

Finally we say a few words about the relevance of the above calculations to practical flows. In the obvious practical situations where Görtler vortices are thought to be a likely cause of transition the basic state is three–dimensional. Thus for example there is little doubt that the flow over a turbine blade is three–dimensional and our results suggest that it could therefore not support Görtler vortices. On a swept wing the basic state is three–dimensional and, for order one values of the angle of sweep, we can be confident that Görtler vortices cannot exist. However though the size of crossflow required to formally destroy the mechanism is of size $Re^{-\frac{1}{2}}G^{\frac{5}{6}}$ which is necessarily small because of the definition of the Görtler number the numerical constant multiplying this factor will be a function of the particular basic state. It could well be that for some swept-wing flows the Görtler mechanism might survive to modest angles of sweep appropriate to practical situations. Clearly this matter should be the topic of a careful experimental investigation of the Görtler mechanism in three-dimensional flows.

Acknowledgements.

The authors wish to thank SERC and USAF for support for part of the work reported on above. Further thanks are due to ICASE where part of this work was carried out by one of us (PH).

REFERENCES

Bassom, A.P. 1989 On the effect of crossflow on nonlinear Görtler vortices in curved channel flows. *Q. Jl. appl. Math.*, **42**, 495–510.

Bassom, A.P. & Gajjar, J.S.B. 1988 Non-stationary cross-flow vortices in three-dimensional boundary layer flows. *Proc. R. Soc. Lond. A.*, **417**, 179–212.

Cooke, J.C. 1950 The boundary layer of a class of infinite yawed cylinders. *Proc. Camb. phil Soc.*, **46**, 645–648.

Denier, J.P., Hall, P. & Seddougui, S.O. 1990 On the receptivity problem for Görtler vortices: vortex motions induced by wall roughness. *ICASE Rep. No. 90-31. To appear in Phil. Trans. R. Soc. Lond. A*

Görtler H. 1940 Uber eine dreidimensionale instabilität laminare Grenzschubten an Konkaven Wänden. *NACA TM 1357.*

Gregory, N., Stuart, J.T. & Walker, W.S. 1955 On the stability of three dimensional boundary layers with application to the flow due to a rotating disk. *Phil. Trans. R. Soc. Lond. A*, **248**, 155–199.

Hall, P. 1982*a* Taylor-Görtler vortices in fully developed or boundary layer flows. *J. Fluid Mech.*, **124**, 475–494.

Hall, P. 1982*b* On the nonlinear evolution of Görtler vortices in non-parallel boundary layers. *J. Inst. Maths. Applics.*, **29**, 173–196.

Hall, P. 1983 The linear development of Görtler vortices in growing boundary layers. *J. Fluid Mech.*, **130**, 41–58.

Hall, P. 1985 The Görtler vortex instability mechanism in three-dimensional boundary layers. *Proc. R. Soc. Lond. A.*, **399**, 135–152.

Hall, P. 1988 The nonlinear development of Görtler vortices in growing boundary layers. *J. Fluid Mech.*, **193**, 247–266.

Hall, P. & Lakin, W.D. 1988 The fully nonlinear development of Görtler vortices in growing boundary layers. *Proc. R. Soc. Lond. A*, **415**, 421–444.

Hall, P. & Seddougui, S. 1989 On the onset of three-dimensionality and time-dependence in Görtler vortices. *J. Fluid Mech.*, **204**, 405–420.

Hämmerlin, G. 1956 Zur Theorie der dreidimensionalen Instabilität laminar Grenschichten. *Z. Agnew. Math. Phys.*, **1**, 156–167.

Jones, C.W. & Watson, E.J. 1963 Two-dimensional boundary layers. In: *Laminar Boundary Layers* (L. Rosenhead, Ed.), Chap. 5. Oxford University Press.

Malik, M.R., Chuang, S. & Hussaini, M.Y. 1982 Accurate numerical solution of compressible, linear stability equations. *ZAMP*, **33**, 189–201.

Peerhossaini, H. & Wesfreid, J.E. 1988*a* On the inner structure of streamwise Görtler rolls. *Intl J. Heat Fluid Flow*, **9**, 12–18.

Peerhossaini, H. & Wesfreid, J.E. 1988*b* Experimental study of the Taylor-Görtler instability. In *Propagation in Systems Far from Equilibrium* (ed. J.E. Wesfreid, H.R. Brand, P. Manneville, G. Albinet & N. Boccara). Springer Series in Synergetics, vol 41, pp. 399–412. Springer.

Seddougui, S.O. & Bassom, A.P. 1990 On the instability of Görtler vortices to nonlinear travelling waves. *ICASE Rep. No. 90-1. To appear in IMA J. Appl. Math.*

Smith, A.M.O. 1955 On the growth of Taylor-Görtler vortices along highly concave walls. *Q. Appl. Math.*, **13**, 233–262.

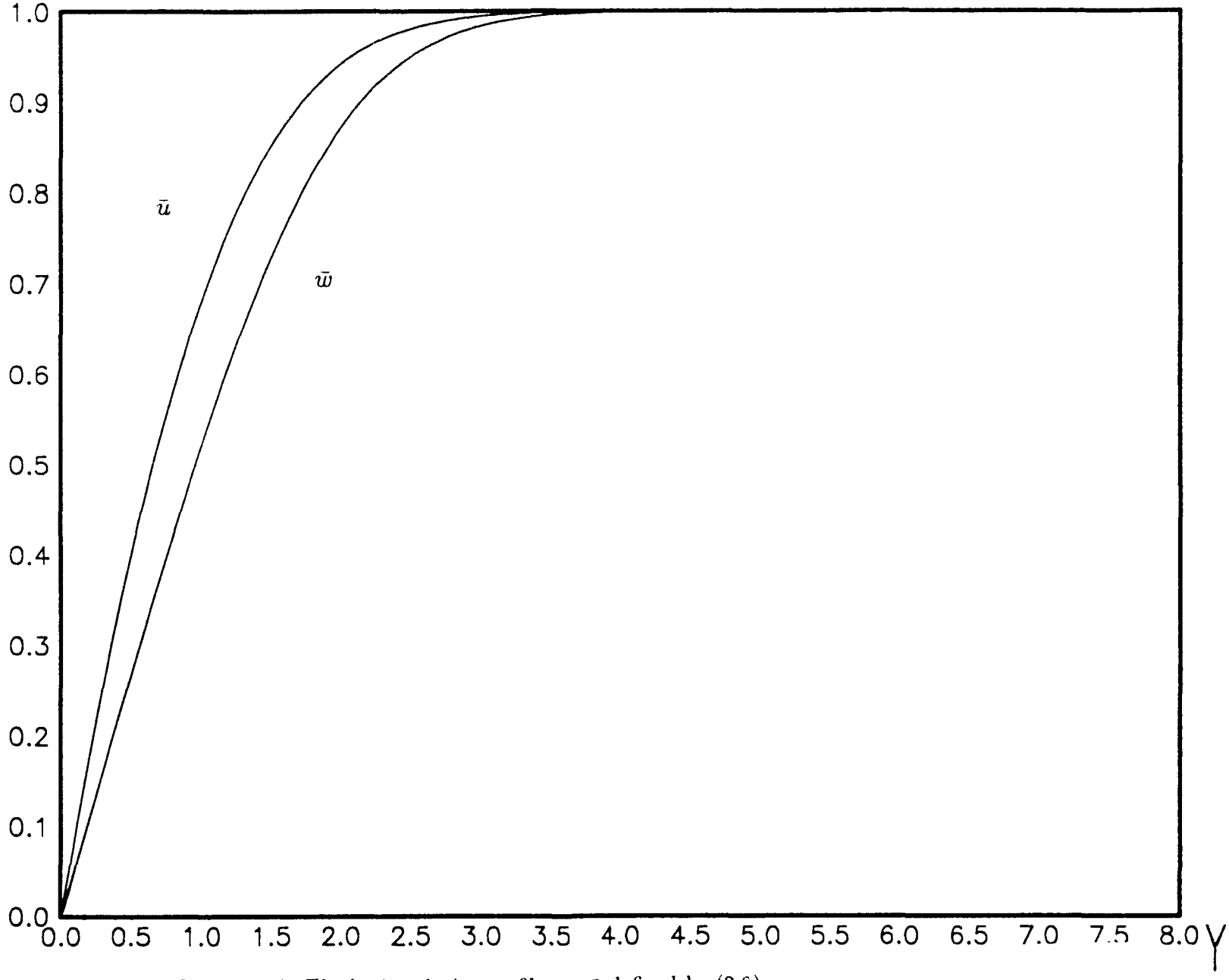

Figure (2.1). The basic velocity profiles $\bar{u}$, $\bar{w}$ defined by (2.9).

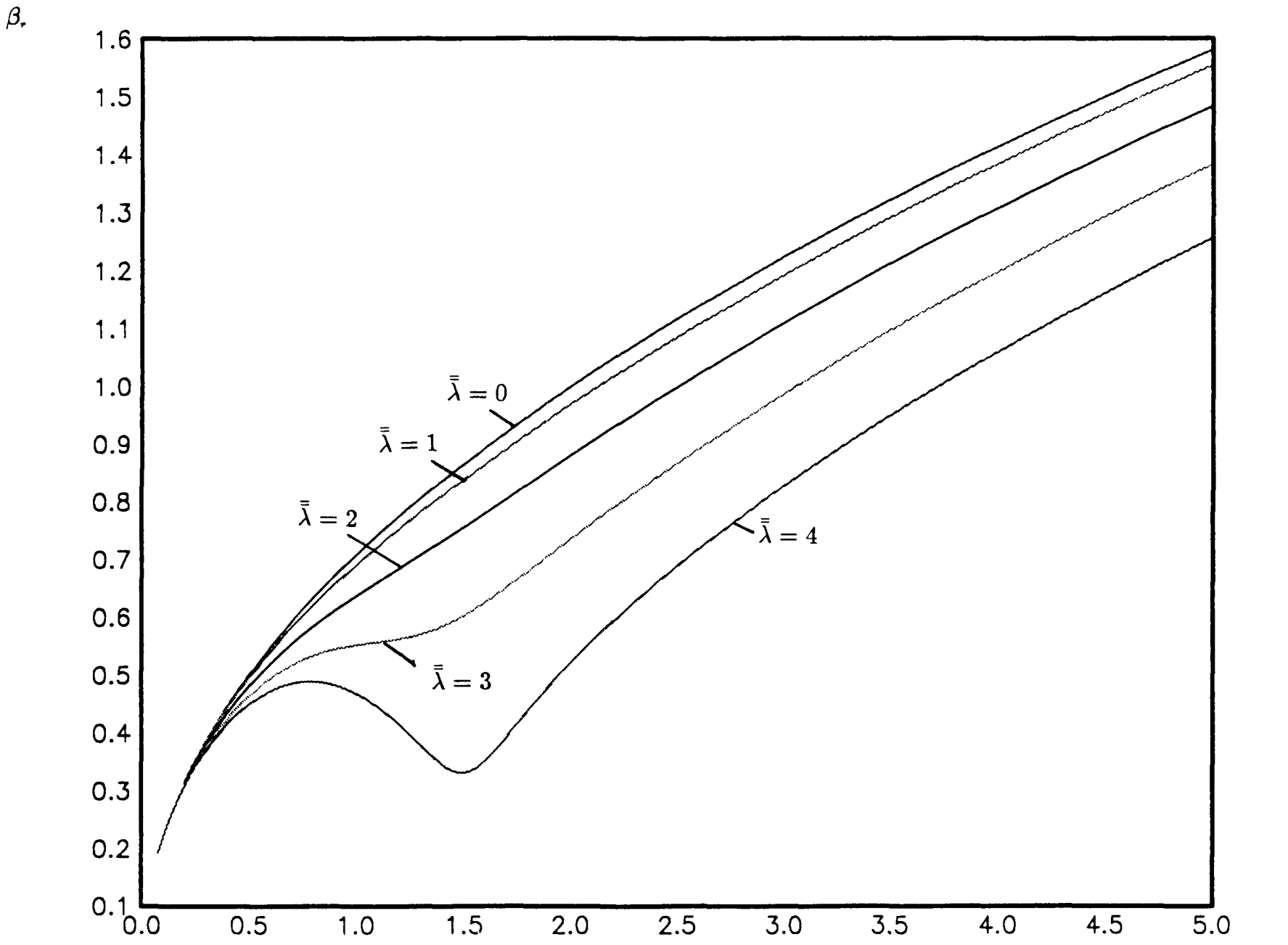

Figure (2.2). Real parts of the amplification parameter β defined by (2.6a) for various values of scaled crossflow $\bar{\bar{\lambda}}$. a) $\bar{\bar{\lambda}} = 0, 1, 2, 3$ and 4, b) $\bar{\bar{\lambda}} = 4.5, 4.75$ and 5.

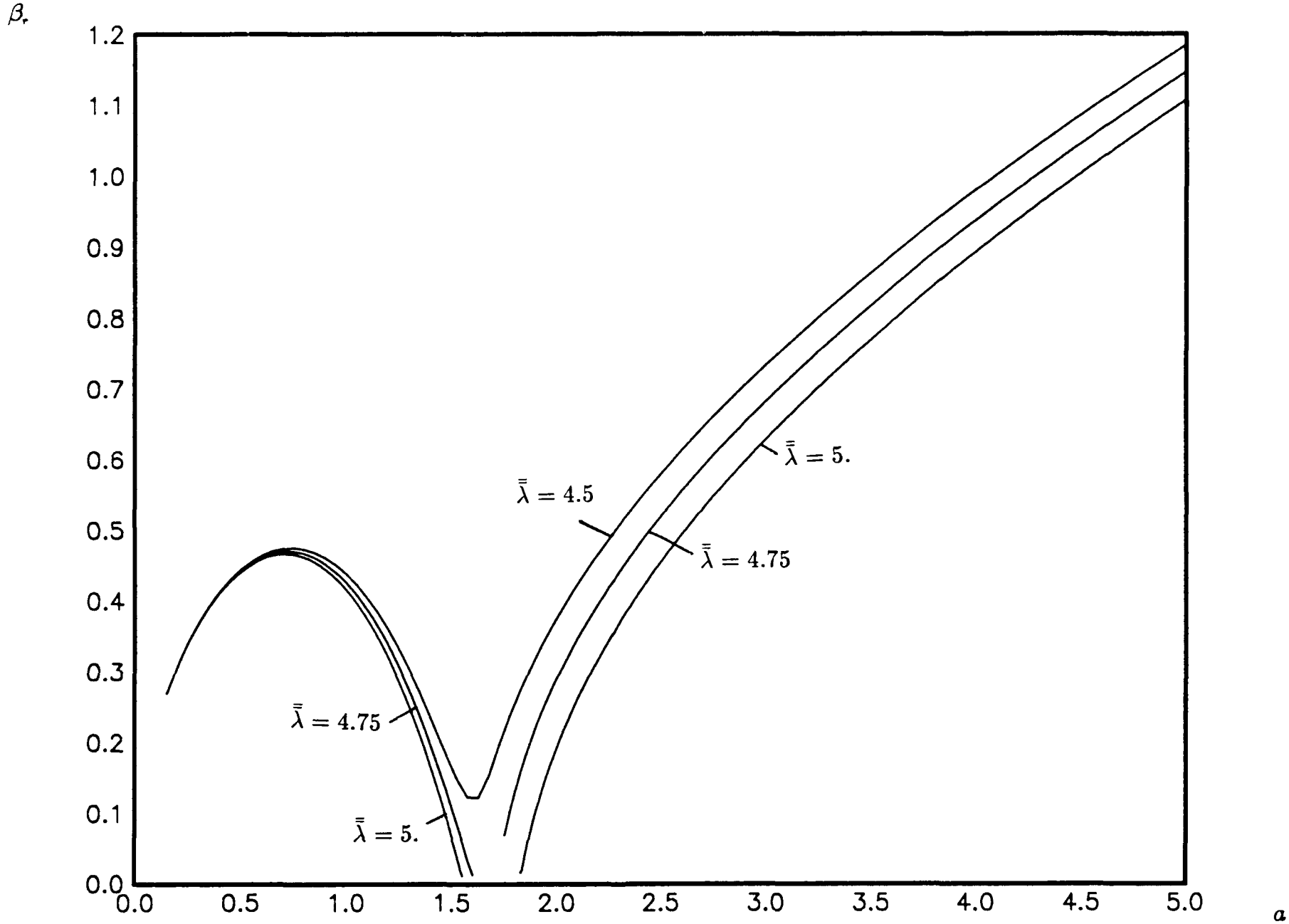

Figure (2.2). Real parts of the amplification parameter β defined by (2.6a) for various values of scaled crossflow $\bar{\bar{\lambda}}$. a) $\bar{\bar{\lambda}} = 0, 1, 2, 3$ and 4, b) $\bar{\bar{\lambda}} = 4.5, 4.75$ and 5.

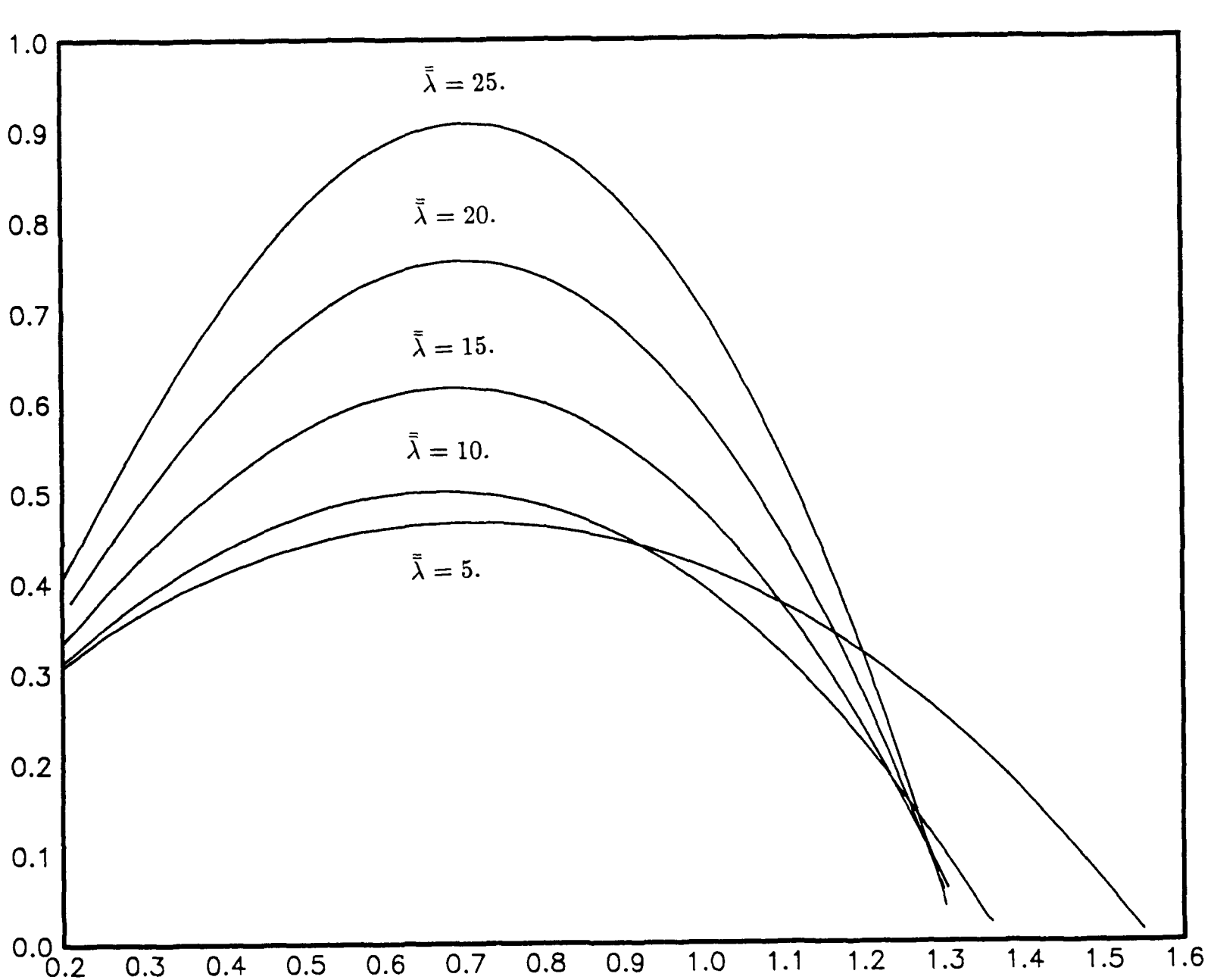

Figure (2.3). Real parts of the amplification parameter β for larger crossflows, $\bar{\bar{\lambda}} = 5, 10, 15, 20$ and 25.

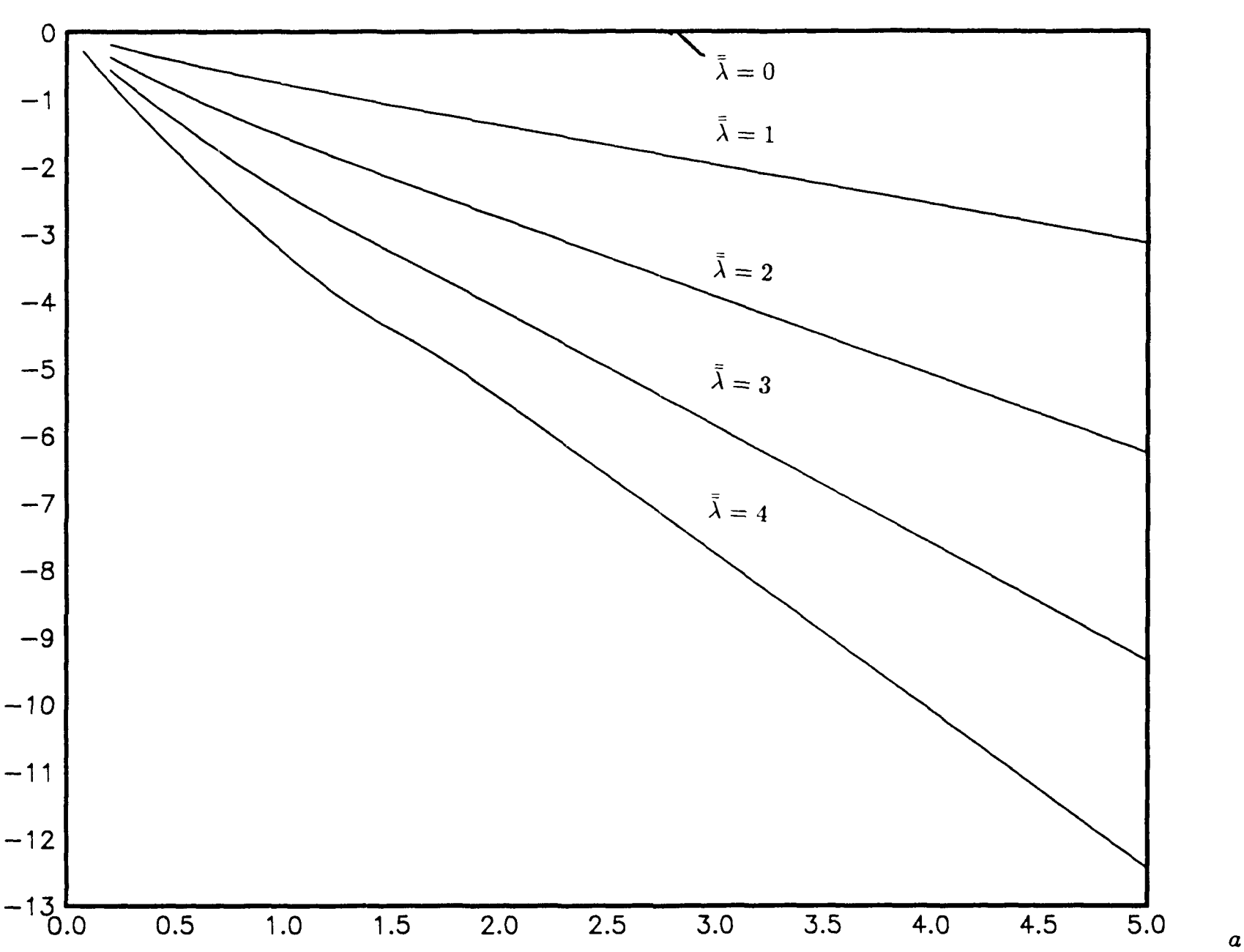

Figure (2.4a,b). Imaginary parts of the amplification parameter β for various values of scaled crossflow $\bar{\bar{\lambda}}$. a) $\bar{\bar{\lambda}} = 0, 1, 2, 3$ and 4, b) $\bar{\bar{\lambda}} = 4.5, 4.75$ and 5.

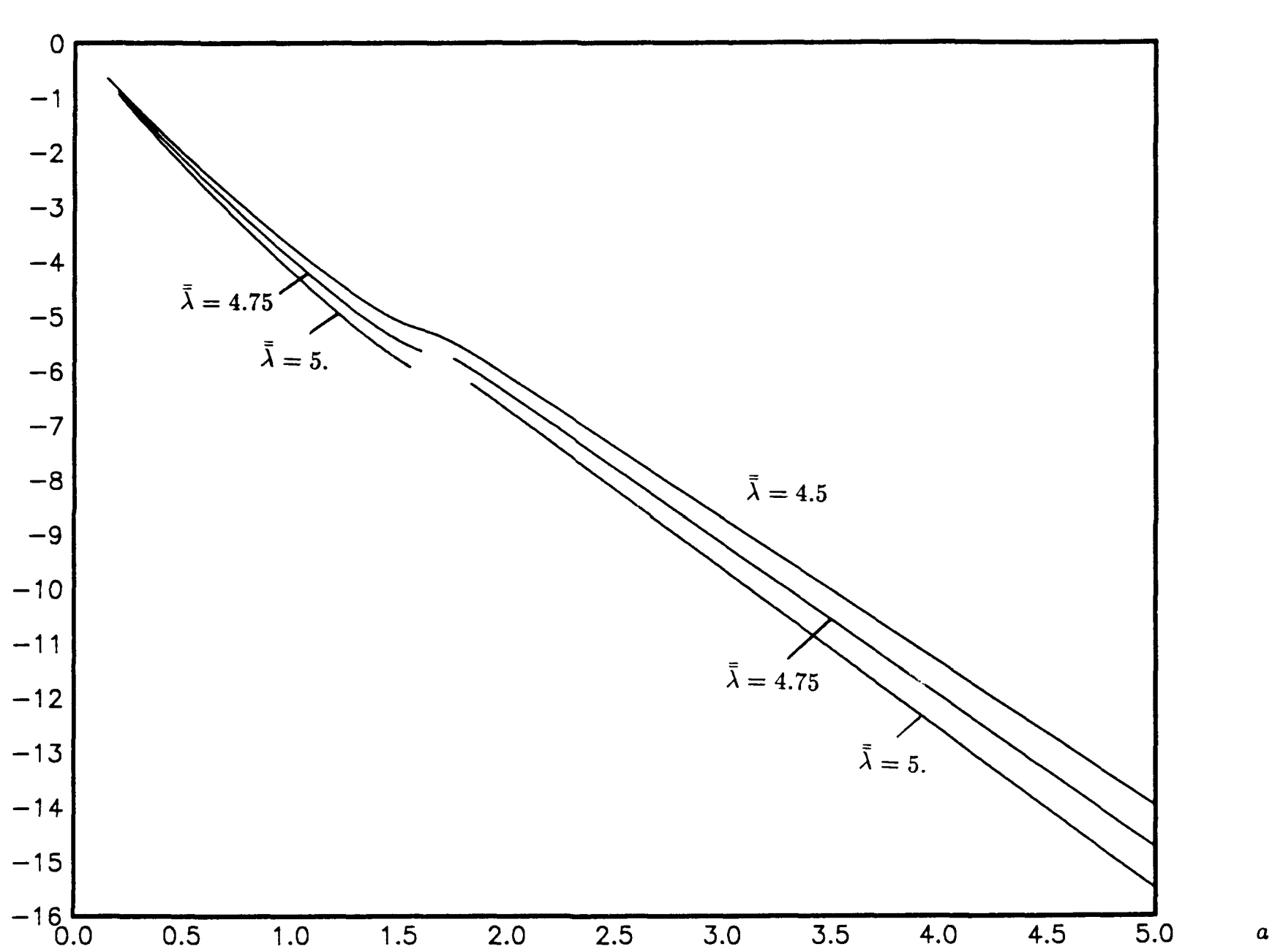

Figure (2.4a,b). Imaginary parts of the amplification parameter β for various values of scaled crossflow $\bar{\bar{\lambda}}$. a) $\bar{\bar{\lambda}} = 0, 1, 2, 3$ and 4, b) $\bar{\bar{\lambda}} = 4.5, 4.75$ and 5.

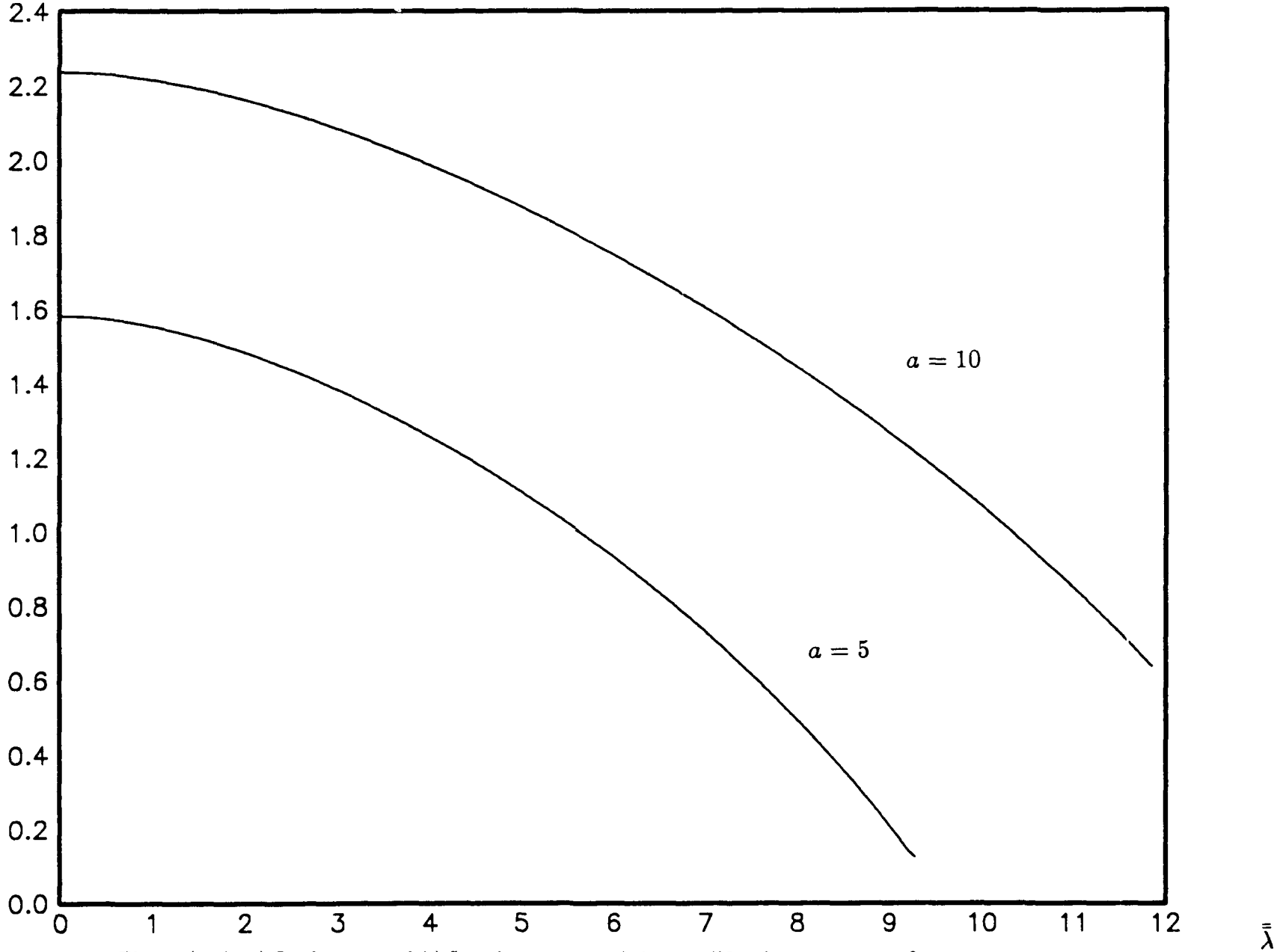

Figure (2.5). a) Real parts and b) Imaginary parts of the amplification parameter β as functions of crossflow $\bar{\bar{\lambda}}$ for vortex wavenumbers $a = 5$, 10.

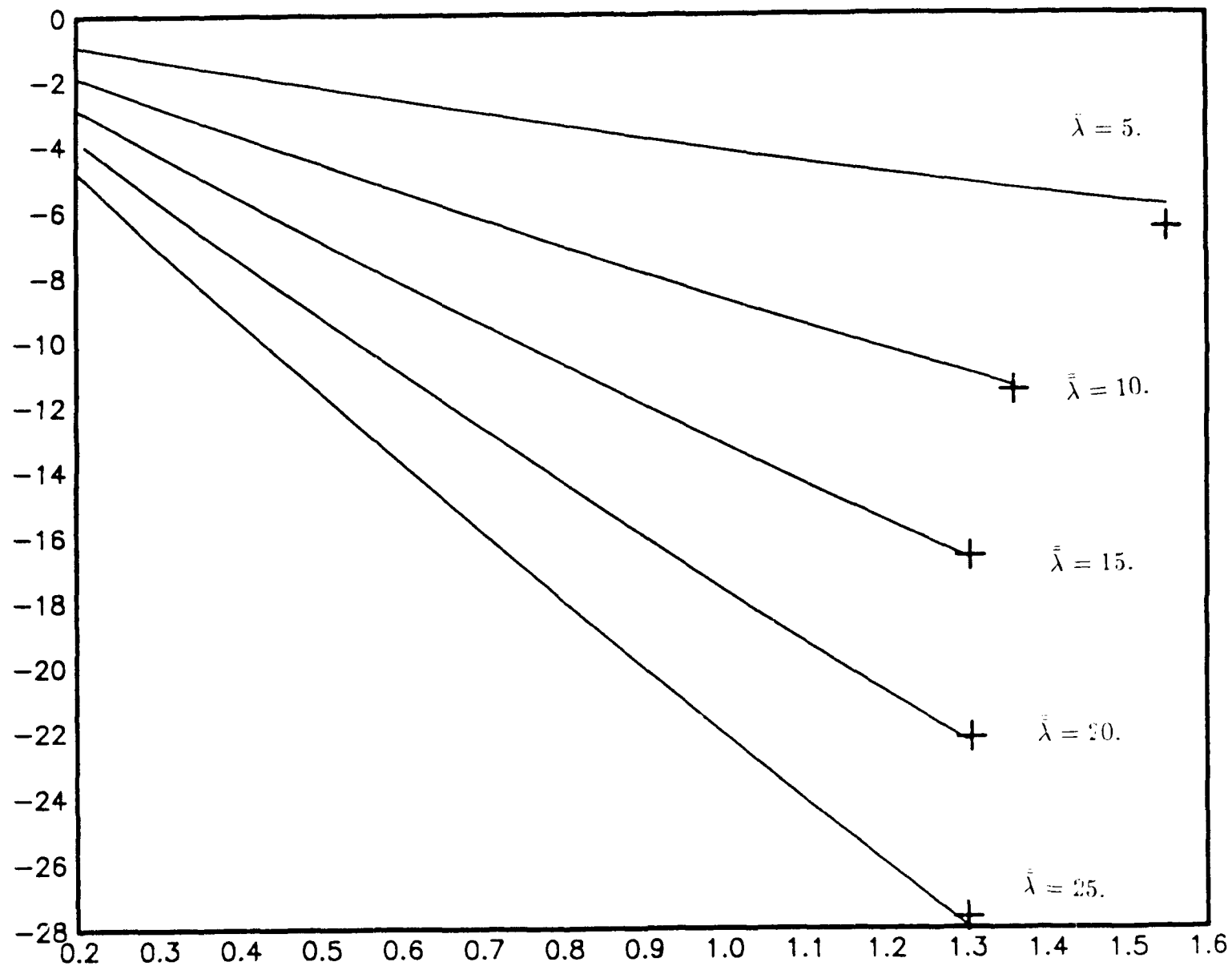

Figure (2.4c). Imaginary parts of the amplification parameter β for crossflow sizes $\bar{\lambda} = 5, 10, 15, 20$ and 25. For each crossflow the cross indicates the classical value of γ such that (2.12) is satisfied and so neutrally stable solutions of the GSW crossflow instability problem arise.

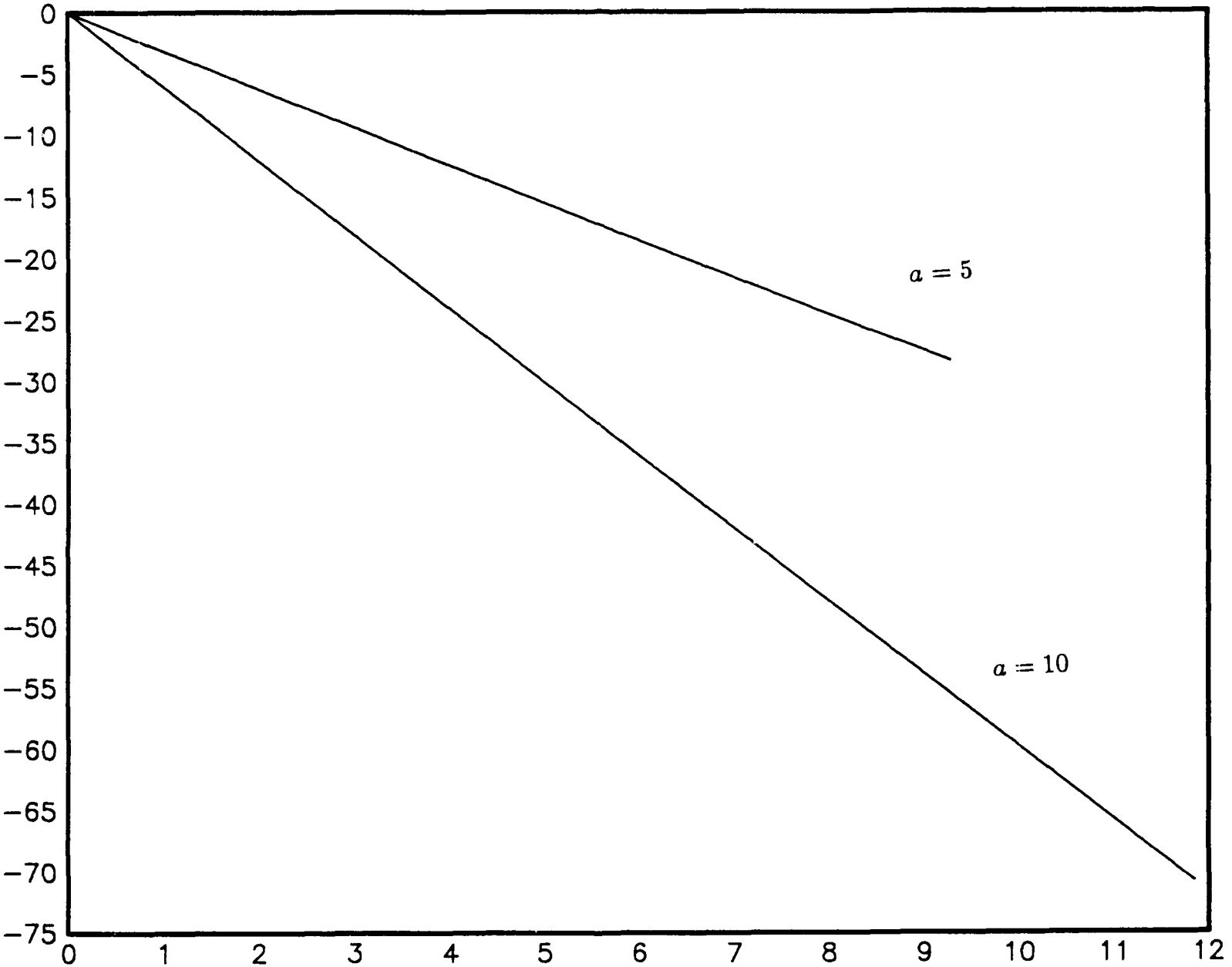

Figure (2.5). a) Real parts and b) Imaginary parts of the amplification parameter β as functions of crossflow $\bar{\bar{\lambda}}$ for vortex wavenumbers a = 5, 10.

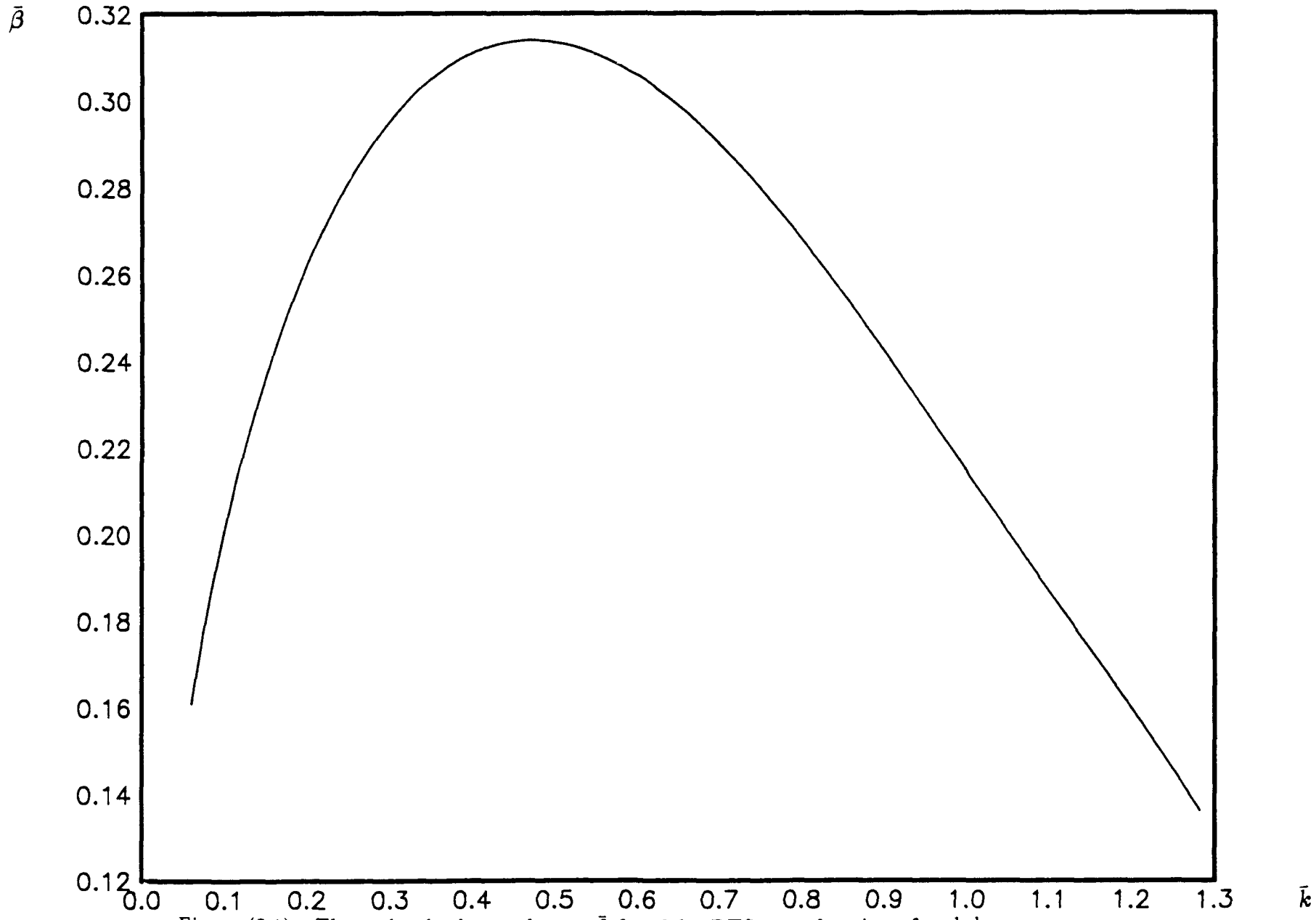

Figure (3.1). The real-valued growth rate $\bar{\beta}$ found by DHS as a function of scaled wavenumber $\bar{k}$.

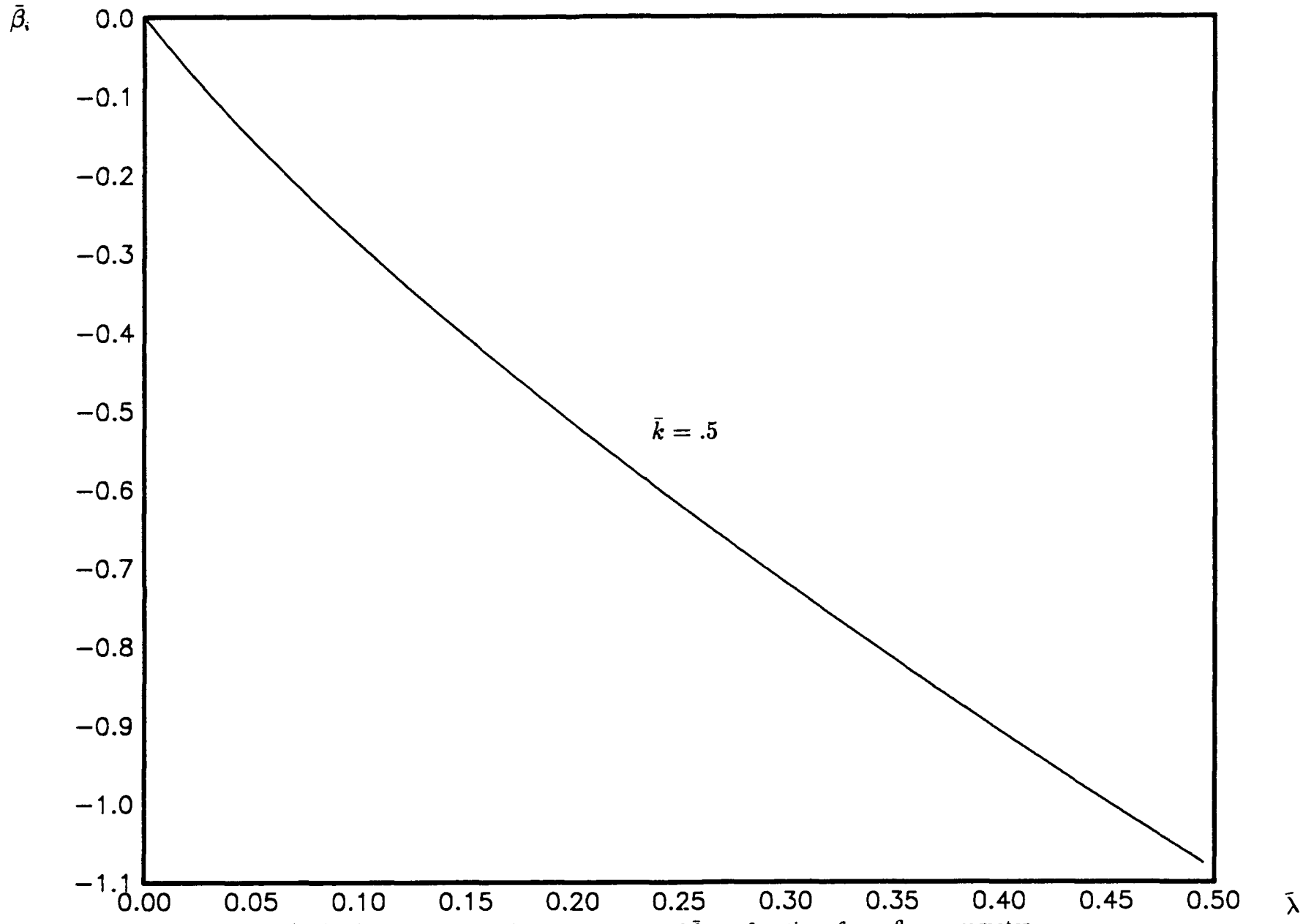

Figure (4.1). a) Real part and b) Imaginary part of $\bar{\beta}$ as a function of crossflow parameter $\bar{\lambda}$ for vortices of zero frequency and wavenumber $\bar{k} = 1/2$.

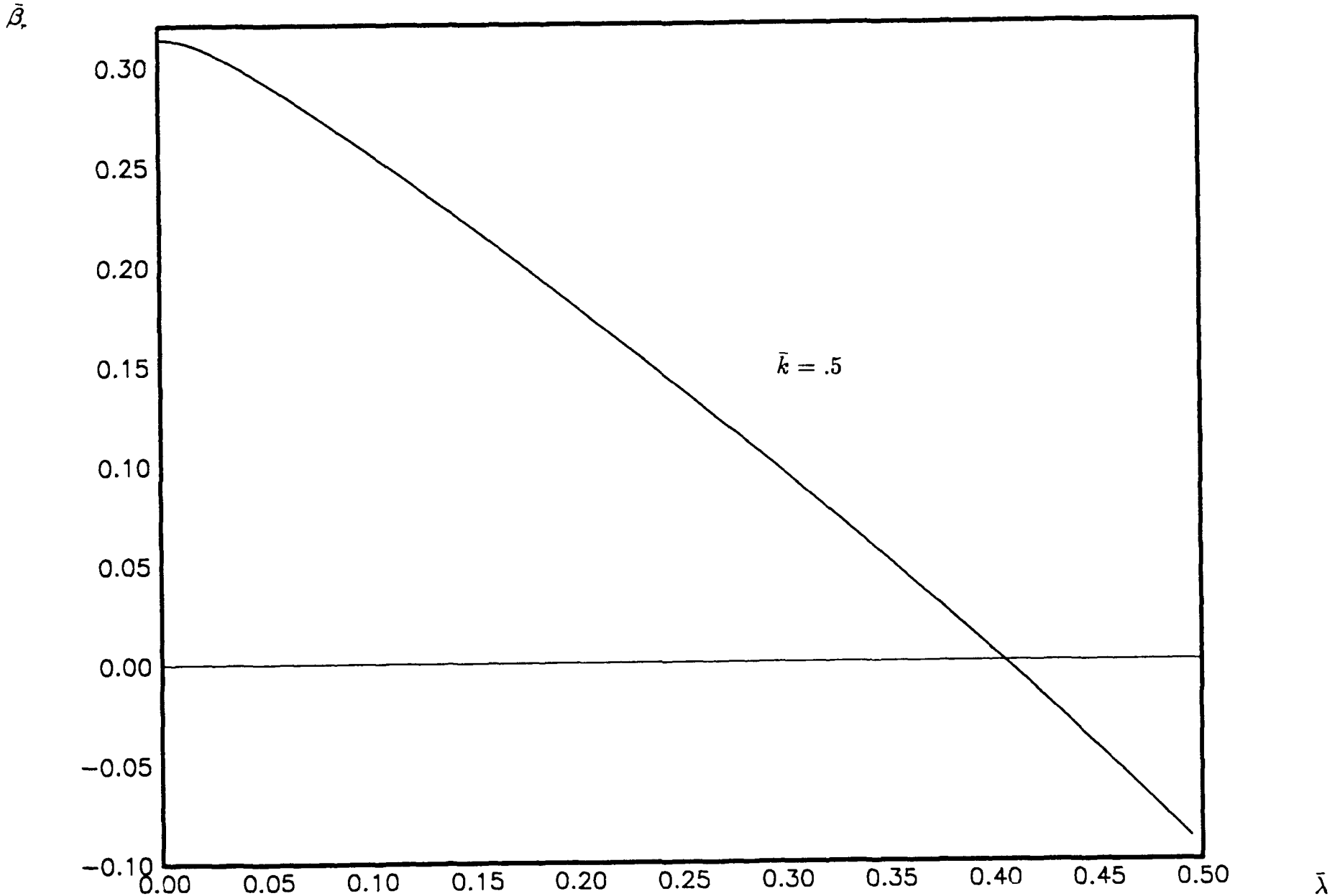

Figure (4.1). a) Real part and b) Imaginary part of $\bar{\beta}$ as a function of crossflow parameter $\bar{\lambda}$ for vortices of zero frequency and wavenumber $\bar{k} = 1/2$.

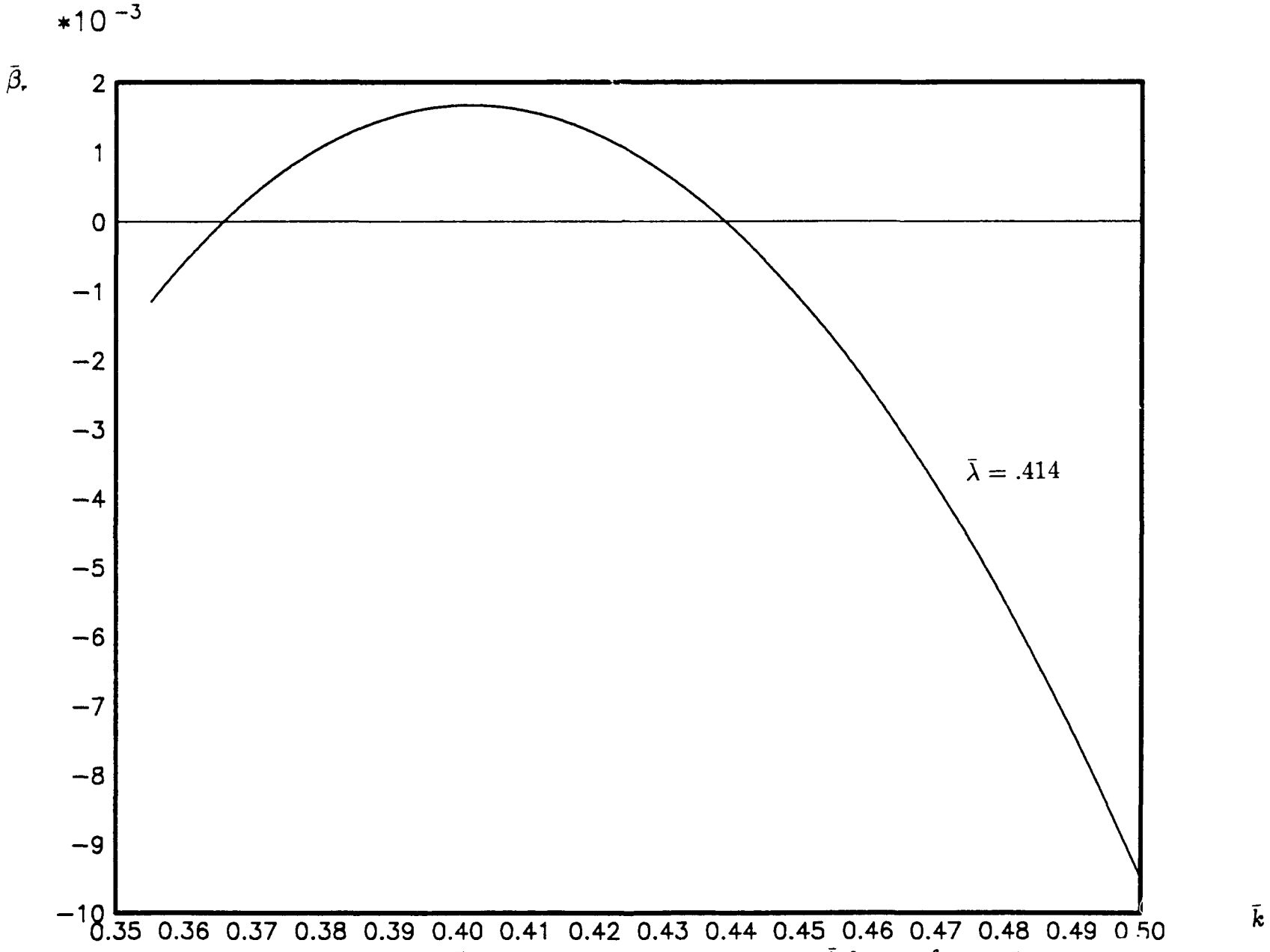

Figure (4.2). Real part of $\bar{\beta}$ as a function of vortex wavenumber $\bar{k}$ for zero-frequency vortices in the presence of crossflows of sizes a) $\bar{\lambda} = 0.414$, b) $\bar{\lambda} = 0.434$.

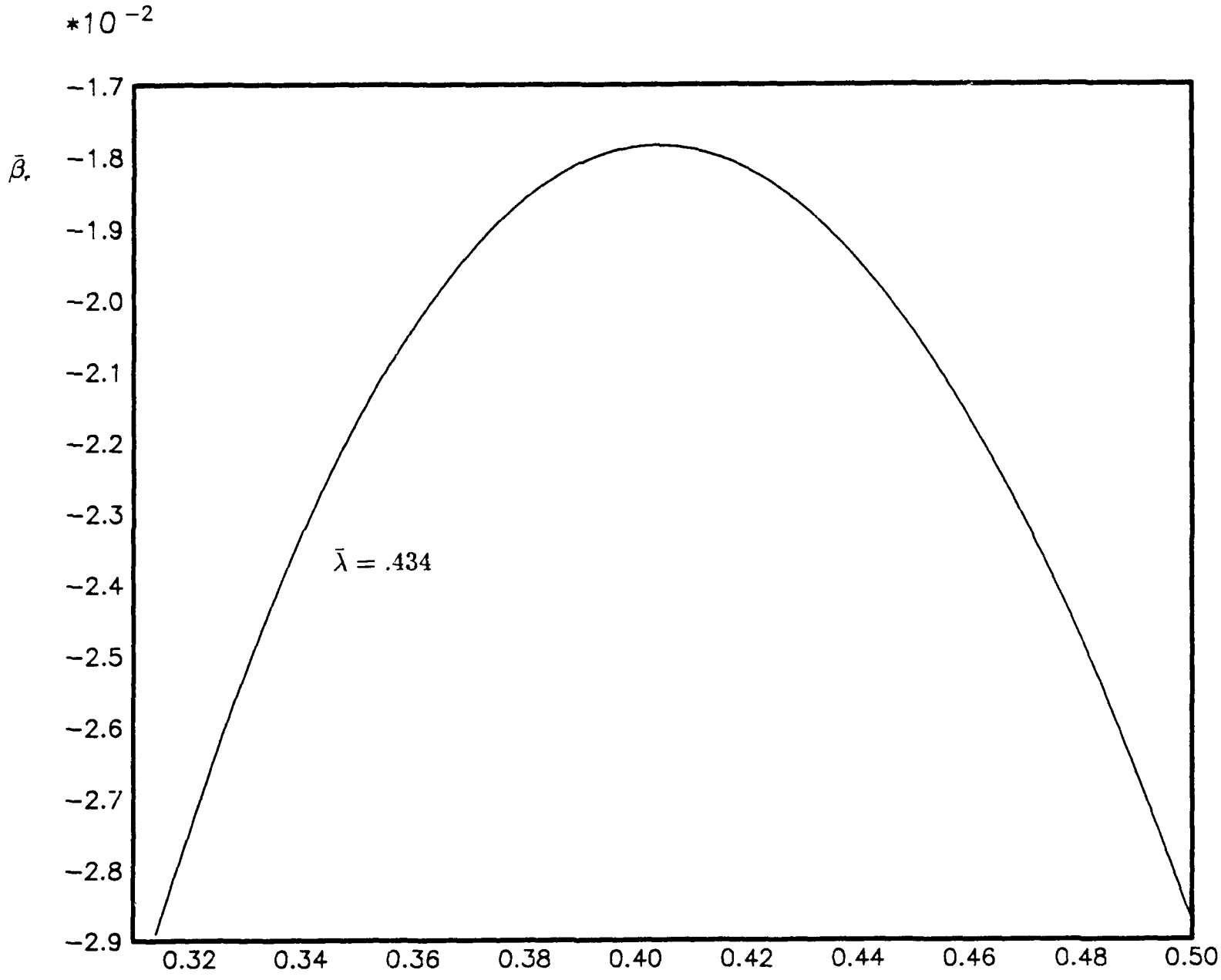

Figure (4.2). Real part of $\bar{\beta}$ as a function of vortex wavenumber $\bar{k}$ for zero-frequency vortices in the presence of crossflows of sizes a) $\bar{\lambda} = 0.414$, b) $\bar{\lambda} = 0.434$.

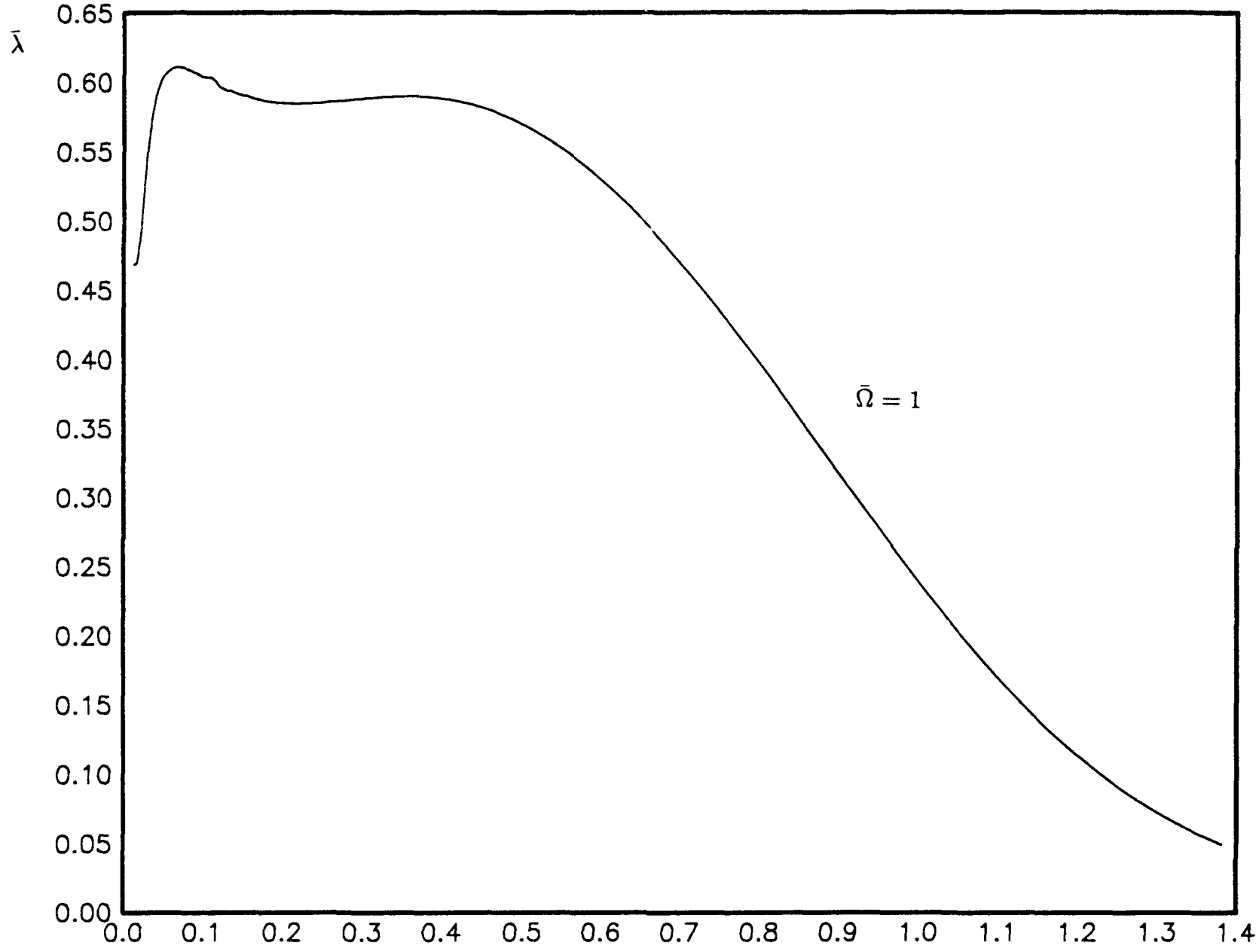

Figure (5.1). Values of crossflow $\bar{\lambda}$ and parameter $\bar{\beta}$ needed in order to ensure that vortices of frequency $\bar{\Omega} = 1$ are neutrally stable. a) $\bar{\lambda}$ and b) $\bar{\beta}$ as functions of vortex wavenumber $\bar{k}$.

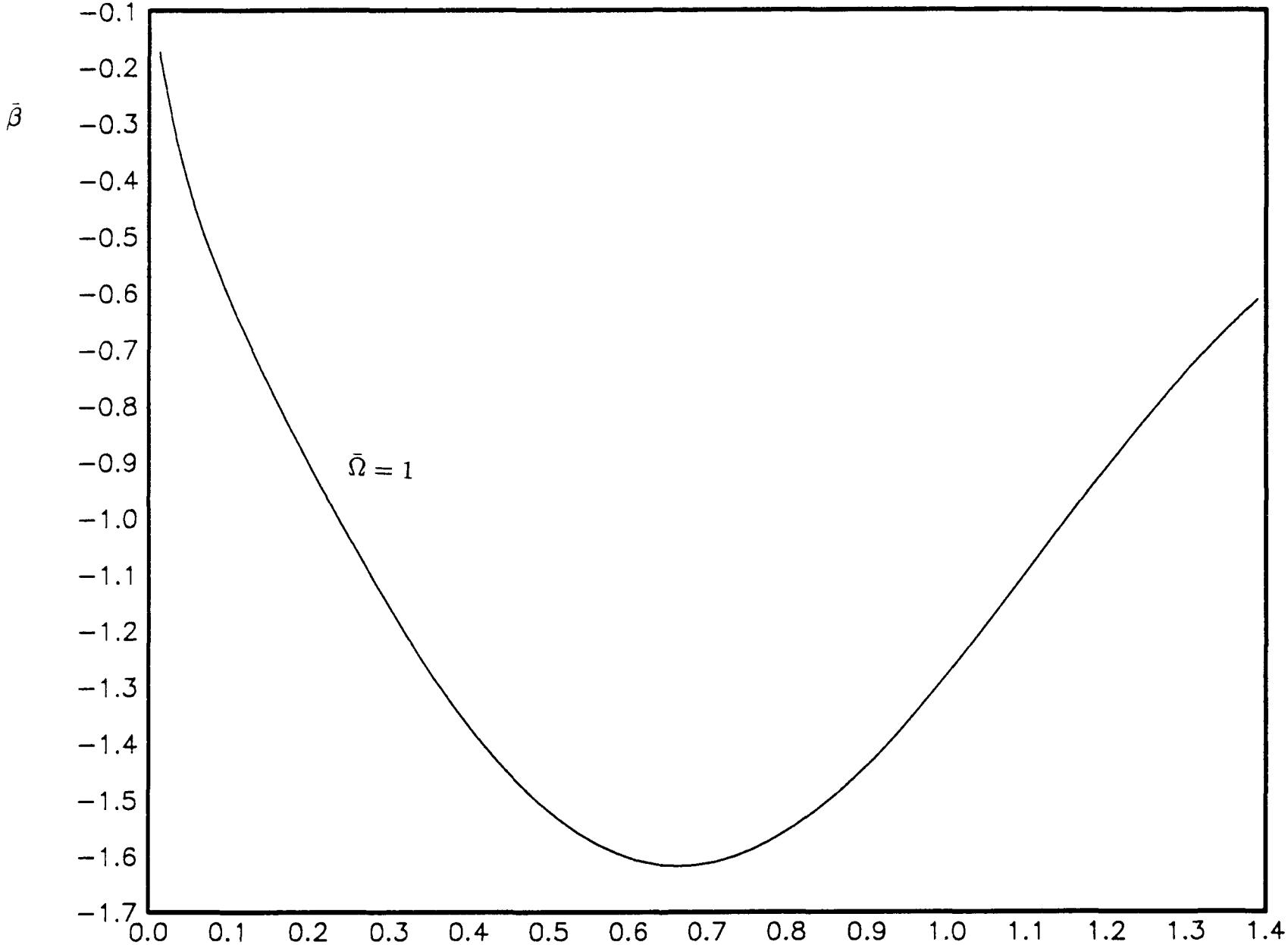

Figure (5.1). Values of crossflow $\bar{\lambda}$ and parameter $\bar{\beta}$ needed in order to ensure that vortices of frequency $\bar{\Omega} = 1$ are neutrally stable. a) $\bar{\lambda}$ and b) $\bar{\beta}$ as functions of vortex wavenumber $\bar{k}$.

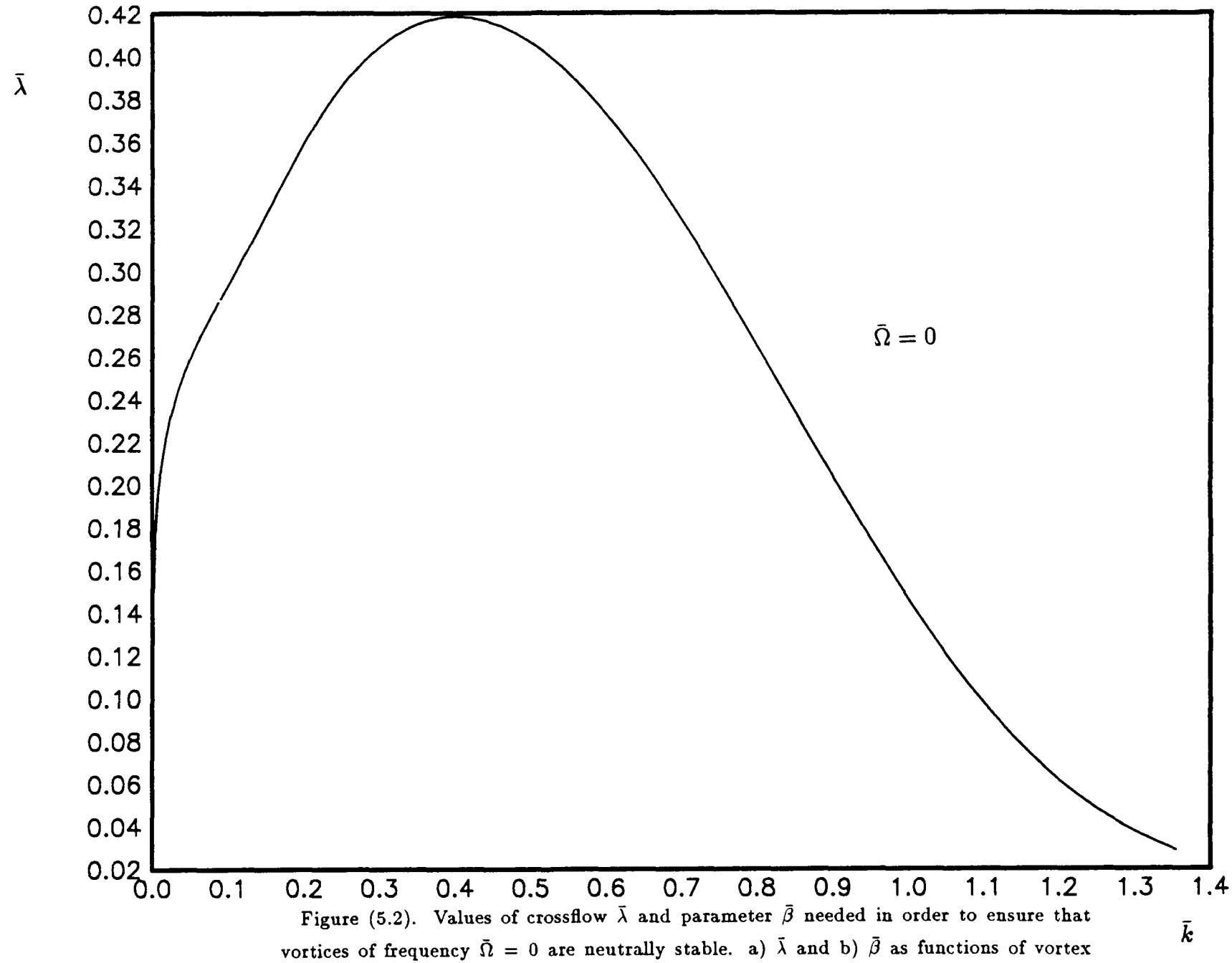

Figure (5.2). Values of crossflow $\bar{\lambda}$ and parameter $\bar{\beta}$ needed in order to ensure that vortices of frequency $\bar{\Omega} = 0$ are neutrally stable. a) $\bar{\lambda}$ and b) $\bar{\beta}$ as functions of vortex wavenumber $\bar{k}$.

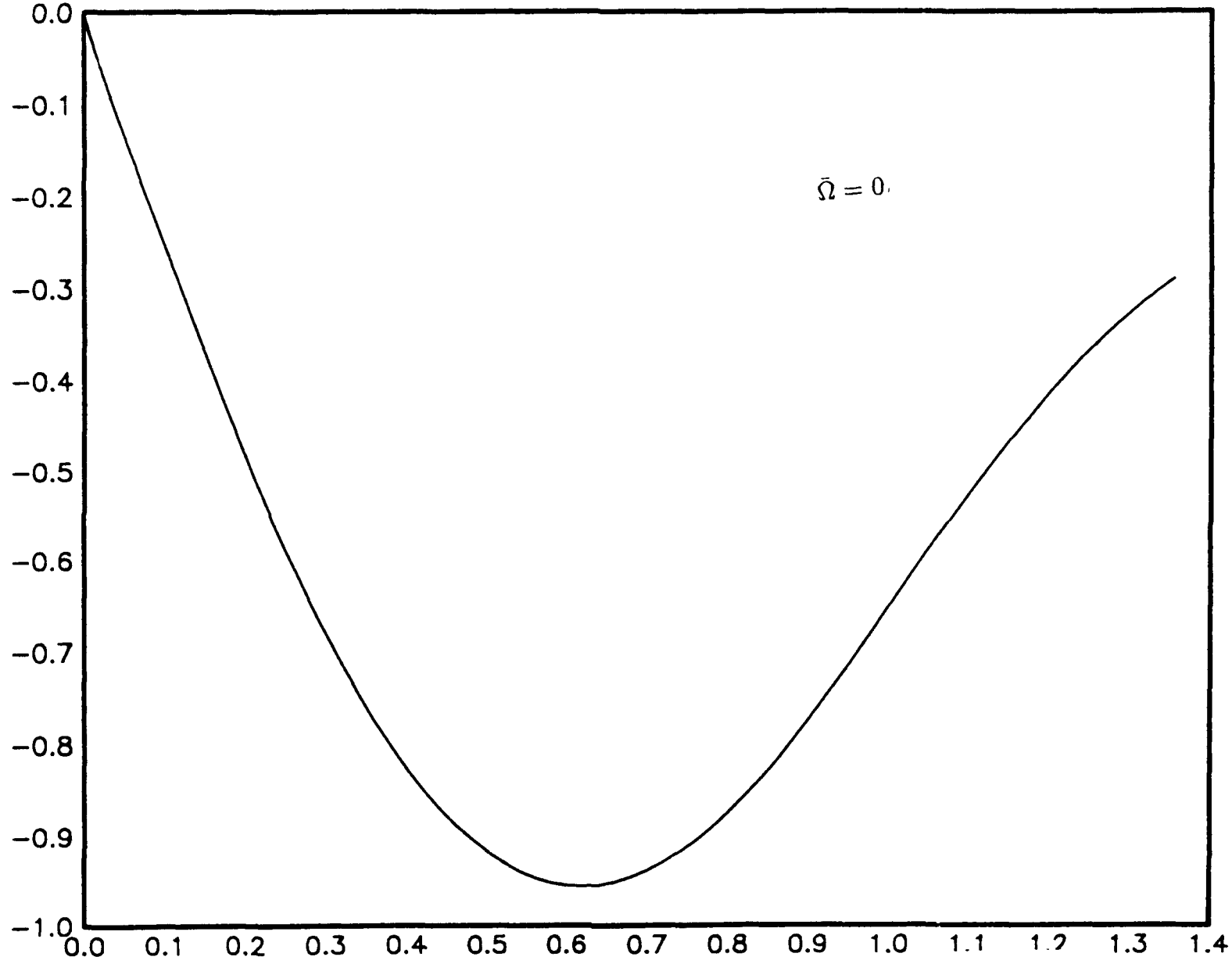

Figure (5.2). Values of crossflow $\bar{\lambda}$ and parameter $\bar{\beta}$ needed in order to ensure that vortices of frequency $\bar{\Omega} = 0$ are neutrally stable. a) $\bar{\lambda}$ and b) $\bar{\beta}$ as functions of vortex wavenumber $\bar{k}$.

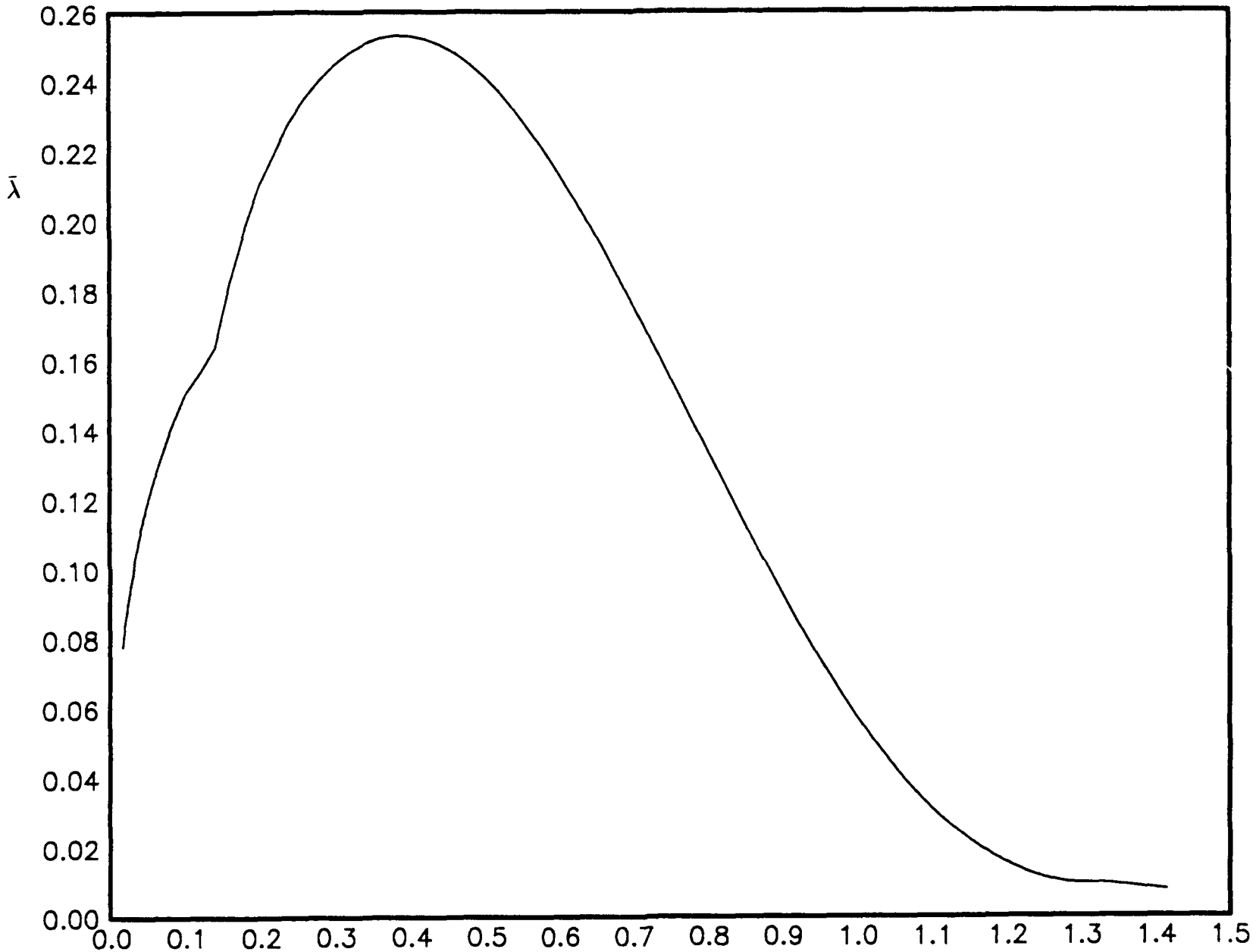

Figure (5.3). Values of crossflow $\bar{\lambda}$ and parameter $\bar{\beta}$ needed in order to ensure that vortices of frequency $\bar{\Omega} = -1$ are neutrally stable. a) $\bar{\lambda}$ and b) $\bar{\beta}$ as functions of vortex wavenumber $\bar{k}$.

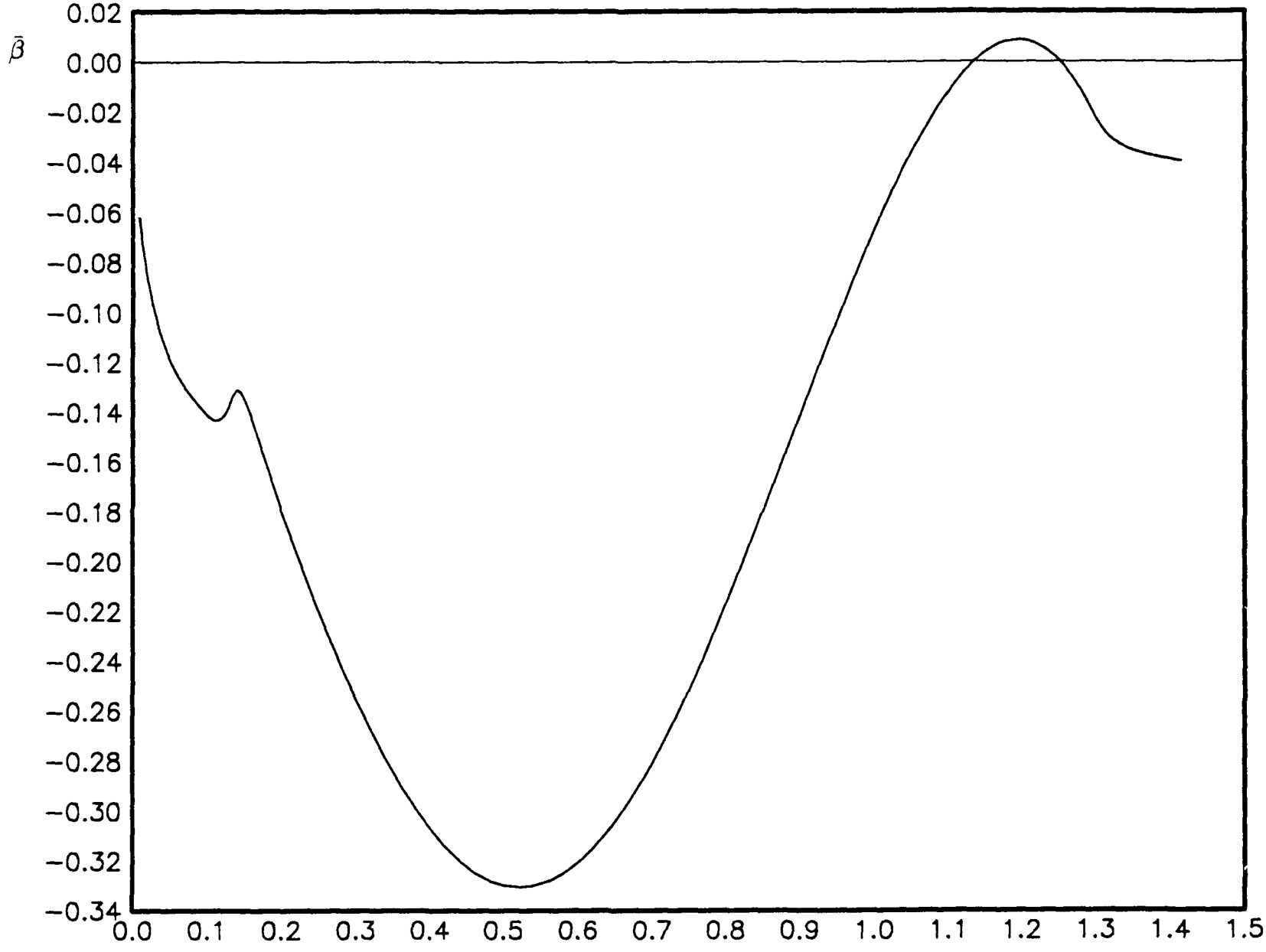

Figure (5.3). Values of crossflow $\bar{\lambda}$ and parameter $\bar{\beta}$ needed in order to ensure that vortices of frequency $\bar{\Omega} = -1$ are neutrally stable. a) $\bar{\lambda}$ and b) $\bar{\beta}$ as functions of vortex wavenumber $\bar{k}$.

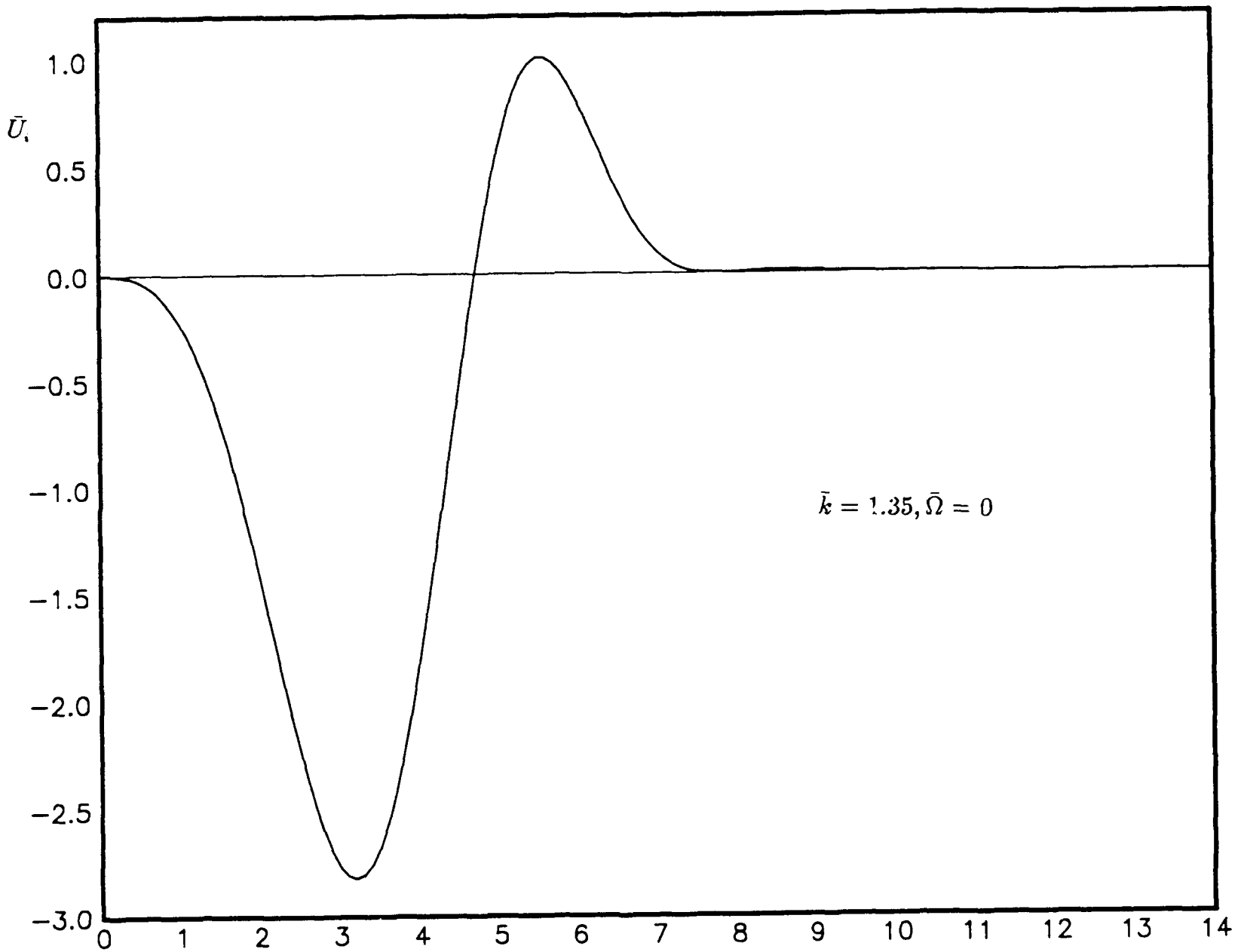

Figure (5.4). Eigenfunctions $\bar{U}$, $\bar{V}$ of (3.10) & (3.11) for neutrally stable vortices with $\bar{k} = 1.35$, $\bar{\Omega} = 0$. a) Re($\bar{U}$), b) Im($\bar{U}$), c) Re($\bar{V}$), d) Im($\bar{V}$).

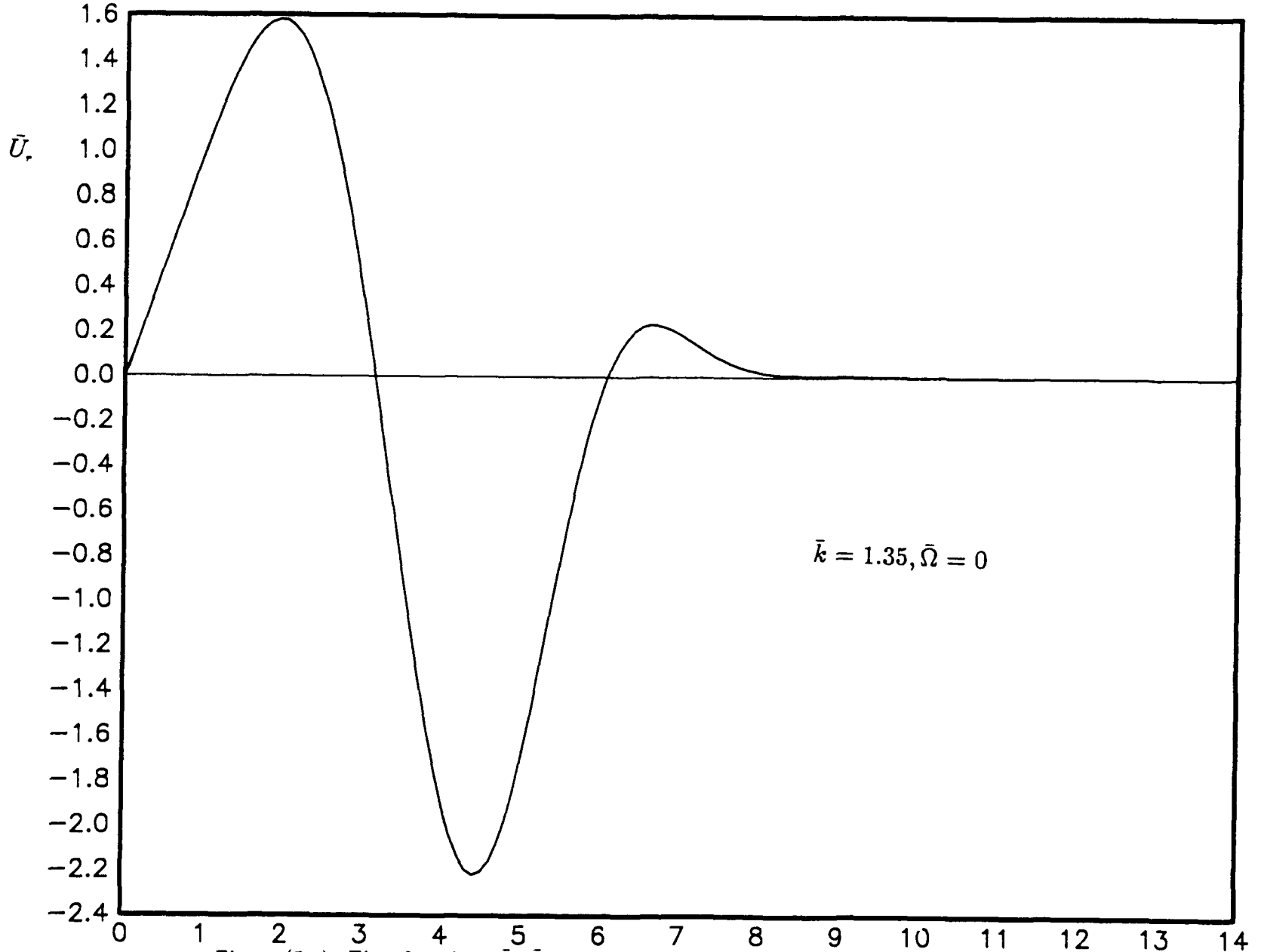

Figure (5.4). Eigenfunctions $\bar{U}$, $\bar{V}$ of (3.10) & (3.11) for neutrally stable vortices with $\bar{k} = 1.35$, $\bar{\Omega} = 0$. a) Re($\bar{U}$), b) Im($\bar{U}$), c) Re($\bar{V}$), d) Im($\bar{V}$).

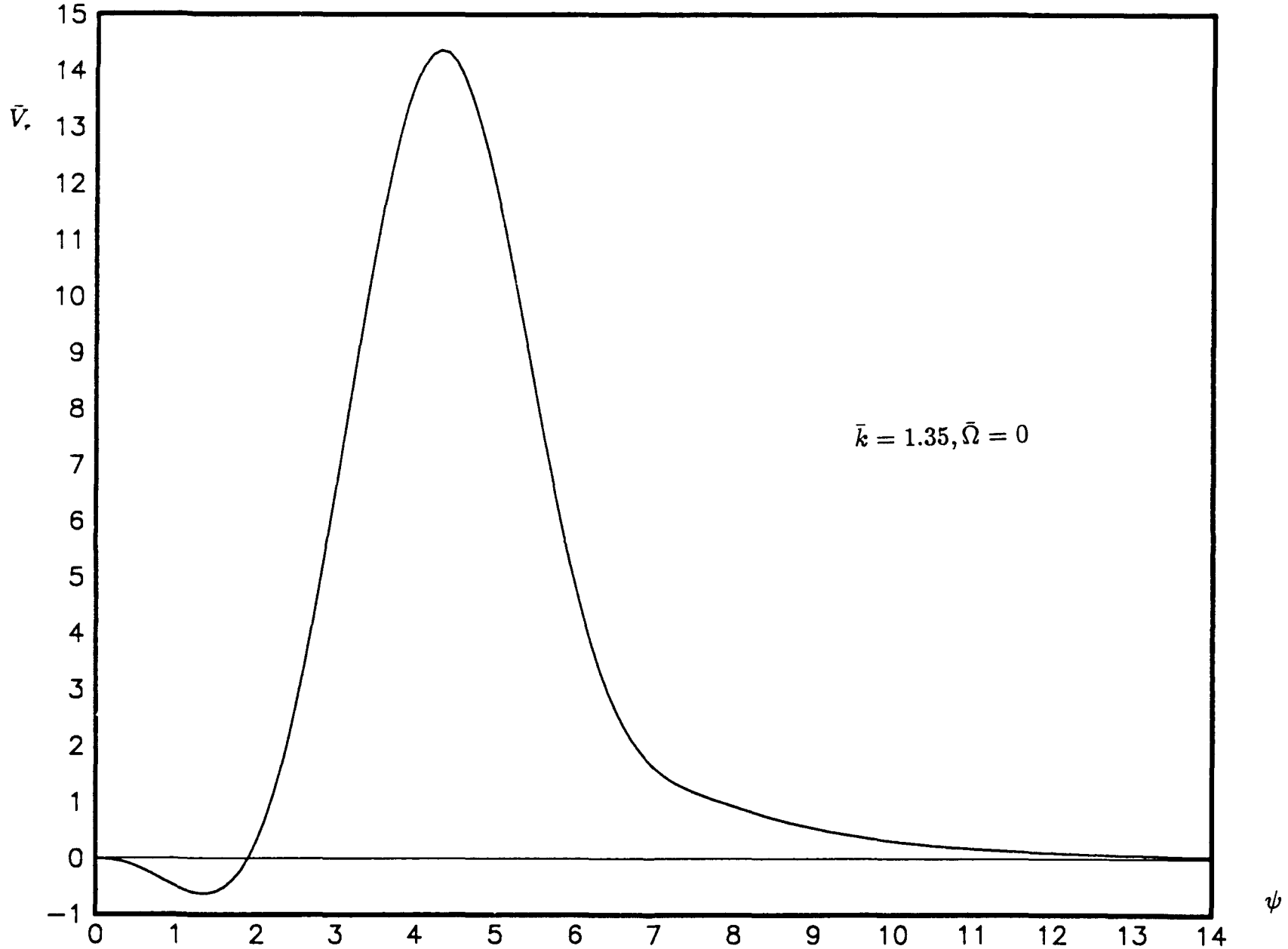

Figure (5.4). Eigenfunctions $\bar{U}$, $\bar{V}$ of (3.10) & (3.11) for neutrally stable vortices with $\bar{k} = 1.35$, $\bar{\Omega} = 0$. a) Re($\bar{U}$), b) Im($\bar{U}$), c) Re($\bar{V}$), d) Im($\bar{V}$).

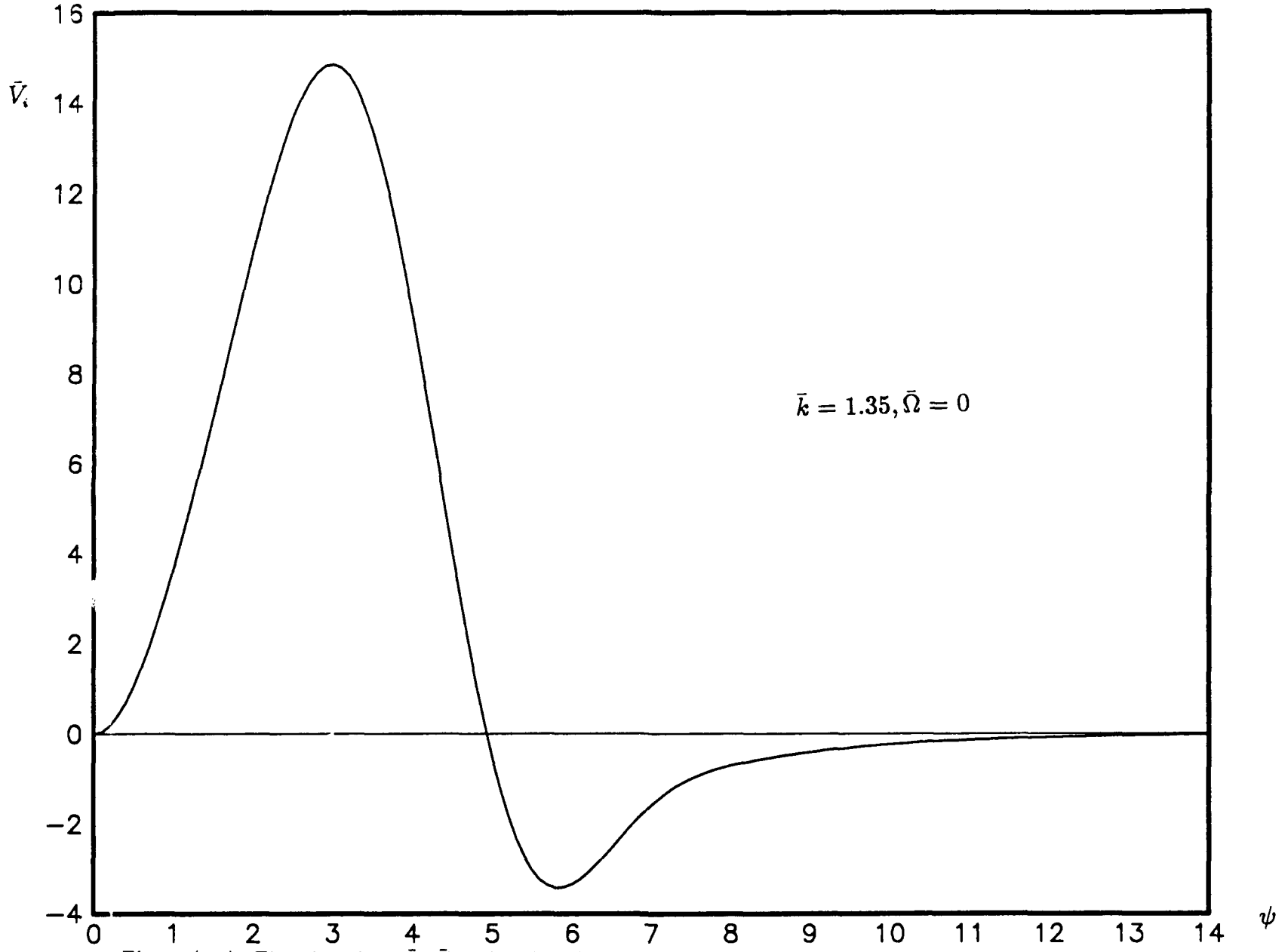

Figure (5.4). Eigenfunctions $\bar{U}$, $\bar{V}$ of (3.10) & (3.11) for neutrally stable vortices with $\bar{k} = 1.35$, $\bar{\Omega} = 0$. a) Re($\bar{U}$), b) Im($\bar{U}$), c) Re($\bar{V}$), d) Im($\bar{V}$).

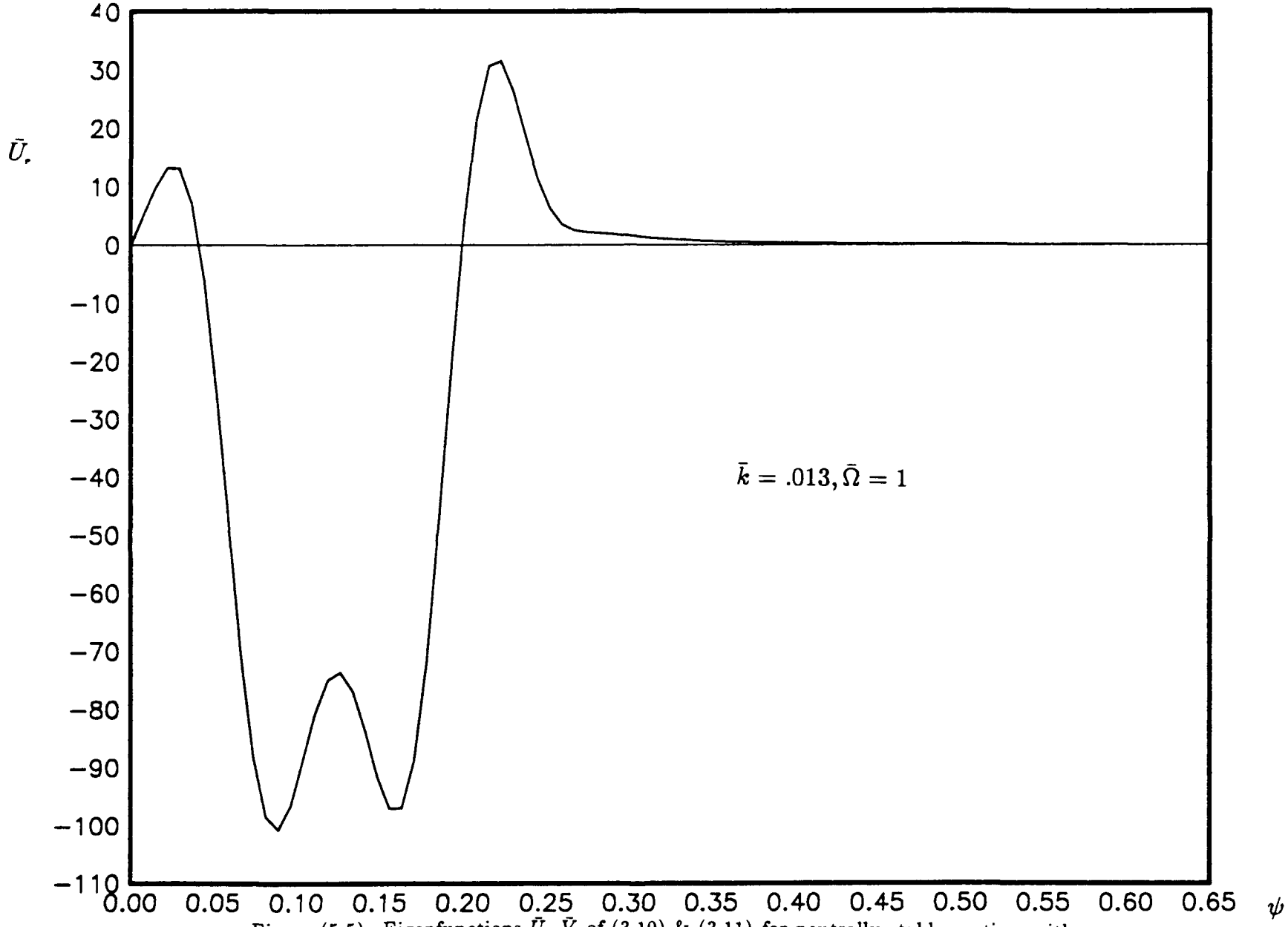

Figure (5.5). Eigenfunctions $\bar{U}$, $\bar{V}$ of (3.10) & (3.11) for neutrally stable vortices with $\bar{k} = 1.3 \times 10^{-2}$, $\bar{\Omega} = 1$. a) Re($\bar{U}$), b) Im($\bar{U}$), c) Re($\bar{V}$), d) Im($\bar{V}$).

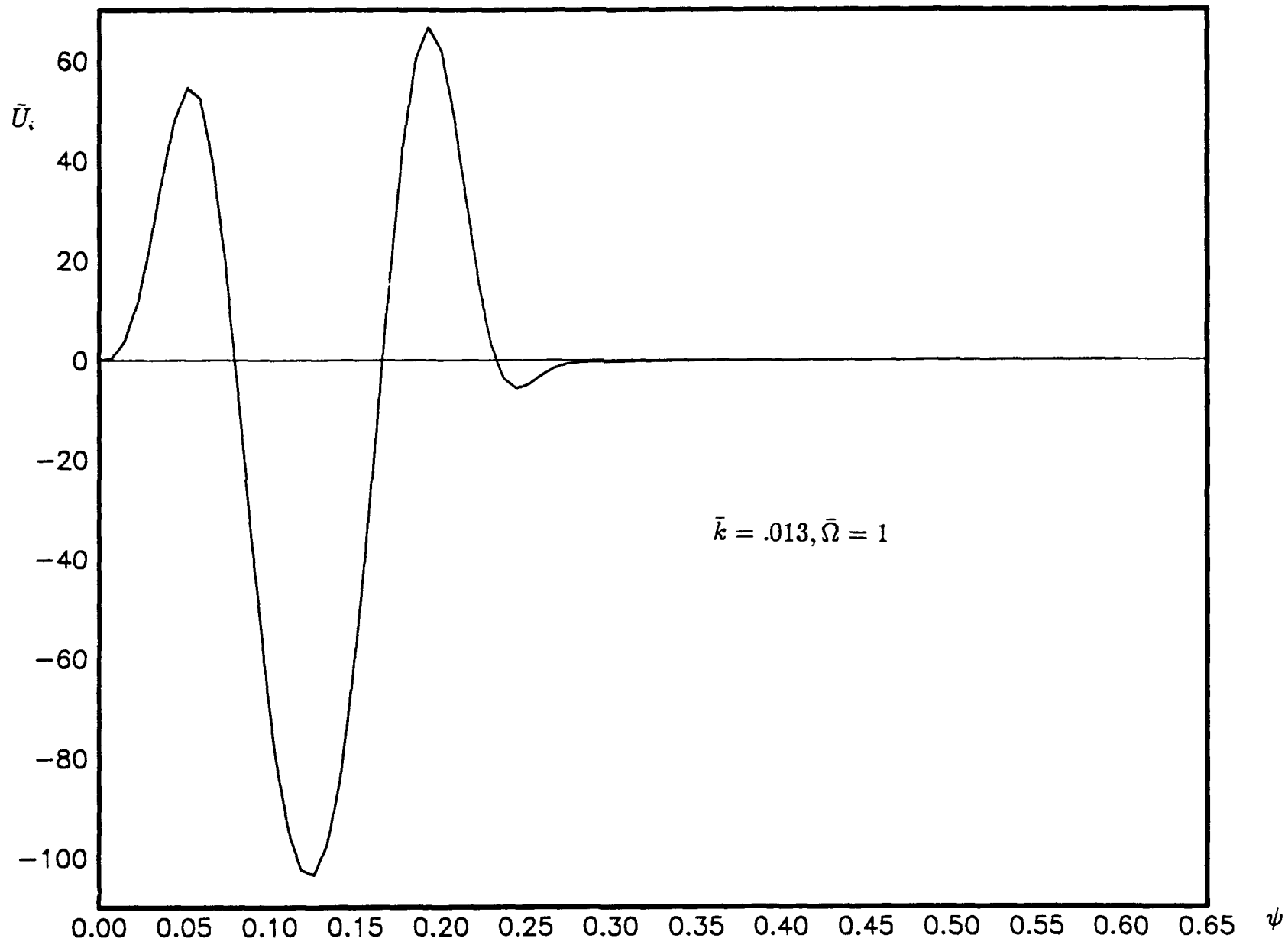

Figure (5.5). Eigenfunctions $\bar{U}$, $\bar{V}$ of (3.10) & (3.11) for neutrally stable vortices with $\bar{k} = 1.3 \times 10^{-2}$, $\bar{\Omega} = 1$. a) Re($\bar{U}$), b) Im($\bar{U}$), c) Re($\bar{V}$), d) Im($\bar{V}$).

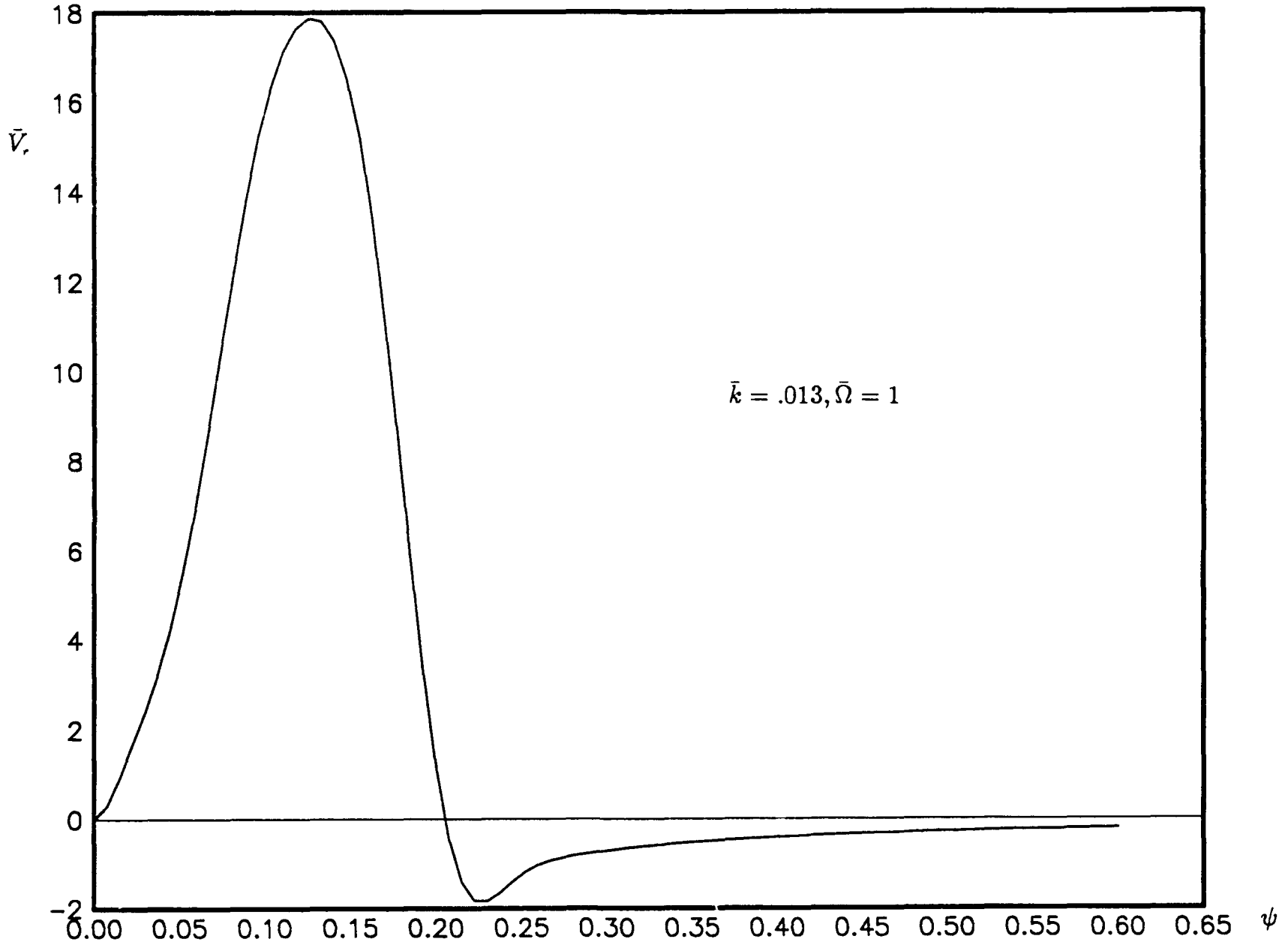

Figure (5.5). Eigenfunctions $\bar{U}$, $\bar{V}$ of (3.10) & (3.11) for neutrally stable vortices with $\bar{k} = 1.3 \times 10^{-2}$, $\bar{\Omega} = 1$. a) Re($\bar{U}$), b) Im($\bar{U}$), c) Re($\bar{V}$), d) Im($\bar{V}$).

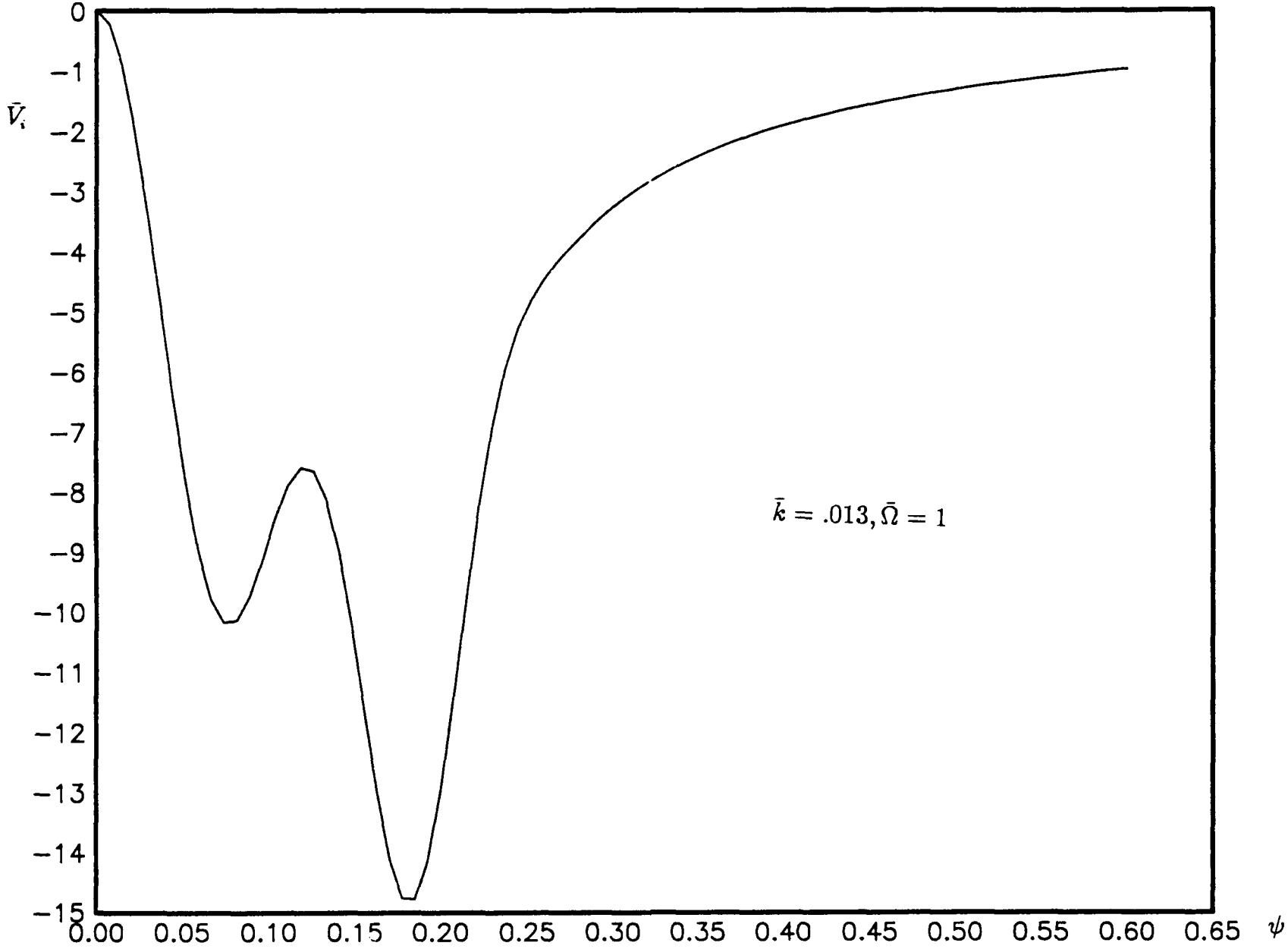

Figure (5.5). Eigenfunctions $\bar{U}$, $\bar{V}$ of (3.10) & (3.11) for neutrally stable vortices with $\bar{k} = 1.3 \times 10^{-2}$, $\bar{\Omega} = 1$. a) Re($\bar{U}$), b) Im($\bar{U}$), c) Re($\bar{V}$), d) Im($\bar{V}$).

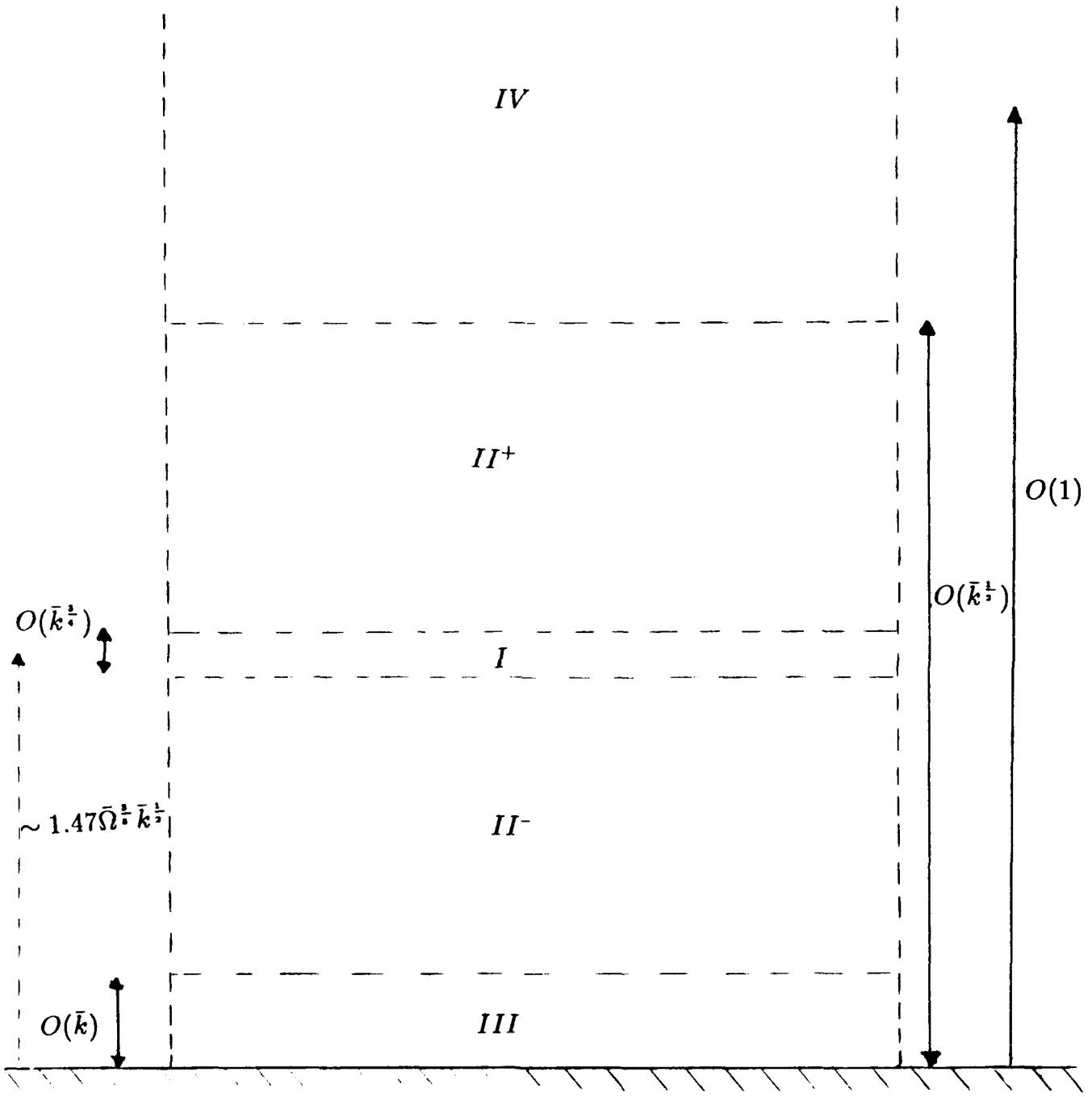

Figure (5.6). Schematic diagram of asymptotic structure of the solution of (3.10) & (3.11) for the case of small vortex wavenumber $\bar{k} \ll 1$. The solution configuration divides into four distinct zones: Zone (I) is a thin region of depth $O(\bar{k}^{\frac{2}{3}})$ at a distance $O(\bar{k}^{\frac{1}{3}})$ from the wall, see definition (5.7a). This zone is embedded within (II), a region of thickness $O(\bar{k}^{\frac{1}{3}})$, see (5.12). The structure has an additional thin viscous layer at the wall, Zone (III), which enables boundary conditions (3.11a) to be met. Finally, an outer region (IV) of depth O(1) facilitates the exponential decay of the disturbance solutions far from the wall, see (5.21).

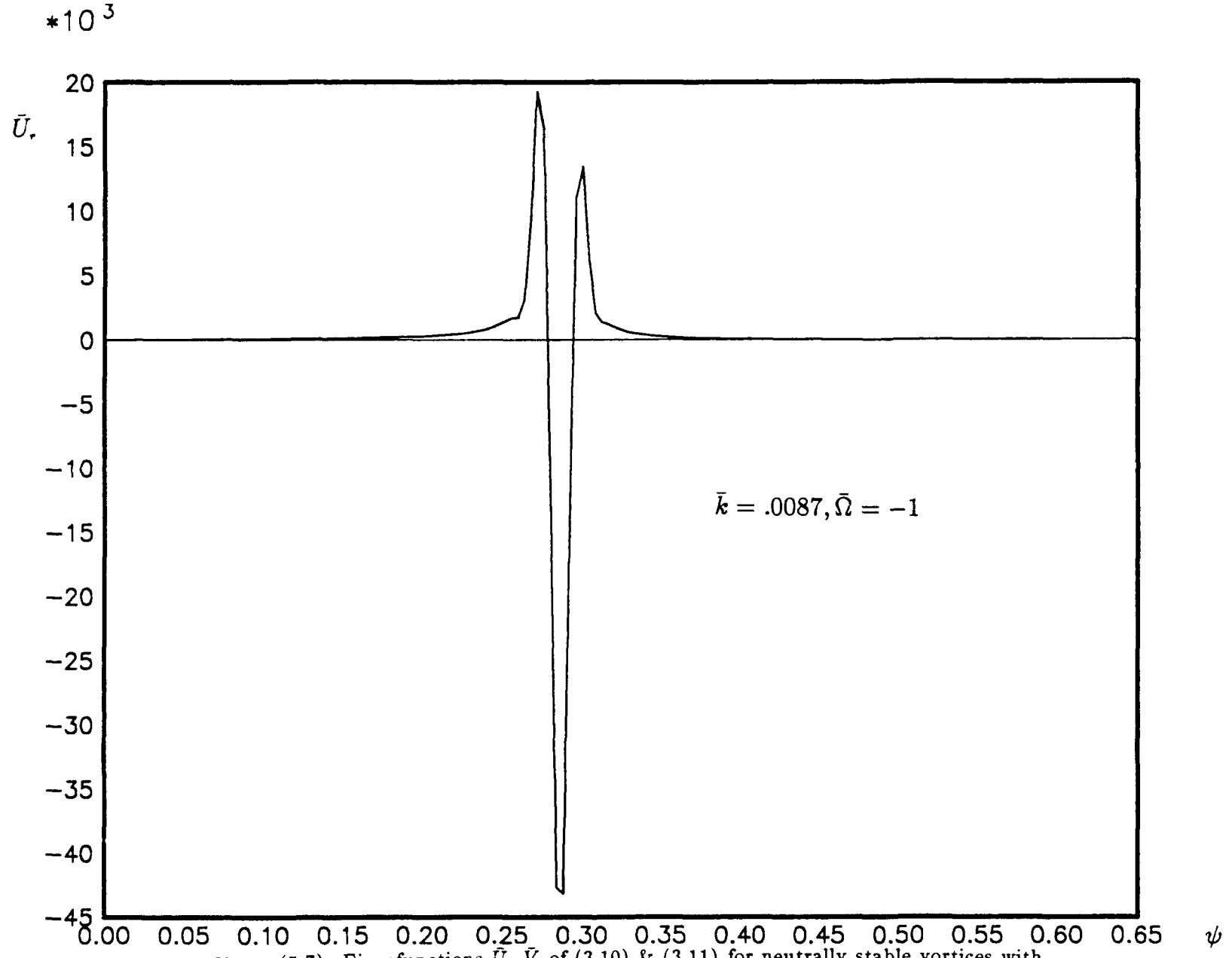

Figure (5.7). Eigenfunctions $\bar{U}$, $\bar{V}$ of (3.10) & (3.11) for neutrally stable vortices with $\bar{k} = 8.7 \times 10^{-3}$, $\bar{\Omega} = -1$. a) Re($\bar{U}$), b) Im($\bar{U}$), c) Re($\bar{V}$), d) Im($\bar{V}$).

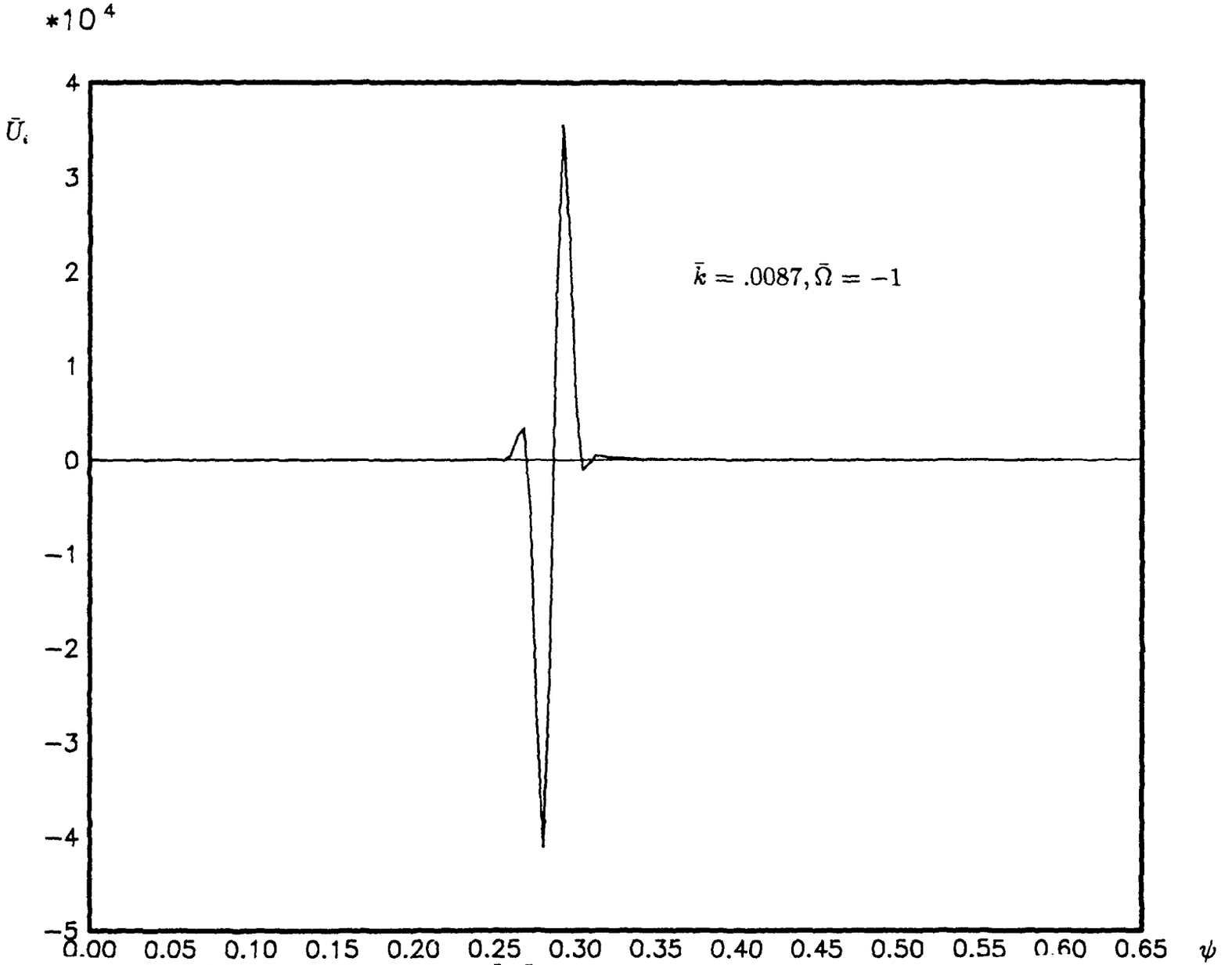

Figure (5.7). Eigenfunctions $\bar{U}$, $\bar{V}$ of (3.10) & (3.11) for neutrally stable vortices with $\bar{k} = 8.7 \times 10^{-3}$, $\bar{\Omega} = -1$. a) Re($\bar{U}$), b) Im($\bar{U}$), c) Re($\bar{V}$), d) Im($\bar{V}$).

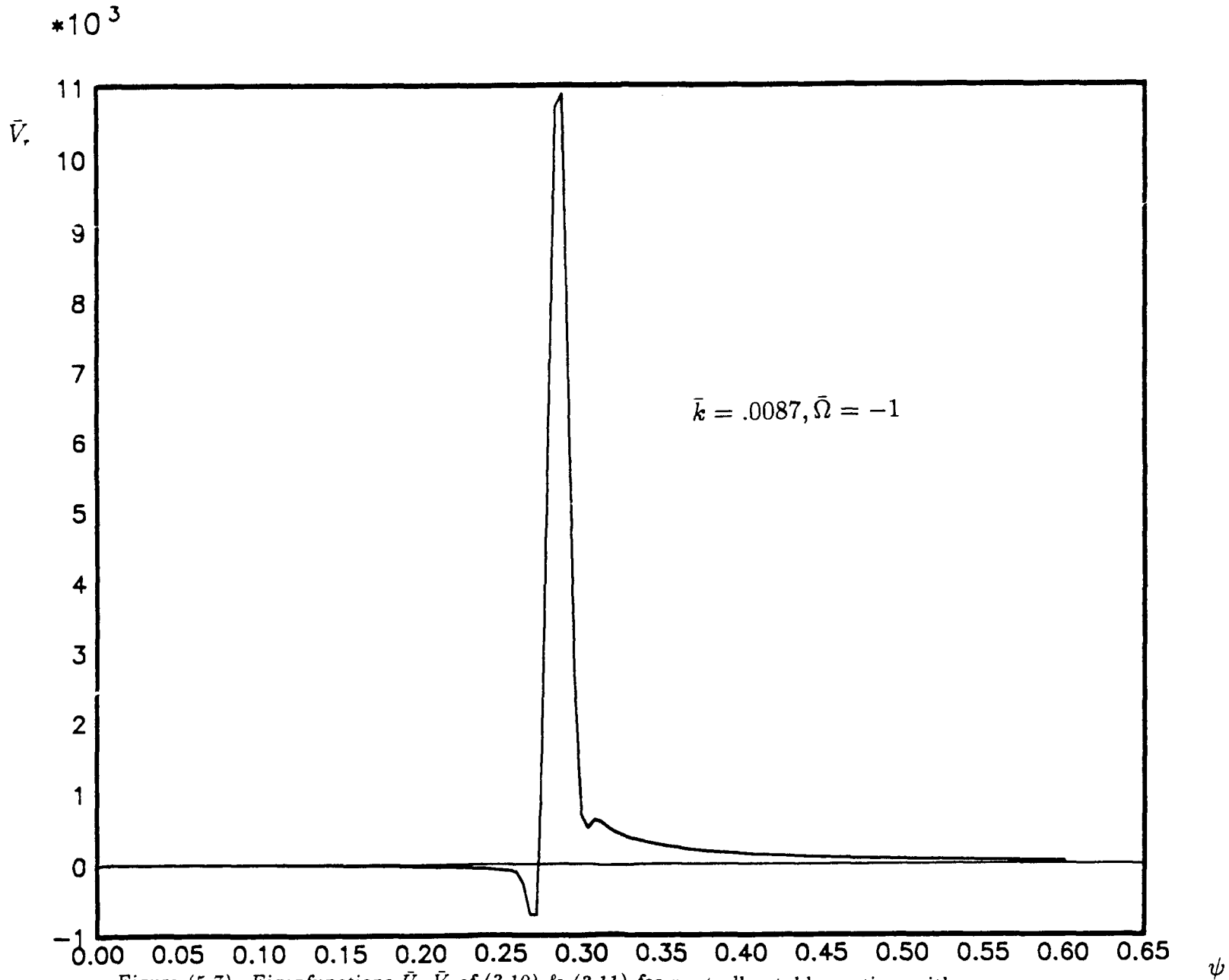

Figure (5.7). Eigenfunctions $\bar{U}$, $\bar{V}$ of (3.10) & (3.11) for neutrally stable vortices with $\bar{k} = 8.7 \times 10^{-3}$, $\bar{\Omega} = -1$. a) Re($\bar{U}$), b) Im($\bar{U}$), c) Re($\bar{V}$), d) Im($\bar{V}$).

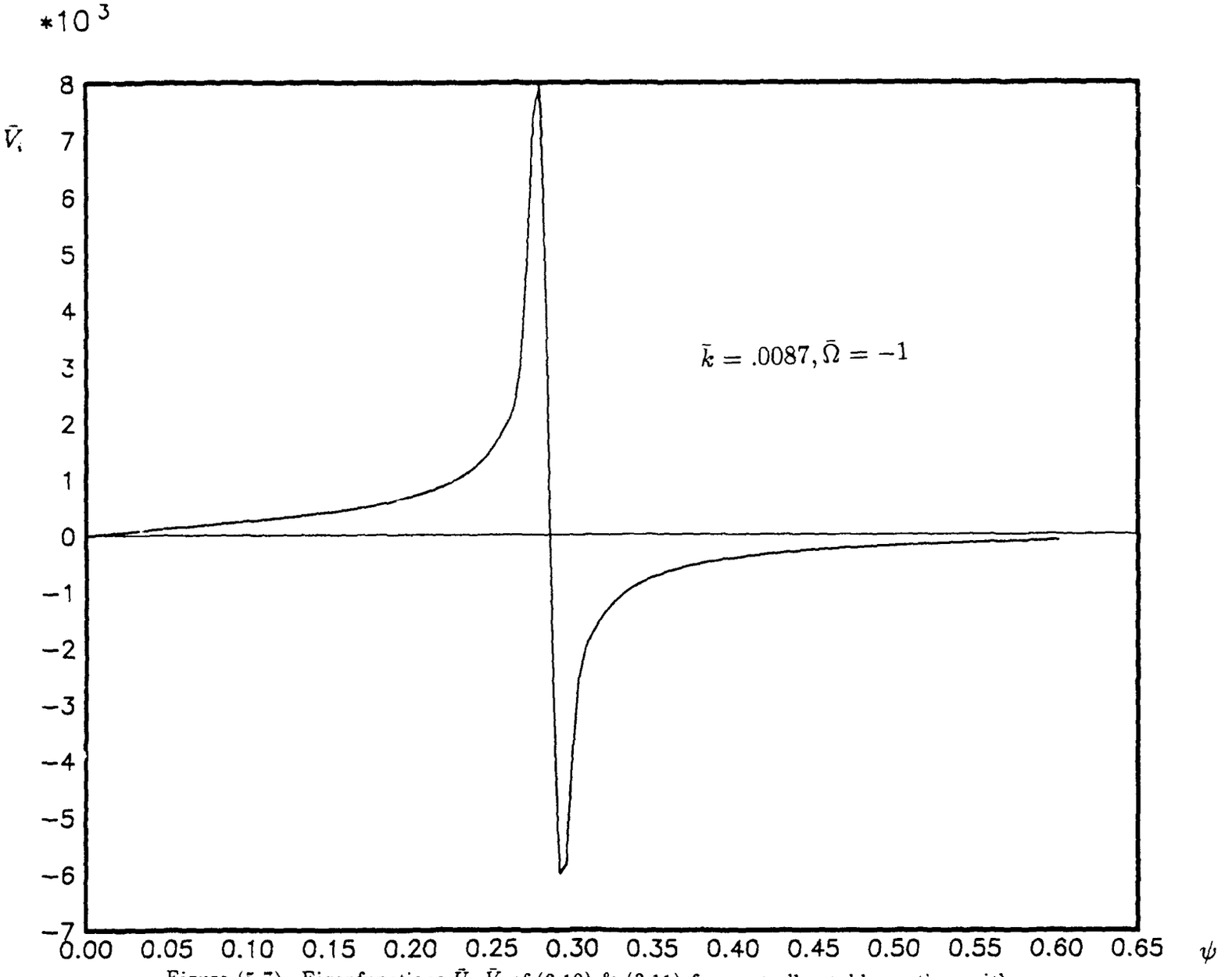

Figure (5.7). Eigenfunctions $\bar{U}$, $\bar{V}$ of (3.10) & (3.11) for neutrally stable vortices with $\bar{k} = 8.7 \times 10^{-3}$, $\bar{\Omega} = -1$. a) Re($\bar{U}$), b) Im($\bar{U}$), c) Re($\bar{V}$), d) Im($\bar{V}$).

Figure (5.8). The growth rates of some unsteady modes of (3.10),a) $\bar{\Omega} = 1$,and b)$\bar{\Omega} = -1$.

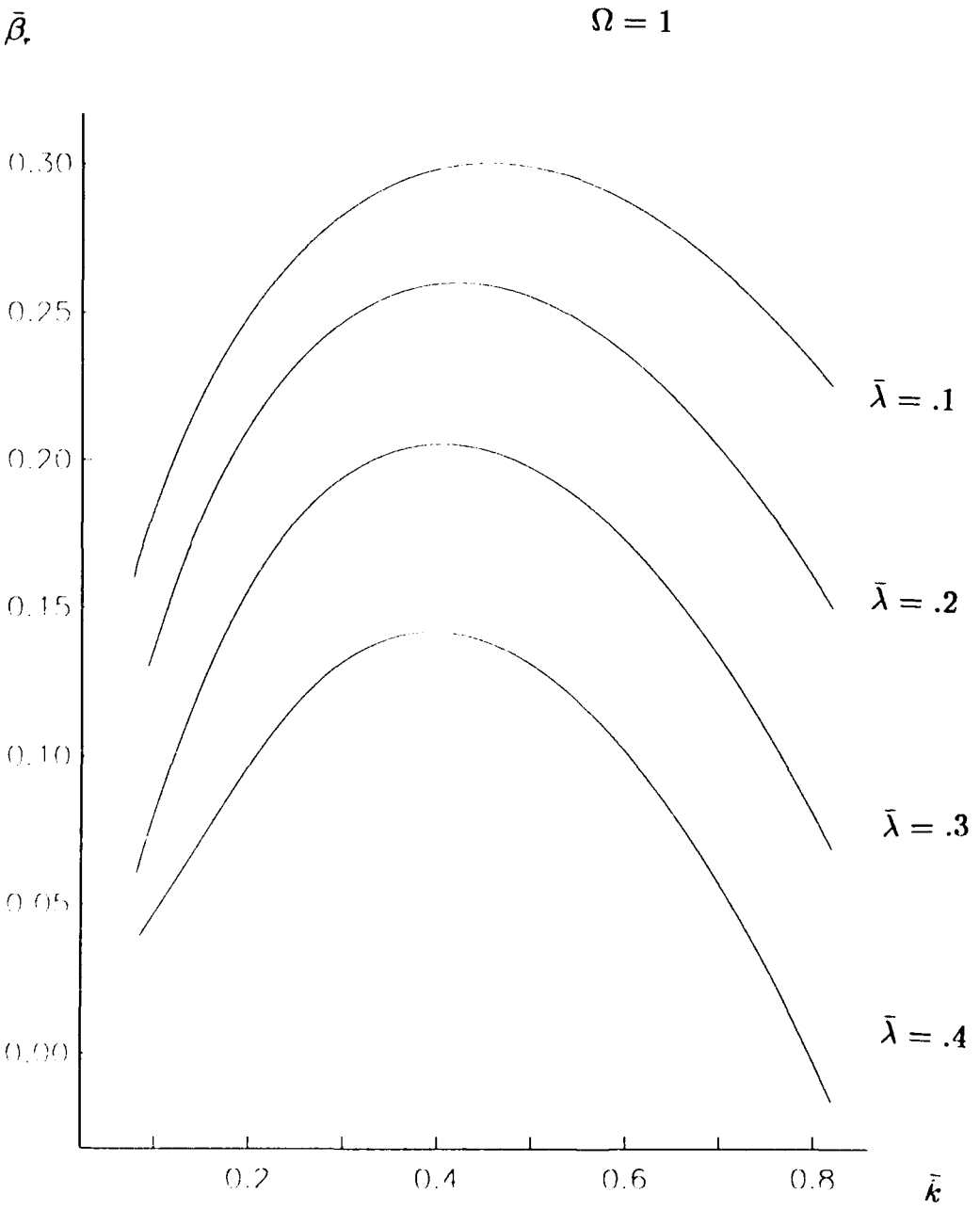

Figure (5.8). The growth rates of some unsteady modes of (3.10),a) $\bar{\Omega} = 1$,and b)$\bar{\Omega} = -1$.

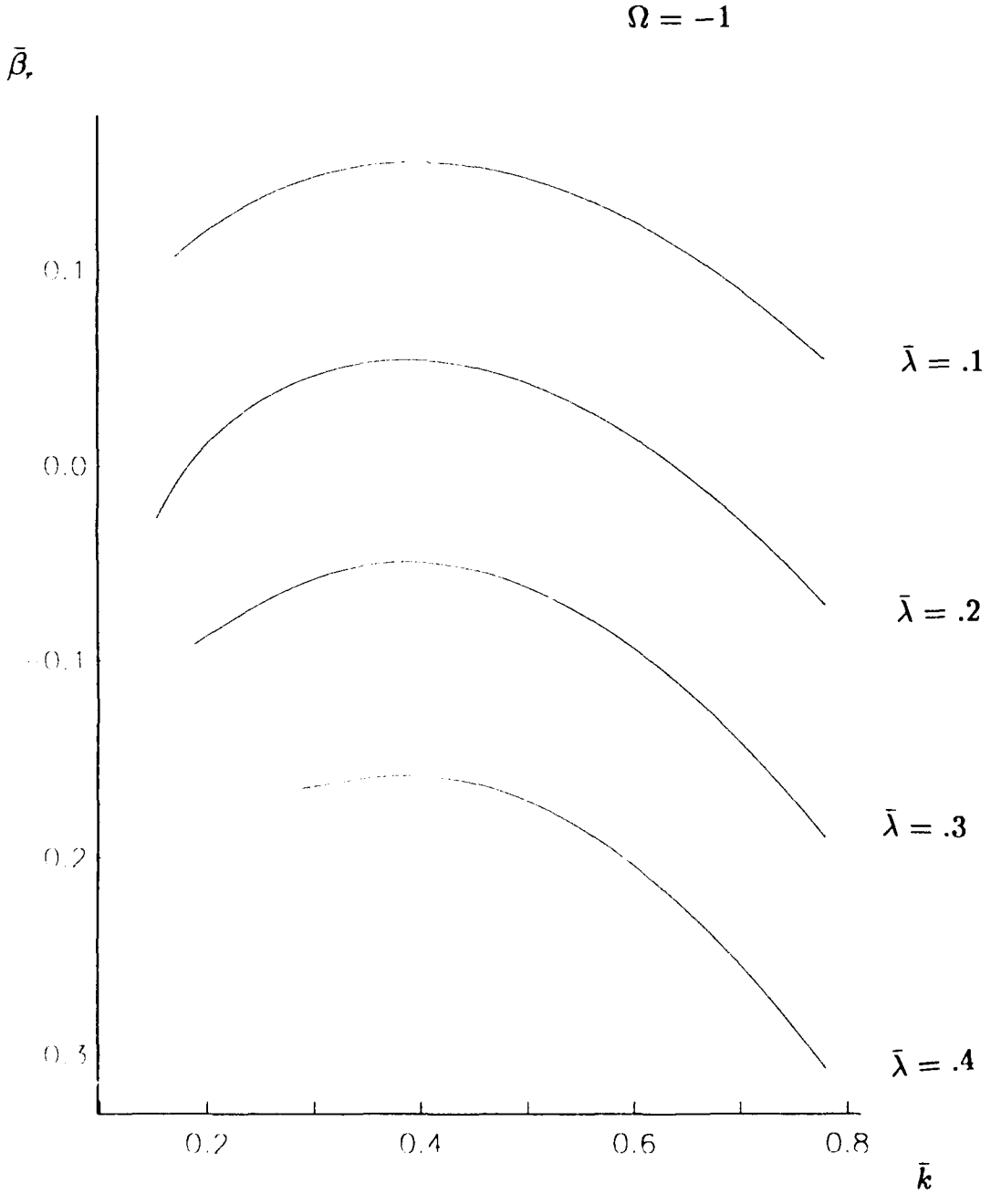

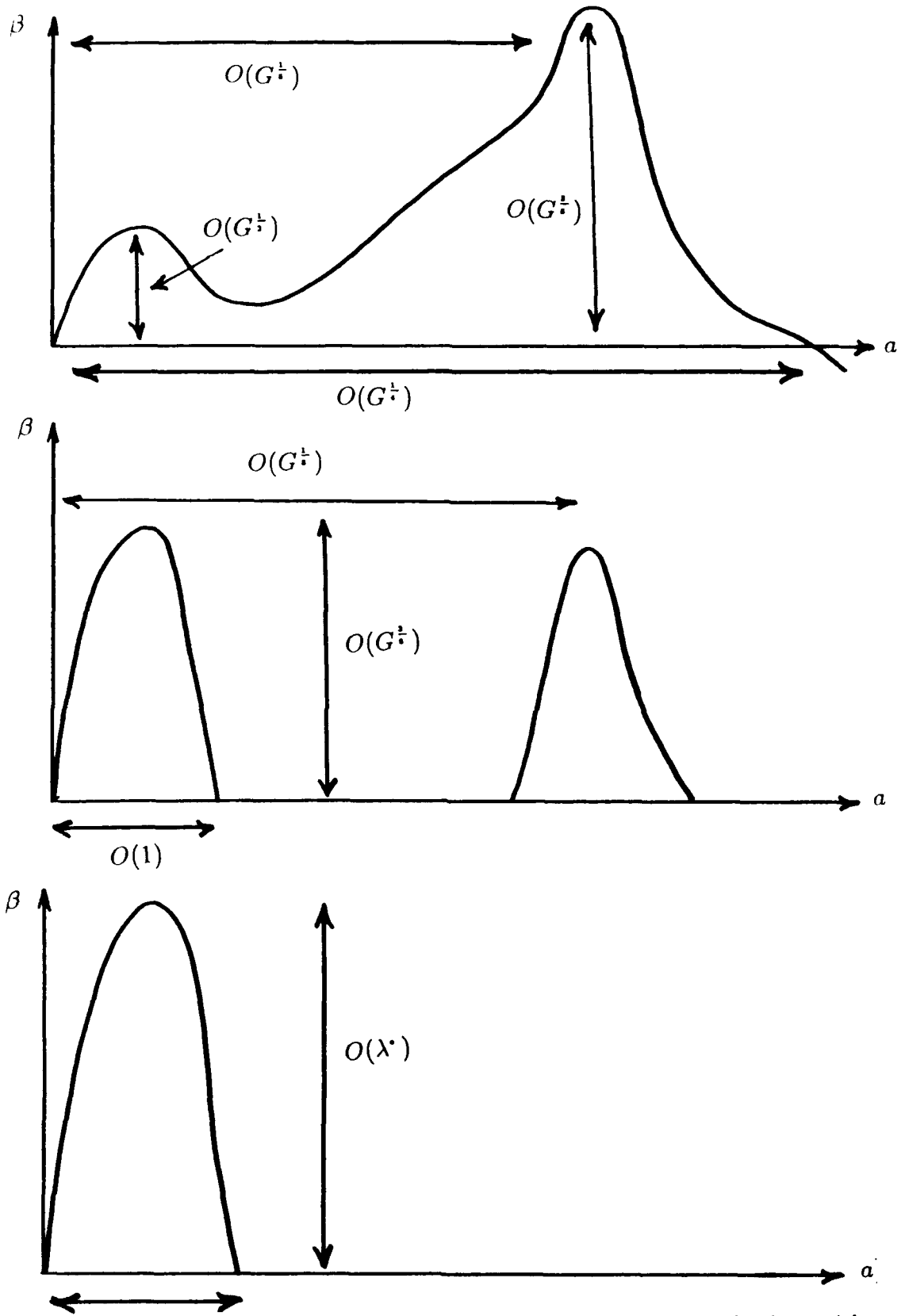

Figure (6.1) A sketch of the growth rate-wavenumber dependence for the crucial crossflow scalings.

NASA

Report Documentation Page

1. Report No	2. Government Accession No	3. Recipient's Catalog No
NASA CR-187456 ICASE Report No. 90-72		

4. Title and Subtitle	5. Report Date
VORTEX INSTABILITIES IN 3D BOUNDARY LAYERS: THE RELATIONSHIP BETWEEN GÖRTLER AND CROSSFLOW VORTICES	October 1990
	6. Performing Organization Code

7. Author(s)	8. Performing Organization Report No
Andrew P. Bassom Philip Hall	90-72
	10. Work Unit No
	505-90-21-01

9. Performing Organization Name and Address	11. Contract or Grant No
Institute for Computer Applications in Science and Engineering Mail Stop 132C, NASA Langley Research Center Hampton, VA 23665-5225	NAS1-18605
	13. Type of Report and Period Covered
12. Sponsoring Agency Name and Address	Contractor Report
National Aeronautics and Space Administration Langley Research Center Hampton, VA 23665-5225	14. Sponsoring Agency Code

15. Supplementary Notes

Langley Technical Monitor:
Richard W. Barnwell

Submitted to Journal of Fluid Mechanics

Final Report

16. Abstract

The inviscid and viscous stability problems are addressed for a boundary layer which can support both Görtler and Crossflow vortices. The change in structure of Görtler vortices is found when the parameter representing the degree of three-dimensionality of the basic boundary layer flow under consideration is increased. It is shown that Crossflow vortices emerge naturally as this parameter is increased and ultimately become the only possible vortex instability of the flow. It is shown conclusively that at sufficiently large values of the crossflow there are no unstable Görtler vortices present in a boundary layer which, in the zero crossflow case, is centrifugally unstable. The results suggest that in many practical applications Görtler vortices cannot be a cause of transition because they are destroyed by the 3-D nature of the basic state. In swept wing flows the Görtler mechanism is probably not present for typical angles of sweep of about 20 degrees. Some discussion of the receptivity problem for vortex instabilities in weakly 3-D boundary layers is given; it is shown that inviscid modes have a coupling coefficient marginally smaller than those of the fastest growing viscous modes discussed recently by Denier, Hall and Seddougui (1990). However the fact that the growth rates of the inviscid modes are the largest in most situations means that they are probably the most likely source of transition.

17. Key Words (Suggested by Author(s))	18. Distribution Statement
vortex, instability, crossflow	02 - Aerodynamics Unclassified - Unlimited

19. Security Classif. (of this report)	20. Security Classif. (of this page)	21. No. of pages	22. Price
Unclassified	Unclassified	76	A05

NASA-Langley, 1990